UNIVERSITAT DE BARCELONA

Characterization of the 40S-LARP1 complex in a model of ribosome biogenesis-addicted tumors

Carolina Martínez Herráez

UNIVERSITAT DE BARCELONA

FACULTAT DE FARMÀCIA I CIÈNCIES DE L'ALIMENTACIÓ

Characterization of the 40S-LARP1 complex in a model of ribosome biogenesis-addicted tumors

CAROLINA MARTÍNEZ HERRÁEZ

APRIL, 2024

Doctoral Program in Biomedicine

Thesis submitted by Carolina Martínez Herráez to apply for the PhD degree at the Universitat de Barcelona

Characterization of the 40S-LARP1 complex in a model of ribosome biogenesis-addicted tumors

Dr. Antonio Gentilella	Dr. Albert Tauler i Girona	Carolina Martínez Herráez
Co-director and tutor	Co-director	PhD student

Universitat de Barcelona

Facultat de Farmàcia i Ciències de l'Alimentació

Departament de Bioquímica i Fisiologia

Institut d'Investigació Biomèdica de Bellvitge (IDIBELL)

Laboratori de Metabolisme del Càncer (LMC)

ABSTRACT

In the process of neoplastic transformation, hyperactivation of proliferative signaling and the deregulation of cellular metabolism are required to ensure uncontrolled cellular growth and proliferation as well as high levels of energy production. To do so, hyperactivation of key oncogenes like MYC and oncogenic pathways such as mTOR, PI3K/AKT, Ras/MEK and WNT/β-catenin are essential to maintain high levels of protein synthesis and to sustain the production of ribosomes, the proteins factories of the cell. Ribosomes are ribonucleoprotein complexes composed by 80 ribosomal proteins (RPs) and 4 rRNA. The generation of new ribosomes is a multi-step and high energy-demanding process that requires a tight regulation from transcription to translation and beyond. In this regard, the production of RP is coordinated at the post-transcriptional level through a cis¬-element, termed Terminal Oligopyrimidine (TOP) motif, present at the transcriptional start site of their cognate transcripts. mTOR, which senses the external and internal metabolic cues in the cell, acts as a translational switch of this family of 5'TOP mRNAs accordingly. Our group has discovered that 5'TOP mRNAs are stabilized and preserved in a biochemical complex composed by the RNA-binding protein LARP1 and the small ribosomal subunit 40S, and that mTOR inhibition triggers the formation of the 40S-LARP1-5'TOP complex. Importantly, we recently described that the 40S-LARP1-5'TOPs complex acts as an anabolic storage in the form of stable pools of translationally-inactive mRNAs upon restrained metabolic limitations characterized by mTOR inhibition such as treatment with pharmacological inhibitors or by amino acid or serum deprivation. This reservoir of anabolic capacity can be rapidly spent by the cells to generate new ribosomes when conditions return permissive and mTOR is reactivated, suggesting that the mTOR / 40S-LARP1 axis could constitute a cell instrinsic mechanism of metabolic resistance to adverse growth conditions. This might have important implications in the process of tumorigenesis and in the treatment of cancers addicted to ribosome biogenesis. However, little is known regarding the formation of this biochemical complex and its molecular makeup in response to limiting metabolic

constraints. To this end, we have characterized the 40S-LARP1 complex interactome in normal growing conditions and under different mTOR inhibiting conditions by Mass Spectrometry. This characterization has shown that the 40S-LARP1 complex interacts with proteins involved in multiple steps of RNA regulation and translation as well as ribosome biogenesis, mitochondrial translation or intracellular organization. Furthermore, we have evaluated the subcellular localization of LARP1 protein, which we have proved to be widespread and mainly cytoplasmic but sensitive to the mTOR pathway. We have observed that LARP1 increases its co-localization with markers of the endoplasmic reticulum and the mitochondria upon mTOR inhibition. An initial analysis on the functional role of the 40S-LARP1 complex(es) interactors has revealed that the RNA binding protein ILF3 and the mitochondrial protein PHB1 are new players in the regulation of 5'TOP mRNAs. Of note, the interaction of the 40S-LARP1 complex with these two partners does not appear to be concomitant, pointing to a model of different 40S-LARP1 complexes co-existing in the cell at the same time. Indeed, LARP1 colocalizes with PHB1 in the mitochondria, which might confer specific functions to the 40S-LARP1 complex confined to such subcellular compartment and distinct of other 40S-LARP1 complexes. Intriguingly, ILF3 and PHB1 have been already described as negative prognostic markers in cancer and chemoresistance, respectively, suggesting a potential role of the 40S-LARP1 anabolic reservoir in those contexts. Furthermore, we have evaluated the subcellular localization of LARP1 protein, which we have proved to be widespread and mainly cytoplasmic but sensitive to the mTOR pathway. We have observed that LARP1 increases its co-localization with markers of the endoplasmic reticulum and the mitochondria upon mTOR inhibition. Understanding this will shed light on the metabolic pathways fed by the anabolic storage, and consequently on new potential targets in RiBi-addicted cancers.

RESUMEN

Las células cancerígenas requieren altos niveles de síntesis de proteínas para mantener el crecimiento tumoral. De esta forma, en muchos tipos de tumores como el cáncer colo-rectal, la síntesis de ribosomas se encuentra frecuentemente hiperactivada para alcanzar la alta demanda anabólica. Nuestro grupo ha descubierto un complejo bioquímico compuesto por la proteína de unión a ARN LARP1 y la subunidad pequeña del ribosoma 40S que estabiliza la familia the ARNm 5'TOP, los cuales codifican componentes de la síntesis de ribosomas. Bajo condiciones de crecimiento desfavorables que derivan en la inhibición de mTOR, el principal sensor del metabolismo celular, el complejo 40S-LARP1 protege los tránscritos 5'TOP en condiciones de supresión de la traducción. Bajo estas condiciones, el complejo 40S-LARP1-ARNms 5'TOP actúa como un almacenamiento de poder anabólico, el cual las células pueden utilizar para generar nuevos ribosomas y, por tanto, nueva capacidad de síntesis de proteínas, cuando las señales internas y externas vuelven a ser favorables. Sin embargo, se desconoce cómo este complejo bioquímico se forma en respuesta a las condiciones metabólicas restrictivas, así como su composición molecular. Con este objetivo, hemos caracterizado el interactoma del complejo 40S-LARP1 bajo diferentes condiciones de inhibición de mTOR por espectrometría de masas. Esta caracterización ha demostrado que el complejo 40S-LARP1 interacciona con proteínas relacionadas con eventos de la regulación de ARN y la traducción, así como síntesis de ribosomas, traducción mitocondrial y organización intracelular. Un análisis funcional ha revelado que la proteína de unión a ARN ILF3 y la proteína mitocondrial PHB1 son potenciales nuevos reguladores de los tránscritos 5'TOP. De manera destacable, ILF3 y PHB1 han sido descritos como marcadores negativos de pronóstico en cáncer y en resistencia a quimioterápicos, respectivamente, sugiriendo nuevos papeles del reservorio anabólico 40S-LARP1 en dichos contextos. Este conocimiento ayudará a descifrar las rutas metabólicas a las cuales este almacenamiento suministra y, por tanto, nuevas dianas en cánceres adictos a la síntesis de ribosomas.

INDEX

LIST OF FIGURES

LIST OF ABBREVIATIONS

3’ / 5’ UTR: 3’ / 5’ Untranslated Region

4E-BP1 / 2: eukaryotic translation Initiation Factor 4E- Binding Protein 1 / 2

5’TOP: 5’ Terminal Olygopyrimidine

5-FU: 5-Fluorouracil

APC: Adenomatous Polysposis Coli

ASC-1: Activating Signal Cointegrator 1

ATAD3: ATPase Family AAA Domain Containing 3

BCL-2: B-Cell Lymphoma 2

BCLAF1: BCL2 Associated Transcription Factor 1

CANX: Calnexin

CAPRIN1: Cytoplasmic Activation/Proliferation-Associated Protein-1

CCR4-NOT (CNOT): Carbon Catabolite Repression-Negative on TATA-less

CDD: Conserved Domain Database

CDS: Coding Sequence

ChIP: Chromatin Immunopreciptation

CHX: Cyclohexamide

COAD: Colorectal Adenocarcinoma

CPSF1: Cleavage and Polyadenylation Specificity Factor

CRC: Colorectal Cancer

CRISPR: Clustered Regularly Interspaced Short Palindromic Repeats

dsRBM: dsRNA Binding Motifs

dsRNA: double-stranded RNA

eEF2: eukaryotic Elongation Factor 2

eEF2K: eukaryotic Elongation Factor 2 Kinase

eIF: eukaryotic translation Initiation Factor

eIF2α: eukaryotic translation Initiation Factor 2α

eIF4A / 4B / 4E / 4F / 4G: eukaryotic translation Initiation Factor 4A / 4B / 4E / 4F / 4G

ER: Endoplasmic Reticulum

ERAD: ER-Associated Degradation

ERLIN1 / 2: Endoplasmic Reticulum Lipid Raft Associated 1 / 2

ERα: Estrogen Receptor α

EXOSC6 / 10: Exosome Component 6 /10

FDR: False Discovery Rate

FLZ: Fluorizoline

FOLFOX: 5’FU + Oxaliplatin

G3BP1 / 2: Ras GTPase-Activating Protein-Binding Protein 1 / 2

GFP: Green Fluorescent Protein

GM: Growing Media

GO: Gene Ontology

HBB: Hemoglobin Subunit Beta

HCC: Hepatocellular Carcinoma

hnRNP: heterogeneous nuclear Ribonucleoprotein

IgG: Immunoglobin G

IL-2: Interleukin 2

ILF2 / 3: Interleukin Enhancer-Binding Factor 2 / 3

IMM: inner mitochondrial membrane

IP: Immunoprecipitation

IRBC: impaired ribosome biogenesis checkpoint

IRES: internal ribosome entry site

ISR: Integrated Stress Response

ISRIB: Integrated Stress Response Inhibitor

ITPR1 / 2 / 3: Inositol 1,4,5-Trisphosphate Receptor Type 1 / 2 / 3

KO: Knock-Out

L32MUT: TetO-MUT-L32TOP-β-Globin-MS2(12X)

L32WT: TetO-WT-L32TOP-β-Globin-MS2(12X)

LAM: La-motif

LARP: La Related Protein

LARP1: La Related Protein 1

LC/MS-MS: Liquid Chromatography coupled to Tandem Mass Spectrometry

LIR: LC3-Interacting Region

LSG1: Large 60S Subunit Nuclear Export GTPase 1

M1: Manders Coefficient 1

MAMs: Mitochondria-Associated Membranes

MAPK: Mitogen-Activated Protein Kinase

MEK: Mitogen-Activated Protein Kinase Kinase

mLST8: mammalian Lethal with Sec13 Protein 8

mRNA: messenger RNA

mTOR: mechanistic Target Of Rapamycin

mTORC1 / 2: mechanistic Target Of Rapamycin Complex 1 / 2

NAT10: N-Acetyltransferase 10

NB: Non-Bound

NF45 / 90 / 110: Nuclear Factor 45 / 90 / 110

NOLC1: Nucleolar and Coiled-Body Phosphoprotein 1

NP GM: non-polysomal growth medium

NP SS: non-polysomal serum starvation

NP TAK: non-polysomal +TAK228

OXPHOS: Oxidative Phosphorylation

P GM: polysomal growth medium

PABP: Poly-A Binding Protein

PAM2: Poly-A Binding Protein Binding Motif 2

PAR: Parental

PAR-CLIP: Photoactivatable Ribonucleoside-enhanced Crosslinking and Immunoprecipitation

PBs: P-Bodies

PDCD4: Programmed Cell Death Factor 4

PHB(s): Prohibitin(s)

PHB1 / 2: Prohibitin 1 / 2

PI3K: Phosphatidylinositol 3-Kinase

PKR: Protein Kinase R

PLA: Proximity Ligation Assay

PLEC: Plectin

POP1: Processing of Precursors 1

PRKDC: Protein Kinase, DNA-Activated, Catalytic Subunit

PRPF6 / 8: Pre-mRNA Processing Factor 6 / 8

RANBP2: RAN binding protein 2

RAP: Ribosome Associated Protein

RAPTOR: Regulatory Associated Protein of mTOR

RBP: RNA-Binding Protein

RBR: Ribosome Binding Region

rDNA: ribosomal DNA

RiBi: Ribosome Biogenesis

RICTOR: Rapamycin Insensitive Companion of mTOR

RIP: RNA Immunoprecipitation

RNA Pol I/II/III: RNA polymerase I/II/III

RNP: Ribonucleoprotein

RP: Ribosomal Protein

RRBP1: Ribosome Binding Protein 1

RRM: RNA Recognition Motif

rRNA: ribosomal RNA

RT-qPCR: Real Time quantitative PCR

S6K1/2: Ribosomal Protein S6 Kinase 1 / 2

SA: Sodium Arsenite

SAINT: Significance Analysis of INTeractome

SASP: Senescence-Associated Secretory Phenotype

sgRNA: single guide RNA

SGs: Stress Granules

siNT: silencing RNA non-targeting

siRNA: silencing RNA

snoRNA: small nucleolar RNA

snRNP: small nucleolar Ribonucleoprotein

SPFH: Stomatin/Prohibitin/Flotillin/HflKC

SPOP: Serine-Glycine-One-Carbon

SS: Serum Starvation

STAU1: Staufen 1

TCGA: The Cancer Genome Atlas

TCOF1: Treacle Ribosome Biogenesis Factor 1

THRAP3: Thyroid Hormone Receptor Associated Protein 3

TOP: Terminal Olygopyrimidine

TORi: mTOR inhibition

tRNA: transfer RNA

TSC1 / 2: Tuberous Sclerosis Complex 1 / 2

TSS: Transcription Start Site

USP1O: Ubiquitin Specific Peptidase 10

VEGF: Vascular Endothelial Growth Factor

WNT: Wingless/int1

INTRODUCTION

1. Ribosome Biogenesis and Cancer

1.1 The Ribosome: composition and structure

The ribosome is the cellular machinery in charge of translating the genetic information into functional proteins (Green & Noller, 1997). The eukaryotic 80S ribosome is a ribonucleoprotein (RNP) particle composed by the 40S and the 60S subunits. Specifically, the 40S ribosome is formed by the 18S ribosomal RNA (rRNA) and 33 ribosomal proteins (RPs), while the 60S consists of 3 rRNA molecules (5S, 5.8S and 28S), and 47 RPs (Table I-1) (Lecompte et al., 2002; Spahn et al., 2001).

Table I-1. Ribosomal Protein composition of the Human 80S ribosome

Large 60S Ribosome				Small 40S Ribosome		
L3	L13	L24	L36	RACK1	S11	S23
L4	L13A	L26	L36A	SA	S12	S24
L5	L14	L27	L37	S2	S13	S25
L6	L15	L27A	L37A	S3	S14	S26
L7	L17	L28	L38	S3A	S15	S27
L7A	L18	L29	L39	S4	S15A	S27A
L8	L18A	L30	L40	S5	S16	S28
L9	L19	L31	L41	S6	S17	S29
L10	L21	L32	LP0	S7	S18	S30
L10A	L22	L34	LP1	S8	S19	
L11	L23	L35	LP2	S9	S20	
L12	L23A	L35A		S10	S21	

From the early days most of the knowledge obtained on the ribosome is based on studies of the prokaryotic ribosome, whereas *S. cerevisiae* has been deeply studied as a model system for the eukaryotic ribosome. Common elements of the prokaryotic and

eukaryotic ribosomes compose the evolutionary conserved core, responsible for the basic mechanism of polypeptide chain formation, while the eukaryotic specific parts are present at the surface, important for binding to regulatory factors (Ben-Shem et al., 2011; Wilson & Cate, 2012). In order to carry out the polypeptide chain synthesis from the messenger RNA (mRNA), eukaryotic and prokaryotic ribosomal subunits have three binding sites for the transfer RNA (tRNA) named A site, that accommodates the amino-acyl tRNA, the P site, where the nascent peptide chain is hold to the tRNA, and the E site or exit site, occupied by the deacylated tRNA after a new peptide bond has been formed. In a nutshell, the small ribosomal subunit is in charge of binding and scanning the mRNA, monitoring the codon-anticodon pairing, while the large subunit mediates the peptide bond formation between the nascent peptide in the P site and the charged-tRNA in the A site (Ramakrishnan, 2002). Besides these commonalities, mechanisms involved in mRNA decoding, translocation, elongation and termination differentiate eukaryotic from prokaryotic protein synthesis (Wilson & Cate, 2012).

While the ribosome has been largely described as a conserved and invariant machinery, in the last years, new insights into the heterogeneity of the ribosome have emerged particularly within higher metazoans phyla. Many studies have described variability in the core RP and rRNA composition, but also in terms of ribosome associated proteins (RAPs). This diversity in composition can occur both at the intracellular level or depending on the cellular subtype or tissue, and it is believed to confer specificity for specific families of transcripts as well as for their localizations or translational status [Reviewed in (Emmott et al., 2019; Genuth & Barna, 2018)].

1.2 Ribosome Biogenesis: Ribosome Assembly

Ribosome biogenesis (RiBi) is a multistep process that involves more than 200 assembly factors, which in eukaryotes takes place in the nucleolus. In the first steps, the three RNA polymerases synthesize the rRNAs and RP mRNAs: RNA polymerase I (Pol I) transcribe the rDNA into the 47S pre-rRNA, a precursor transcript that gives rise to the 18S, 5.8S and 28S rRNAs in the nucleolus. RNA polymerase III (Pol III) transcribes 5S rRNA

and RNA Polymerase II (Pol II) produces RP mRNAs, both in the nucleoplasm. RP mRNAs, as well as the transcripts encoding for other assisting factors, are translated in the cytoplasm and reimported into the nucleolus to assist the ribosome assembly.

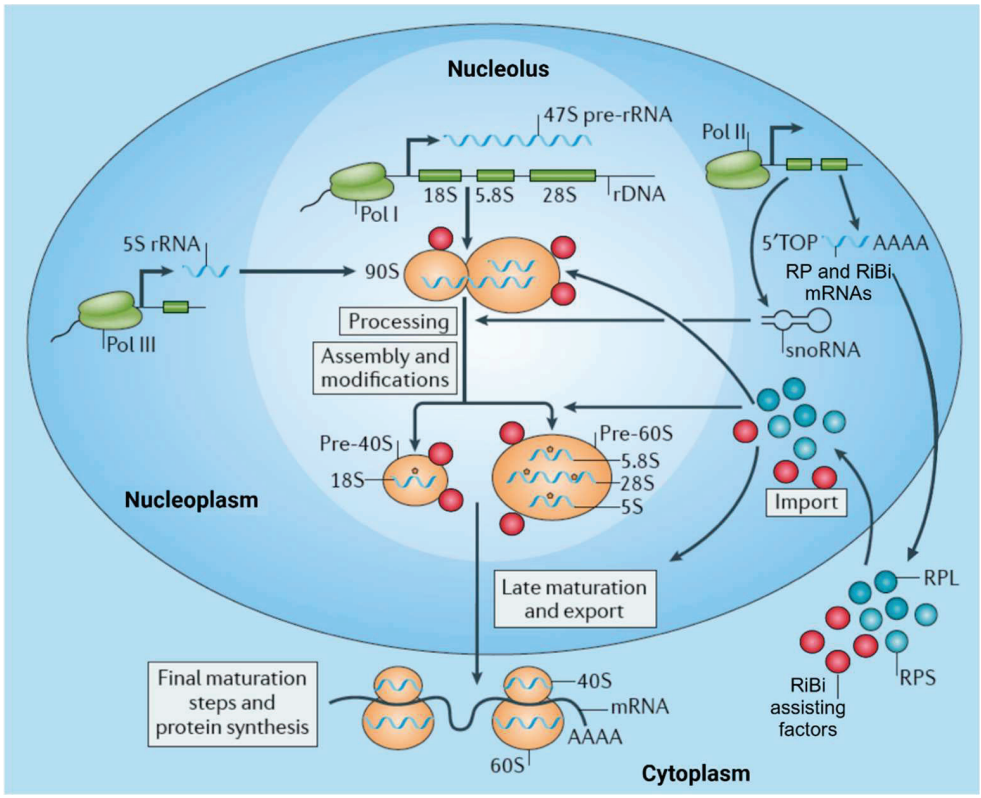

Figure I-1. Ribosome Biogenesis. The mature eukaryotic 80S ribosome is composed by the 40S and the 60S subunits. The majority of the steps of the RiBi process occur in the nucleolus. RNA Pol I transcribes the 47S precursor rRNAs (47S pre-rRNAs), which contains the sequences of 18S, 5.8S and 28S rRNAs. In the nucleoplasm, the 5S rRNA is transcribed by RNA Pol III, whereas RPs and other RiBi assisting factors mRNAs by RNA Pol II. The latter are exported to the cytoplasm for translation into their cognate proteins, which are subsequently re-imported in the nucleolus. There, rRNA and RPs get assembled into the 90S processome. During the maturation of the 90S processome into pre-40S and pre-60S ribosomal subunits, pre-rRNA is modified and processed through mechanisms that involve ~200 small nucleolar RNAs (snoRNAs) and RiBi assisting factors. A few additional RPs are assembled into pre-40S and pre-60S ribosomal subunits in the nucleoplasm and the cytoplasm, giving rise to the mature 80S ribosome. Figure adapted from Pelletier *et al.*, 2018 (Pelletier et al., 2018).

In more details, the rRNA precursors and most RPs are progressively assembled into the 90S processome that is processed and modified by a set of small nucleolar RNA (snoRNAs), nucleases and modifying enzymes to generate the pre-40S and pre-60S ribosomes. Finally, additional modifications and the last set of RPs are assembled in the nucleoplasm or the cytoplasm, where fully mature ribosomes are able to carry out translation (Granneman & Baserga, 2004; Tschochner & Hurt, 2003) (Figure I-1).

The idea of a fixed RiBi process has been challenged by new studies that describe more dynamic mechanisms of cytosolic RPs assembly and exchange. Different groups have described local translation of RP mRNAs far from the perinuclear cytosol, in protrusions of migrating cells (Dermit et al., 2020), as well as in neuronal axons (Biever et al., 2020; Fusco et al., 2021; Shigeoka et al., 2019). Interestingly, in axons, the incorporation of these newly synthesized RP into functional pre-existing ribosomes was observed (Fusco et al., 2021; Shigeoka et al., 2019), suggesting non-canonical RiBi events of local repair or specialization.

1.3 Ribosome Biogenesis Coordination

To guarantee an efficient ribosome assembly, the cell should produce all the ribosomal components and the RiBi assisting factors in a coordinated and balanced manner, investing high levels of energy to complete the process (Kressler et al., 2017). In this regard, the modulation of the RiBi process is controlled by pathways that respond to the metabolic status of the cell, being MYC and mechanistic Target Of Rapamycin (mTOR) the two main regulators of RiBi (Lempiäinen & Shore, 2009).

1.3.1 mTOR pathway

The production of new ribosomes must be tightly related to the energetic status of the cell. Regarding this, mTOR signaling pathway is the main sensor and coordinator of the cellular metabolism.

mTOR is a serine/threonine kinase that serves as the core enzyme of two complexes, mTOR complex 1 (mTORC1) and mTOR complex 2 (mTORC2) (Hara et al., 2002; D. H.

Kim et al., 2002). Among other regulatory proteins, the core of mTORC1 is composed by the catalytic component mTOR, the regulatory protein associated to mTOR (RAPTOR), in charge of substrate recruitment through recognition of TOR signaling (TOS) motif on target proteins (Nojima et al., 2003; Schalm et al., 2003), and mammalian lethal with Sec13 protein 8 (mLST8), required for the kinase activity of the complex (Yang et al., 2013). On the other hand, mTORC2 contains mTOR, mLST8 and rapamycin insensitive companion of mTOR (RICTOR), which has a similar role to RAPTOR (Jacinto et al., 2004; Sarbassov et al., 2004) and assists the scaffolding of the complex (Figure I-2).

mTORC1 and mTORC2 are the major sensors of external and internal cues defining the cellular metabolic status of the cell and, as a response, adjust the catabolic and anabolic routes accordingly. mTORC1 constitutes the nodal hub to which many pathways converge to signal cellular stresses as well as the availability of amino acids, oxygen and energy. In this regard, PI3K/AKT and RAS/MEK pathways are key signaling routes for the detection of external growth factors that impinge on the inhibition of Tuberous Sclerosis Complex (TSC), a key negative regulator of mTORC1 (Inoki et al., 2002; L. Ma et al., 2005; Manning et al., 2002). To do so, when TSC1/2 are inactive, the active form of Rheb (Rheb-GTP) is on the lysosomal surface to activate mTOR (Inoki, Li, et al., 2003; Tee et al., 2003). Both amino acids and growth factors are essential for mTORC1 activation. Indeed, in conditions of amino acid availability, Rag GTPases ensure that mTORC1 is recruited to the lysosomal surface to get activated by Rheb-GTP (E. Kim et al., 2008; Sancak et al., 2008). AMPK, which is activated in situations of DNA damage, hypoxia and energy deficit, is another key inhibitor of mTORC1 (Brugarolas et al., 2004; Feng et al., 2007; Gwinn et al., 2008; Inoki, Zhu, et al., 2003). On the other hand, mTORC2 upstream regulation is based on its interconnection with the PI3K/AKT pathway (Yang et al., 2015). Importantly, there is an additional regulation between mTORC1 and mTORC2. Indeed mTORC2 activates mTORC1 through AKT, however, mTORC1 indirectly inactivates mTORC2 by a negative feedback loop through the inhibition of PI3K signaling (Hsu et al., 2011; Yu et al., 2011) and insulin receptor sensor 1 (ISR1) (Um et al., 2004).

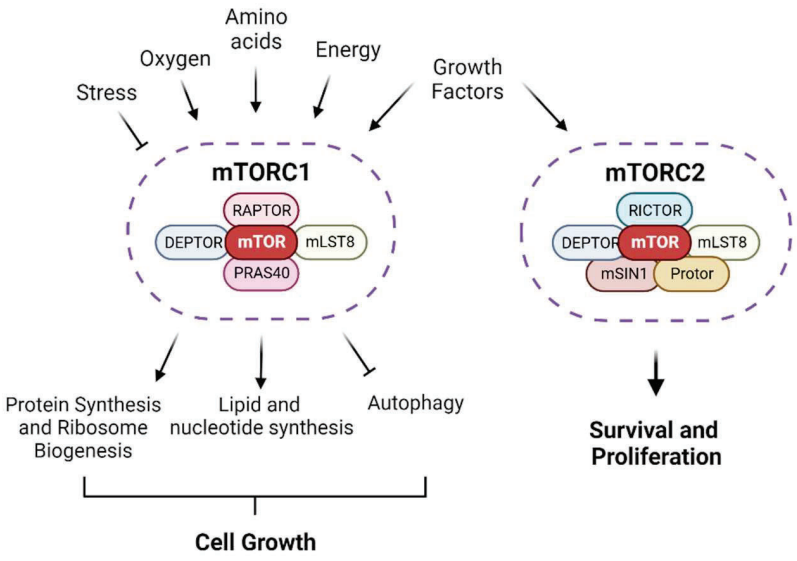

Figure I-2. mTORC1 and mTORC2. mTORC1 and mTORC2 are composed by the catalytic core, the mTOR kinase. Accessory proteins specific to each complex confer specificity to upstream and downstream signaling pathways. mTORC1 is composed by RAPTOR, mLST8 and the inhibitory subunits DEPTOR and PRAS40. mTORC2 is composed by mLST8 and RICTOR, as well as Protor 1/2, mSIN1 and the inhibitory protein DEPTOR. Together, mTORC1 and mTORC2 sense nutrient availability, energy levels, growth factors and stresses to activate or inhibit cell growth and proliferation accordingly. Figure adapted from Saxton and Sabatini, 2017 (Saxton & Sabatini, 2017).

Regarding the downstream pathways that these complexes regulate, mTORC1 sustain the global anabolism by activating lipid synthesis, energy production and particularly, protein synthesis and ribosome biogenesis. At the same time, it also inhibits catabolic pathways such as autophagy and lysosome biogenesis. mTORC2 mainly controls cell survival routes and cytoskeletal organization. Collectively, they control and promote cell growth and proliferation in response to nutrient availability, energy levels, growth factors and stresses [reviewed in (Saxton & Sabatini, 2017)] (Figure I-2).

Its central role in the cellular anabolism has turned the mTOR pathway as a promising target for anti-proliferative treatments including antibiotics, immunosuppressant or

cancer therapeutics (Mao et al., 2022). In this regard, the naturally occurring anti-fungal drug rapamycin, which allowed for the isolation of mTOR, and its subsequently developed analogs (rapalogs), are allosteric inhibitors of mTOR. However they only inhibit the activity of mTORC1, not affecting the mTORC2 activity, at least upon acute treatment. Other molecules, termed second generation mTOR inhibitors, have been developed to target both complexes, these are ATP-site competitive inhibitors of mTOR kinase and include PP242, Torin1 or INK128 (also TAK228 or MLN0128) (Garcia-Echeverria, 2011).

1.3.2 mTOR and Ribosome Biogenesis

RiBi is regulated at several stages by mTORC1 and its main effectors ribosomal S6 kinases (S6Ks) and eIF4E-binding proteins (4E-BPs). Many studies have described the role of mTOR in controlling the three RNA polymerases (Mayer & Grummt, 2006). First, mTORC1 is necessary for the synthesis of 47S pre-rRNA (Hannan et al., 2003; Mayer et al., 2004), as well as 5S rRNA and tRNA (Kantidakis et al., 2010; Shor et al., 2010), directly or by means of S6K1. In addition to this, S6Ks are required for the transcription of a number of nucleolar factors involved in RiBi (Chauvin et al., 2014). Furthermore, mTORC1 indirectly sustains RiBi through purine and pyrimidine biosynthesis that feed rRNA production (Ben-Sahra et al., 2013, 2016). Finally, mTORC2 regulates AKT, which has been described to promote rRNA synthesis cooperating with MYC (Chan et al., 2011) (Figure I-3).

On an additional layer, mTORC1 also exerts its function controlling different steps of translation initiation and elongation. On one hand, mTOR facilitates global translation through phosphorylation and inactivation of eIF4E-BP1 and 2 (4E-BPs), which in their hypophosphorylated state (mTOR inactive) sequester eIF4E, hampering the assembly of the translation initiation complex eIF4F required for CAP-dependent translational initiation (Gingras et al., 1998). On the other hand, the mTORC1 target S6K1 phosphorylates PDCD4, eIF4B and eukaryotic elongation factor 2 (eEF2) kinase (eEF2K),

that eventually promote translation at different steps (Dorrello et al., 2006; Sonenberg & Hinnebusch, 2009; X. Wang et al., 2001).

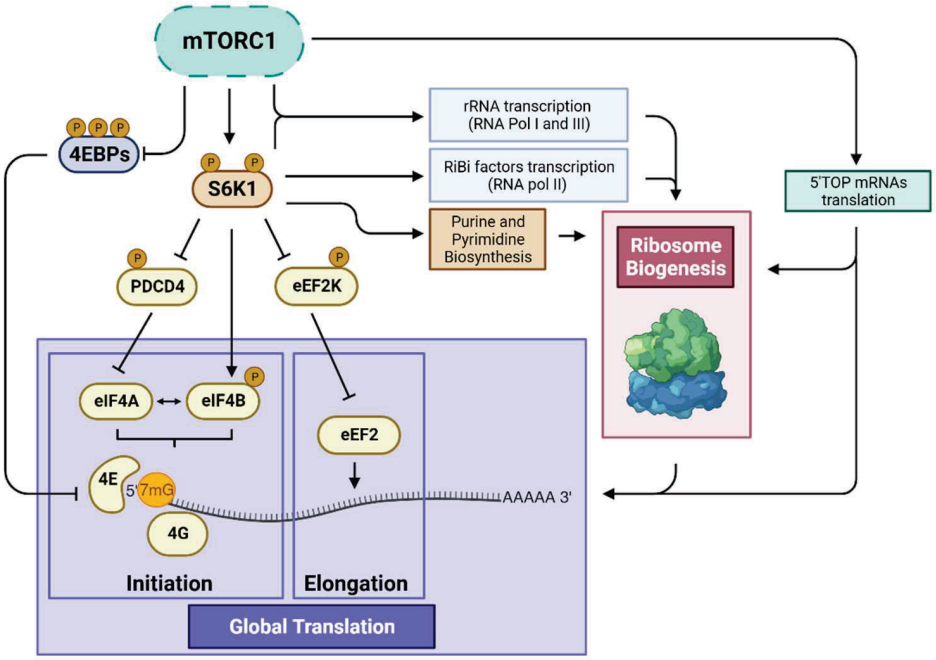

Figure I-3. mTORC1 sustains global translation and ribosome biogenesis. mTORC1 phosphorylates and activates S6K1, which in turn positively regulates mRNA translation initiation, elongation, purine and pyrimidine biosynthesis and the transcription of rDNA and nucleolar factors. mTORC1 phosphorylation on 4E-BPs relieves the inhibitory effect on translation initiation. mTORC1 activates translation of 5'TOP mRNAs that encode for ribosomal proteins, ribosome biogenesis assisting factors and translational factors, feeding ribosome biogenesis and translation. Figure adapted from Gentilella *et al.*, 2015 (Gentilella *et al.*, 2015).

In addition to these mechanisms of control of global translation, mTOR specifically regulates the translation of the family of mRNAs encoding for RPs, translational factors and other RiBi assisting factors (Hsieh et al., 2012; Jefferies et al., 1997; Meyuhas, 2000; Thoreen et al., 2012). This family is characterized by the presence of a *cis*-regulatory element at the Transcriptional Start Site (TSS) defined by a polypyrimidine tract with a Cytosine in the position +1 and termed 5' Terminal Oligopyrimidine (5'TOP) (Jefferies et

al., 1994). Regarding the mechanism involved, the stress granules associated proteins TIA-1 and TIAR were first identified as important 5'TOP mRNAs translational repressors in response to amino acid starvation (Damgaard & Lykke-Andersen, 2011). Additionally, different studies had pointed out to a specific role of 4E-BP1 and 2 in the regulation of 5'TOP mRNAs (Hsieh et al., 2012; Thoreen et al., 2012). Importantly, in the last decade, the RNA-binding protein (RBP) La Related Protein 1 (LARP1) has emerged as the key connector of mTOR signaling and the 5'TOP mRNAs translational regulation (See Introduction section 2.2) (Fonseca et al., 2015; Tcherkezian et al., 2014) (Figure I-3).

1.3.3 MYC and Ribosome Biogenesis

As extensively reviewed in Van Riggelen *et al.* (Van Riggelen et al., 2010), MYC transcription factor has been described as a multifaceted regulator of RiBi and translation. On one hand, it activates the transcription of rDNAs by RNA Pol I and RNA Pol III, facilitating the formation of pre-47S rRNA and 5S rRNA, respectively (Arabi et al., 2005; Gomez-Roman et al., 2003; Grandori et al., 2005). Moreover, it has been also described to induce the RNA Pol II-dependent transcription of genes encoding RPs and assembly factors, such as proteins required for rRNA processing and for nuclear-cytoplasmic export of ribosome components (Boon et al., 2001; Schlosser et al., 2003)(Boon et al., 2001; Schlosser et al., 2003). To further promote RiBi, MYC also intervenes in the translational process by activating the transcription of tRNA (Gomez-Roman et al., 2003) and eukaryotic translation initiation factors (eIFs) eIF4E, eIF2α, eIF4A1 and eIF4G1 (Schmidt, 2004), favoring cap-dependent translation that drives the production of the above-mentioned proteins.

1.3.4 Additional Checkpoints

Along with the control of the synthesis of RiBi factors, the cell requires other mechanisms of regulation of ribosome content and quality. A first mechanism for the maintenance of ribosome proteostasis consists in the disposal of the excess of non-incorporated RPs, as well as misfolded proteins by dedicated chaperones and the ubiquitin-proteasome system (UPS) (Kressler et al., 2017). Importantly, imbalances in

ribosomal components necessary for ribosome biogenesis can lead to the activation of a dedicated checkpoint named the Impaired Ribosome Biogenesis Checkpoint (IRBC). Upon impaired RiBi, a precursor complex formed by newly synthesized 5S rRNA, RPL5 and RPL11, instead of being incorporated into the pre-60S ribosome, is redirected to bind and inhibit HDM2, thus stabilizing p53, which in turn orchestrate a protective response leading to cell cycle arrest (Donati et al., 2013; Gentilella et al., 2017a).

1.4 Ribosome Biogenesis addicted Cancers

1.4.1 Hyperactivation of Ribosome Biogenesis

The ribosome is the ultimate effector of the protein synthetic process, which is essential for the generation of new building blocks essential for cell growth and proliferation (Lempiäinen & Shore, 2009). The hyperactivation of RiBi, and hence the protein synthetic capacity of the cell, driven by mutations in key oncogenes and tumor suppressor genes, is critical to sustain the uncontrolled cell proliferation in a number of tumor types (Pelletier et al., 2018). This ascribe a pivotal role to the above-mentioned regulators of RiBi, MYC and mTOR, in the development of tumors that depend on an aberrant RiBi rate.

Deregulation of MYC expression is a common feature of a wide range of cancers (Van Riggelen et al., 2010). Along this line, different studies have approached RiBi as a therapeutic target in MYC-driven tumorigenesis. Indeed, the benefits of RNA Pol I inhibition in restraining cancer progression have been investigated in the mice model of spontaneous lymphoma driven by MYC (Eμ-*Myc*), characterized by an exacerbated protein synthesis rate (Bywater et al., 2012). Importantly, Barna *et al.* demonstrated that restoring global translation to normal levels in Eμ-*Myc* mice by means of an heterozygous mutation in an RP gene (*Rpl24+/-*), significantly increased the disease-free survival rates, constituting one of the most determinant studies in support of the dependence of MYC-driven tumors on ribosome production (Barna et al., 2008). Recently, the activation of the IRBC and the subsequent p53-dependent apoptosis has

been proposed as the mechanism underlying the therapeutic benefits of RiBi blockade in MYC-driven lymphoma regression (Domostegui et al., 2021).

The role of mTORC1 over RiBi coordination is particularly important in cancer, given that it acts as one of the main downstream effectors of several oncogenic pathways such as Ras, PI3K, Wnt or MYC. Indeed, mTORC1 signaling is upregulated in most solid tumors (Gentilella et al., 2015; Saxton & Sabatini, 2017). Oncogenic alterations in components of the PI3K/AKT and RAS/MEK pathways, like gain of function mutations in PI3K or loss of function mutation in the tumor suppressor PTEN, usually lead to hyperactivation of mTOR (Dienstmann et al., 2014), which in turn increases global translation. Additionally, activating mutations in Wnt pathway also lead to mTOR hyperactivation via TSC2 phosphorylation. This way, inhibition of mTOR can block Wnt-induced cell growth and tumor development in mammary cancer cells *in vivo* (Inoki et al., 2006). mTOR is also downstream of TNFα pathway through TSC1, connecting inflammation, tumor angiogenesis and development (Lee et al., 2007). Finally, the liaison between MYC and mTOR and its relevance in lymphomagenesis was underscored by the finding that mTOR-dependent phosphorylation of 4E-BP1 is required for human MYC-dependent tumor initiation and maintenance (Pourdehnad et al., 2013). Accordingly, many mTOR inhibiting drugs have been approved as anti-cancer therapeutical treatments, however recurrent resistance is still an unresolved issue. In this regard, targeting RiBi could constitute a more precise strategy to attack the development of those cancers addicted to the hyperproduction of ribosomes, preventing a widespread toxicity in normal cells (Gentilella et al., 2015).

1.4.2 Qualitative dysregulations of Ribosome Biogenesis

Of note, quantitative dysregulations of RiBi have been linked to pro-tumorigenic roles, as well as qualitative changes and alterations in the RiBi process (Bustelo & Dosil, 2018). This is the case of ribosomopathies, congenital disorders characterized by an impairment in the ribosome production and function, that counterintuitively correlate with increased cancer risk (Narla & Ebert, 2010). Different categories of genetic

alterations, spanning from haploinsufficient mutations in RP genes, in rRNA or RiBi assisting factors, shape a heterogenous ribosome composition that can drive on one hand defects in translational fidelity that might generate alternative proteins. On the other hand, they create a set of specialized ribosomes that preferentially translate certain mRNAs encoding oncogenic proteins, as in the case of BCL-2 and MYC (Kampen et al., 2019; Marcel et al., 2013). These two possibilities could lead to changes in the cell proteome composition that ultimately support malignant transformation (Farley & Baserga, 2016; Genuth & Barna, 2018). Interesting examples of "onco-ribosomes" include the mutation in RPL10 (RPL10-R98S), which activates an internal ribosome entry site (IRES)-dependent translation of the anti-apoptotic protein BCL-2 mRNA, supporting T-cell leukemia progression (Kampen et al., 2019). Post-transcriptional modifications in ribosomal components can also alter the cancer translatome. This is the case of p53-inactivated cancer cells that present high levels of FLB, an rRNA-methyl transferase, leading to altered rRNA 2'-O-methylation and an increase in IRES-dependent translation of cancer genes mRNAs, like IGF1R or MYC (Marcel et al., 2013).

1.4.3 Colorectal Cancer

Among the tumor types dependent on RiBi, colorectal cancer (CRC) is one of the most characterized, also underscored by the fact that almost every step in the RiBi process presents an alteration in CRC [reviewed in (Nait Slimane et al., 2020)].

In the progressive development of sporadic colorectal cancer (sCRC), 80% of cases present initial somatic mutations in the Adenomatous Polysposis Coli (*APC*) gene, component of the Wnt signaling pathway, associated with the appearance of non-malignant small adenomas. In most cases, these mutations drive MYC overexpression by activation of its transcription by β-catenin / TCF4 (Muzny et al., 2012). Subsequently, activating mutations in *KRAS* oncogene promote the growth of the adenomas, which followed by inactivating mutations in tumor suppressor genes like *TP53*, *PTEN* or *SMAD4* leads to the development of malignant carcinomas (Figure I-4). Recent studies have related both MYC and mutated KRAS (KRASG13D) to activation of a RiBi signature in

HCT116 colorectal cancer cell lines (Charitou et al., 2019; Lafita-Navarro et al., 2018). In support of this dependence of CRC by RiBi, the first line chemotherapeutic regimen for CRC patients consisting in the combination of 5-Fluorouracil (5-FU) and oxaliplatin (FOLFOX) inhibits this process, by inhibiting the pre-rRNA processing, in the case of 5-FU, and the rDNA transcription in the case of oxaliplatin (Burger et al., 2010). Overall, these data support the use of human colorectal cancer cell lines as a model for study of ribosome biogenesis addicted cancers.

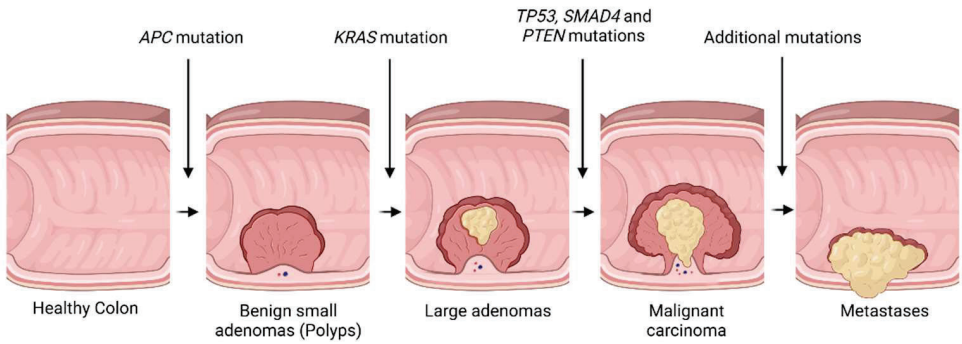

Figure I-4. Sporadic colorectal cancer progression. sCRC is initiated in 80% of cases with inactivating mutations in tumor suppressor *APC* gene that generates benign polyps. *KRAS* mutations drive adenoma growth and additional inactivating mutations in the tumor suppressor genes *TP53*, *SMAD4* or *PTEN* lead to development of malignant carcinomas. Figure created with BioRender.com.

2. LARP1 and the regulation of 5'TOP mRNAs

2.1 LARP1 structure

2.1.1 La-Related Proteins Family

LARP1 is a member of the La-Related Proteins (LARPs) family, including six more members, LARP1b, LARP3, LARP4, LARP4b, LARP6 and LARP7, and named so due to the presence of a common La-motif (LAM), original observed in the Genuine La protein (LARP3). In close proximity of the LAM, these proteins also present at least one RNA recognition motif (RRM) or an RRM-like. The LARP family is evolutionary conserved and

the different members have been linked to specific RNA regulatory functions, ranging from transcription to control of stability and translation (Bousquet-Antonelli & Deragon, 2009). Interestingly, this family has been widely studied for its role in cancer, with LARP1 the most extensively studied in oncogenesis [reviewed in (Stavraka & Blagden, 2015)]

2.1.2 LARP1 domains and structure

Over the years, studying the different domains that compose LARP1 have been defining a more precise picture of LARP1 structure and function (Figure I-5). Prediction studies against the Conserved Domain Database described that LARP1's LAM and RRM-like motifs, named the La-Module, were in the middle of the polypeptide sequence (Bousquet-Antonelli & Deragon, 2009). Another study defined in *C. elegans* a conserved RNA binding C-terminal domain, present only in the LARP1 protein and termed DM15 domain (Nykamp et al., 2008). Later studies determined the structure of the DM15 domain in human LARP1 (Lahr et al., 2015), which binds the TOP motif along with the 7-methylguanosine cap structure of the mRNA (Lahr et al., 2017; Philippe et al., 2018). Subsequently, the interaction of LARP1 with Poly-A Binding Protein (PABP) was described in *Drosophila* (Blagden et al., 2009) and confirmed in human cell lines (Burrows et al., 2010), in which the association was ascribed to the PABP Binding Motif (PAM2), within the La-module (Fonseca et al., 2015; Mattijssen et al., 2021). Different studies aiming at defining the phosphoproteome of mTORC1 discovered LARP1 as major hit (Hsu et al., 2011; Kang et al., 2021; Yu et al., 2011). Posterior studies defined the interaction between LARP1 and RAPTOR, component of the mTORC1 complex (Fonseca et al., 2015; Tcherkezian et al., 2014), through a yet not well defined motif at the C-terminus of LARP1 and in non-physiological condition of RNA depletion (RNAse treatment) (J. J. Jia et al., 2021). This discovery and the further description of LARP1 function over 5'TOP mRNAs downstream mTORC1 pathway (See Paragraph 2.2) led to seek for the phosphorylation sites of LARP1. Phospho-proteomic analysis and *in vitro* work have characterized serine and threonine amino acids spanning the adjacent region to the DM15 domain as candidate LARP1 residues that affect LARP1-RAPTOR or LARP1-5'TOP binding (Hong et al., 2017; J. J. Jia et al., 2021). Finally, our group demonstrated

that to regulate the 5'TOP mRNAs family, LARP1 must form a complex with the 40S ribosome (Gentilella et al., 2017a). Importantly, the cryo-electron microscopy density map of such interaction has been recently published, defining the ribosome binding region (RBR) of LARP1 spanning the residues between La Module and DM15 domains (Saba et al., 2023).

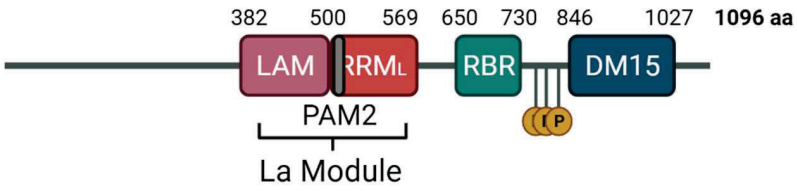

Figure I-5. LARP1 domains. LARP1 protein structure (1096 aa isoform) with the predicted domains and phosphorylation sites by mTOR. The La-Module is composed by the LAM and the RRM-like domains, common to every LARP family member. The RRM-like domain contains a PAM2 motif needed for the association with PABP protein. RBR: Ribosome Binding Region. Yellow circles: mTOR phosphorylation sites described in Hong et al., 2017 and Hsu et al., 2011 (Hong et al., 2017; Hsu et al., 2011). The DM15 domain specifically binds the 5'TOP motif at the 7-mG mRNA cap. Figure created with BioRender.com.

2.1.3 *LARP1* gene and transcripts isoforms

The human *LARP1* gene is located on chromosome 5 at position 5q33.2 and drives the transcription of nine known putative mRNA isoforms. Most of the above mentioned studies describing LARP1 protein role and domain composition are based on the 1019 amino acids (aa) sequence encoded by the LARP1 mRNA transcript variant 1 (NM_015315.5). However, a recent study has demonstrated that the majority of cancer cell lines express a longer mRNA transcript variant 2 (NM_033551.3), that generates a protein of 1096 aa (Schwenzer et al., 2021), used as reference sequence for the numbering of the amino acid residues in Figure I-5.

2.2 LARP1 and 5'TOP mRNAs

2.2.1 LARP1 translational regulation of 5'TOP mRNAs

The main function described for LARP1 relies on its RNA-binding capacity and the regulation of the family of 5'TOP mRNAs. The 5'TOP element in RPs was characterized in a set of vertebrate organisms as a *cis* regulatory motif capable to confer a translational control (Avni et al., 1994) in response to cellular signaling inputs. Indeed, pharmacological or physiological inhibition of mTOR led to a rapid downregulation of the translation of those transcripts (Jefferies et al., 1994; Meyuhas, 2000).

Regarding the intermediates between mTOR and 5'TOP mRNAs translational regulation, LARP1 emerged as the key connector a decade ago. The first study identifying an interconnection between LARP1 and 5'TOP mRNAs by Aoki *et al.*, determined that LARP1 expression correlates with the stabilization of 5'TOP mRNAs (Aoki et al., 2013). However, whether LARP1 is an activator or a repressor of 5'TOP mRNAs translation has been debated for long time, and the studies of the last decade do not reconcile it into a unifying model on how the axis mTORC1-LARP1-5'TOP mRNAs works [reviewed in (Berman et al., 2021)]. Tcherkezian *et al.* observed that LARP1 associates *in vitro* with the 7-methyl-guanosine CAP along with other factors of the preinitiation complex as a function of mTOR activity, thus suggesting that LARP1 is a positive activator of global translation. However, the evidence of a specific role in promoting 5'TOP mRNA translation are poorly tackled (Tcherkezian et al., 2014). In a posterior study in HEK293 cells, the authors observed that mTORC1 inhibition with rapamycin or Torin1 (allosteric and ATP-site mTOR inhibitors, respectively) enhanced the interaction between LARP1 and 5'TOP mRNAs, opposite to eIF4G-5'TOP mRNAs binding, suggesting that LARP1 acts as a translational repressor (Fonseca et al., 2015). Consistent with this model, *in vitro* assays showed that LARP1 outcompetes eIF4E for the binding to the CAP of 5'TOP mRNAs and that RNA immunoprecipitation assays showed that LARP1 association with the 5'TOP inversely correlate with that of eIF4G, a component of the eIF4F complex (Lahr et al., 2017).

Essential to understand these discrepancies, *in vitro* kinase assays indicated that LARP1 is a direct substrate of mTOR kinase, as well as S6K1 and AKT (Hong et al., 2017), suggesting that its phosphorylation status downstream of mTOR signaling could mediate the translational control of 5'TOP mRNAs. Indeed, in a subsequent study, the group of Thoreen showed *in vitro* that mTORC1 inhibition induced the binding of a fragment of LARP1 to a 5'TOP reporter RNAs, while decreasing its translation, supporting the model of LARP1 as an mTORC1-dependent switch of the translation of 5'TOP mRNAs (Philippe et al., 2018) (Figure I-6).

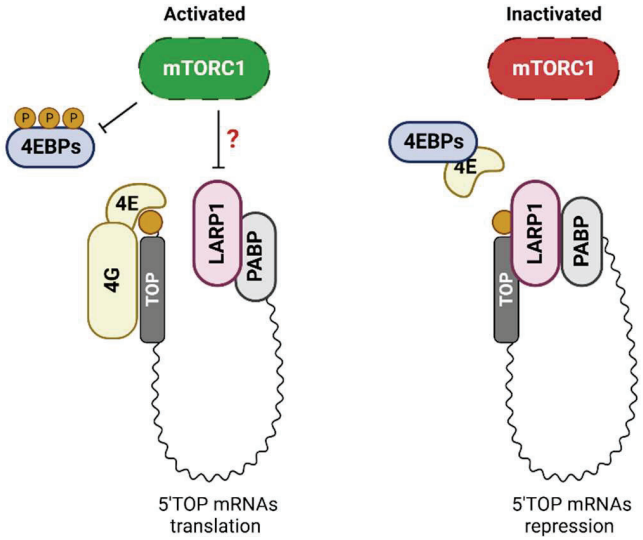

Figure I-6. Proposed model for mTORC1 / LARP1 / 5'TOP mRNAs regulation. By hyperphosphorylating 4E-BPs, mTORC1 relieves the sequestration of eIF4E to facilitate translation initiation. mTORC1 might inhibit the binding of LARP1 to the 5'TOP element by phosphorylation of amino acid residues close to the DM15 domain. mTORC1 inactivation shuts down 5'TOP mRNA translation by releasing the translational inhibitors 4E-BPs, allowing the binding of LARP1 to the 5'TOP motif adjacent to the CAP structure. Figure adapted from Philippe *et al.*, 2018 (Philippe et al., 2018).

Importantly, these studies are based on *in vitro* experiments, however, our group had tackled the role of LARP1 in 5'TOP biology in more complex cellular models with physiological mTOR signaling. In a first study, our group demonstrated that LARP1 stabilizes the 5'TOP mRNAs by forming a tripartite complex with the 40S ribosome and

that this 5'TOP stability complex is lost together with LARP1 genomic locus in 5q-syndrome (Gentilella et al., 2017a). Later, we described that such interaction was further stimulated by mTORC1 inhibition in a set of cellular systems, and that 5'TOP mRNAs stabilization and protection was essential to resume RP synthesis and ribosome production once mTOR was reactivated (See Section 2.2.2) (Fuentes et al., 2021). Additionally, a series of studies have focused on the role of LARP1 in the 5'TOP mRNA stability (Aoki et al., 2013; Mattijssen et al., 2021; Ogami et al., 2022; Park et al., 2023). Consistent with our studies, Ogami *et al.* showed a direct correlation between LARP1 expression and poly-A tail length of 5'TOP mRNAs in HEK293 cells upon mTOR inhibition (Ogami et al., 2022). Indeed, a recent *in vitro* study proposes that LARP1 complexed with PABP are essential for protection of short poly-A tail from deadenylation by the CCR4-NOT complex (Park et al., 2023). These results are essential to understand the role of LARP1 in the translational regulation of 5'TOP mRNAs, as stability and protection from degradation are crucial to enhance their translation and set a priority when the conditions are permissive and global protein synthesis is reestablished.

As described above, the majority of the studies have linked the role of LARP1 and 5'TOP mRNAs regulation downstream mTORC1 pathway. However, alternative kinases governed by other cellular regulatory pathways have been described to phosphorylate LARP1 and in the end, regulate 5'TOP biology. Importantly, the cell cycle-associated kinase CDK1 was identified as a general activator of protein synthesis, with a special effect on 5'TOP mRNAs. They found LARP1, which appears to be a putative phosphor-target of CDK1, to be main effector in the axis CDK1 in the activation of translation of 5'TOP transcripts (Haneke et al., 2020). Additionally, Wilbertz *et al.* described in HeLa cells the preference of Stress Granules (SGs) and P-Bodies (PBs) to accumulate 5'TOP mRNAs upon oxidative stress by sodium arsenite treatment in a LARP1-dependent manner (Wilbertz et al., 2019). Oxidative stress activates the integrated stress response (ISR) leading to the phosphorylation of eIF2α by one of its kinases (HRI, PKR, GCN2 and PERK) and the transcription factor ATF4 upregulation (Pakos-Zebrucka et al., 2016). Indeed, a recent study has described that GCN2 inhibits 5'TOP mRNAs translation upon

amino acid starvation through the transcriptional regulation of LARP1 by ATF4, the main effector of the ISR (Farooq et al., 2022). These set an example on how complex the regulation of LARP1 and the 5'TOP mRNAs can be as a result of the different pathways that come into play depending on the cellular status.

2.2.2 The 40S-LARP1 complex

We first described in Gentilella *et al.* the complex formed by LARP1 and the 40S small ribosome that stabilized the 5'TOP mRNAs. In this study, carried out in colorectal cancer HCT116 cells under growing conditions, our laboratory demonstrated that LARP1 was not essential for RP synthesis nor Ribosome Biogenesis. By contrary, the importance of the 40S-LARP1 complex resides on the stabilization of endogenous 5'TOP mRNAs with the non-polysomes. This effect was TOP specific as the stability of a reporter transcript carrying a mutation in the 5'TOP element was not affected by the knockdown of LARP1 or a ribosomal protein of the small subunit. Importantly, the characterization of the transcriptome bound by the 40S-LARP1 complex revealed not only the presence of the entire ribosome biogenesis and protein synthesis apparatus, but also other anabolic pathways, suggesting that the complex can influence at the translational level the metabolic output of the cells (Gentilella et al., 2017a).

In this regard, to better understand the physiological relevance of the 40S-LARP1 complex, in a second study we observed that upon unfavorable growth conditions leading to mTOR inhibition, the 5'TOP mRNAs stabilization set a priority among the rest of the transcriptome protecting the cellular anabolism at the RNA level (Fuentes et al., 2021). First, we determined that chronic mTOR inhibition by pharmacological ATP-site mTOR inhibitors or deprivation of nutrients such as serum, amino acids or oxygen, lead to the destabilization of endogenous non-TOP mRNAs while RP mRNAs were stabilized only in LARP1 expressing tumoral cells of different origin. Under these conditions of mTOR inhibition, both LARP1 protein and RP mRNAs were accumulated in the 40S and 80S fractions of a polysomal gradient. This stabilization complex was translationally inactive as puromycin treatment, a potent translational elongation inhibitor, did not

affect the formation of the complex. Importantly, we showed that the formation of the 40S-LARP1-5'TOP mRNAs complex is a protective mechanism against mRNA degradation driven by ribophagy, a process of ribosomal autophagy activated upon prolonged mTOR inhibition (Wyant et al., 2018). In this regard, the knockdown of NUFIP1, the main effector of ribophagy, restored the stabilization of total levels of 5'TOP mRNAs lost in LARP1-KO cells upon mTOR inhibition. Characterization of the transcriptome bound to the 40S-LARP1 complex by RNA-seq analysis in LARP1 expressing versus LARP1-KO cells after mTOR inhibition showed a specific stabilization in the anabolic storage of transcripts encoding RP, components of the translational machinery like initiation and elongation factors, or RiBi factors and, more interestingly, mRNAs of mitochondrial components such as the subunits composing the oxidative phosphorylation (OXPHOS) complexes. Indeed, Transcription Starting Site (TSS) analysis of the protected transcripts unveiled the 'non-pure TOP' category of mRNAs, in which OXPHOS transcripts reside and alternative isoforms can present TOP or non-TOP elements. Our study showed that LARP1 almost exclusively protects the isoforms that present a 5'TOP TSS. Finally, we demonstrated that this anabolic storage is used once the inhibition of mTOR is released to produce new protein synthetic machinery and eventually restore ribosome biogenesis and total protein synthesis, which LARP1-KO cells failed to reconstitute (Fuentes et al., 2021).

Altogether, these data propose a model in which under mTOR inhibiting conditions, the 40S-LARP1 complex protects from degradation the transcripts of key components of the protein synthetic machinery, but also other factors required for energy production. When mTOR is reactivated after the release of the stress, these mRNAs are rapidly translated to generate new ribosomes and reactivate the cellular protein synthesis and eventually, cell growth and proliferation (Figure I-7). This model explains at least in part the mechanism underlying the dual roles previously assigned to LARP1. While it can work as a translational repressor upon mTOR inhibition, it selectively preserves the 5'TOP mRNAs and the anabolic architecture of the cell, thus ascribing to the 40S-LARP1 complex an unprecedented role of guardian of cellular anabolism.

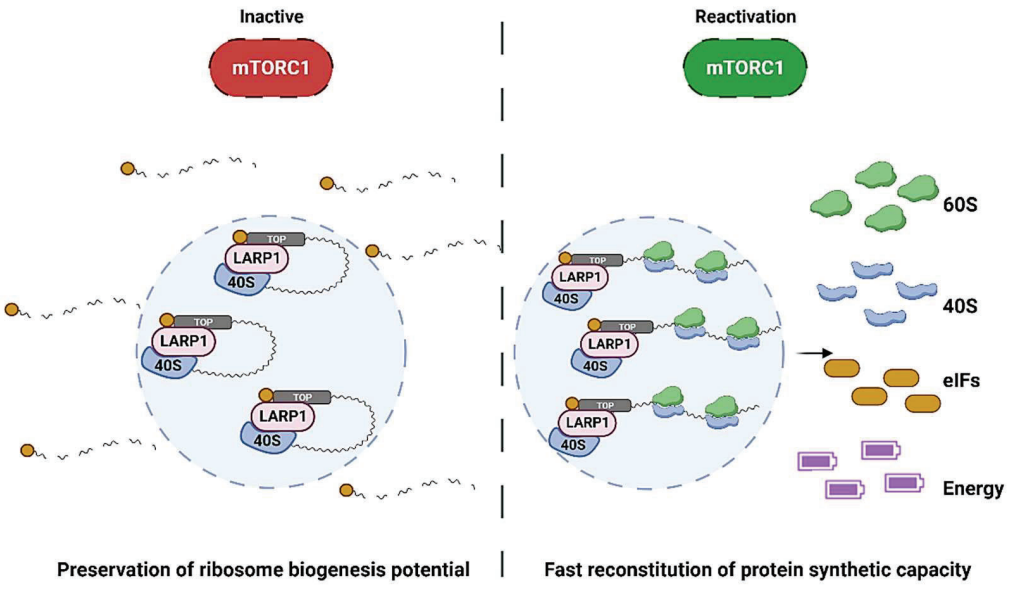

Figure I-7. 40S-LARP1 complex working model. Upon mTOR inhibition, the 40S-LARP1 complex protects the 5'TOP mRNAs from ribophagy-driven degradation, by forming an anabolic reservoir of translationally-repressed mRNAs. mTOR reactivation by an anabolic signal, reconstitutes rapidly the translation of protected 5'TOP mRNAs, reconstituting ribosome content and thus restoring protein synthetic capacity of the cell. Figure adapted from Fuentes *et al.*, 2021 (Fuentes et al., 2021).

2.3 LARP1 and cancer

Initial studies in *C. elegans* and *Drosophila* described that homozygous LARP1 deletion mutants were viable but caused slower growth rates and defects in oogenesis in the first (Nykamp et al., 2008), and embryonic development impairment and infertility in the latter (Blagden et al., 2009). In HEK293 cells, other studies have reported as well defects in cell growth caused by LARP1 effective knockdown (Tcherkezian et al., 2014), although many other tumoral and non-tumoral contexts can survive the absence of LARP1. Many studies have described LARP1 expression to correlate with cancer development in many tumor types. Overexpression of LARP1 in tumor tissue compared to counterpart normal tissues has been described for patients with hepatocellular carcinoma (HCC) (Xie et al., 2013), cervical cancer (Mura et al., 2015), prostate cancer (PCa) (Kato et al., 2015), non-small cell lung cancer (NSCLC) (Xu et al., 2017) and

colorectal cancer (CRC) (Ye et al., 2016). In these settings, the analysis showed that LARP1 was as a bad prognostic marker in patient survival (Xie et al., 2013; Xu et al., 2017; Ye et al., 2016).

Apparently, this might be contradictory with the description of LARP1 as a translational repressor of RP mRNAs, which support RiBi and therefore protein synthesis and growth. In this regard, the group of Blagden has reported in many studies the oncogenic role of LARP1 with respect to the regulation of non-TOP mRNAs. Burrows *et al.* defined in HeLa cells (cervical cancer) that LARP1 knockdown results in cell cycle arrest, apoptosis and reduction of cell migration capacity, probably due to a defect in cytoskeletal organization (Burrows et al., 2010). A subsequent study defined the mRNA interactome of LARP1, the transcripts of which were associated to cancer-related pathways such as cytoskeleton, MAPK, VEGF or the transcript of mTOR itself. Importantly, in this scenario LARP1 promotes tumor growth *in vivo* (Mura et al., 2015). By using ovarian cancer cell lines and xenografts, Hopkins *et al.* also demonstrated the importance of LARP1 in chemotherapeutical resistance, an effect accounted to the LARP1 stabilization capacity of BCL-2 mRNA and destabilization of BIK transcript, which drives apoptosis resistance (Hopkins et al., 2016). However, these evidences are still awaiting to be put in the context of LARP1 as a major interactor of PABP, hence a general indirect interactor of poly-A+ mRNAs.

With respect to the role of LARP1 in 5'TOP mRNAs regulation, cancer development and chemotherapeutical resistance, the model proposed by our group could explain the direct correlation between LARP1 expression and cancer malignancy, as the 40S-LARP1 complex could confer a metabolic advantage to cancer cells in restrained metabolic conditions. The fluctuation in mTOR inhibition is a common feature in cancer. Indeed solid tumors are characterized by local deficiency of nutrients and oxygen and many chemotherapeutical treatments also restrain mTOR activity. Based on our model, we hypothesize that the 40S-LARP1-5'TOP mRNAs complex prepares the cancer cell for a regrowth once revascularization of the tumor occurs or chemotherapy stops. This

makes the mTOR/40S-LARP1 axis an appealing therapeutic target for tumor progression and, more importantly, for tumor recurrence.

3. ILF3

3.1 ILF family: ILF2 and ILF3

3.1.1 ILF2 and ILF3 proteins

Human Interleukin enhancer-binding Factor 2 (ILF2) and Interleukin enhancer-binding Factor 3 (ILF3) proteins were originally purified as a complex that interacts with the promoter of the Interleukin 2 (*IL2*) gene (Corthésy & Kao, 1994). They are encoded by their homonymous genes, *ILF2* (chromosome 1q21.3) and *ILF3* (chromosome 19p13.2) (ncbi.nlm.nih.gov/gene). The transcriptional unit of *ILF3* generates two alternative and mutually exclusive splicing variants that encode for two proteins of 90 kDa and 110 kDa, which differ at the C-terminus (Saunders, Jurecic, et al., 2001). Across the literature, many names have been used to refer to ILF3 isoforms and ILF2. ILF3 small isoform of 90 kDa is also named Nuclear Factor 90 (NF90), Nuclear factor of activated T-cells 90 (NF-AT-90) or Nuclear factor associated with double-stranded RNA (dsRNA) 1 (NFAR-1). In accordance to this, the 110 kDa isoform has corresponding alternative names as NF110, NF-AT-110 or NFAR-2. ILF2 can be generally found in the literature as NF45 or NF-AT-45, recalling its protein size of 45 kDa.

Structurally, the N-terminal end of ILF2 and ILF3 isoforms present a common Zinc Finger-associated (DZF) domain, required for their hetero-dimerization (Wolkowicz & Cook, 2012). Additionally, ILF3 proteins count with a Nuclear Localization Signal (NLS), two dsRNA Binding Motifs (dsRBMs) in the middle of its primary sequence and an RGG motif that interacts with nucleic acids in the C-terminal region (Masuda et al., 2013). As mentioned above, the ILF3 isoforms 90 and 110 kDa have alternative C-termini, the latter presenting a specific GQSY aminoacid sequence-rich region, suggested to interfere with the dsRNA binding activity of ILF3 and to intervene in protein-protein interactions (Reichman & Mathews, 2003; Castella et al., 2014) (Figure I-8). These

structural differences can lead to alternative post-transcriptional and post-translational regulations that govern the subcellular localization of these proteins, which has been observed both in the nucleus and in the cytoplasm (Parrott et al., 2005).

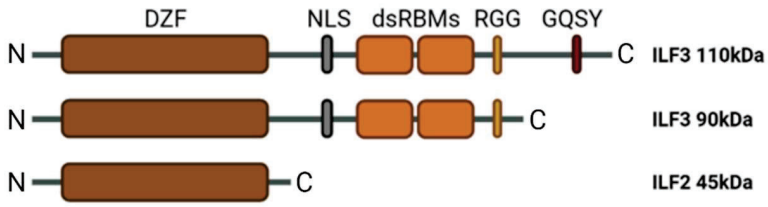

Figure I-8. ILF2 and ILF3 isoforms protein domains. DZF domain: zing-finger associated domain is required for heterodimerization of ILF2 with ILF3 isoforms. NLS: nuclear localization signal. dsRBMs: double-stranded RNA Binding Domains. RGG domain is required for nucleic acids binding. GQSY-rich domain is specific to the C-terminus of 110 kDa ILF3. N- and C- indicate amino- and carboxy- termini, respectively. Figure created with BioRender.com.

3.1.2 ILF2 and ILF3 interaction

Many studies have observed the heterodimerization of ILF2 with one of the two isoforms of ILF3 (NF45/NF90 or NF45/NF110) (Corthésy & Kao, 1994; Guan et al., 2008; Wolkowicz & Cook, 2012). Importantly, there is a post-translational co-regulation between these proteins as the formation of the heterodimers ensure their stabilization (Guan et al., 2008). When downregulating ILF3 expression, ILF2 protein gets destabilized, however when ILF2 is depleted only the 110 kDa ILF3 is affected through an unknown mechanism (Wandrey et al., 2015; G. Yan et al., 2023). Interestingly, phosphorylation of ILF3 isoforms by Protein Kinase R (PKR), also named dsRNA-dependent Protein Kinase, has been shown to reduce ILF2/ILF3 binding, resulting in the retention of ILF3 in the cytoplasm (Harashima et al., 2010). This suggests a model in which ILF3 subcellular distribution can be regulated by its partnership with ILF2, which presents a nuclear localization.

3.2 ILF3 nuclear function

ILF3 proteins are predominantly nuclear proteins localized in both nucleoplasm and nucleoli. Originally, ILF3 was described, together with ILF2, as a DNA-binding protein

that contacted the Antigen Receptor Response Element 2 (ARRE-2) at the promoter of the *IL2* gene (Corthésy & Kao, 1994); and then confirmed by Chromatin Immunoprecipitation (ChIP) in Jurkat T-cells (Shi et al., 2007). Other studies have described the *in vitro* binding capacity of 90 kDa and 110 kDa ILF3 to DNA (Satoh et al., 1999); however, no DNA-binding consensus elements have been ever identified.

Accordingly with the nuclear association of ILF2 and ILF3, the role of the ILF2/ILF3 complex has been widely studied and correlated with many nuclear processes like DNA break repair (Shamanna et al., 2011), mitotic control (Guan et al., 2008), transcription activation upon T-cell activation (Kiesler et al., 2010; H. Tsai et al., 2021) or microRNA (miRNA) biogenesis (Sakamoto et al., 2009) (Figure I-9). ChIP analysis in mouse embryonic cells was used to define the role of the ILF2/ILF3 as a transcriptional coactivator that binds the upstream enhancer and promoter region of *c-Fos* gene, for which their dsRBDs were not required (Nakadai et al., 2015). Importantly, Reichman *et al.* previously had shown that ILF3 has both activating and inhibiting roles in transcription depending on the promoter context, and suggested that this is dependent on the co-recruitment to ILF2 (Reichman et al., 2002). In line with these results, more recent data of ChIP followed by deep sequencing (ChIP-seq) have defined the transcriptional targets of ILF3 isoforms. The transcriptional functions of ILF3 include the upregulation of important transcription factors in proliferation like *MYC* and the downregulation of differentiation factors like *KLF1* (Wu et al., 2018).

However, the majority of the studies on ILF3 have been focused on its RNA binding capacity and thus, its RNA regulatory role. Regarding this, proteomic analysis of the interactome bound by ILF3 proteins identified several proteins of the heterogeneous RNP (hnRNP) family, implicated in the nuclear processing of the pre-mRNA, as well as the splicing factor PSF (Chaumet et al., 2013), suggesting a role in nuclear RNA metabolism (Figure I-9). Previous studies have also observed the interaction of ILF3 with components of the spliceosome machinery (Saunders, Perkins, et al., 2001; Zhou et al., 2002) as well as with pre-mRNA and spliced mRNA *in vitro* (Pfeifer et al., 2008).

According to the shuttling nature of ILF3 between the nucleus and the cytoplasm, different studies have underscored the role of ILF3, together with exportin-5, in the nuclear export of cargo RNA (T. Chen et al., 2004; Gwizdek et al., 2004).

Interestingly, Wandrey *et al.* have described the role of ILF2/ILF3 heterodimer in RiBi and nucleolar morphology. In this study, the authors confirmed the enrichment of ILF2 and the 90 kDa ILF3 in nucleoli of HeLa cells, and the co-precipitation of the 90 kDa isoform with the pre-60S ribosomal particles in HEK293 cells, for which the dsRBD domains are required. In these cells, depletion of either ILF2 or ILF3 by siRNA caused an impairment in RiBi, however how this occurs remains still elusive. Indeed, no alteration in rDNA transcription, rRNA maturation nor in pre-60S export have been detected (Wandrey et al., 2015). Further studies will be needed to confirm this role of ILF2/ILF3 complex and decipher the mechanism behind this defect and at what stage of the RiBi process ILF3 intervenes.

3.3 ILF3 role in translation

Deciphering the cellular role of ILF3 has been a complex task due to ILFs different isoforms and subcellular localizations. The nuclear and cytoplasmic implications of ILF3 in both DNA and RNA regulation, set a double function of ILF3 proteins, as DNA- and RNA-binding proteins (DRBPs), suggesting a role at different levels of gene expression. In this regard, many studies have tried to unravel the regulatory role of ILF3 in translation (Figure I-9).

The dsRBDs of ILF3 were first described to bind highly structured adenoviral RNAs (Liao et al., 1998). Posteriorly, it was demonstrated that phosphorylation of ILF3 by PKR after viral infection in human cells led to ILF3 association with ribosomes and inhibition of viral RNAs translation, a mechanism of host defense against viral infection (Harashima et al., 2010). Pfeifer *et al.* had previously shown that depletion of ILF3 isoforms increased poly-A RNA localization in the cytoplasm and global protein synthesis in HeLa cells (Pfeifer et al., 2008). Other studies have also evidenced the translational inhibitory role of ILF3. The group of Gorospe has established that 90 kDa ILF3 specifically binds

and represses the translation of AU-rich element (ARE)-containing mRNAs, including certain eIFs mRNAs (Kuwano et al., 2009). Of note, they also proposed that 90 kDa ILF3 governs specific translational programs by inhibiting the translation of several factors of the senescence-associated secretory phenotype (SASP) in non-senescent cells, which is reversed in senescent cells by a downregulation of ILF3 expression (Tominaga-Yamanaka et al., 2012).

On the contrary, ILF3 has been also proposed as a translational activator. Regarding the antiviral response, nuclear export of ILF3 is required for IL-2 mRNA stabilization, a step that is required to increase the levels IL-2 production after T-cell activation (Shim et al., 2002). Importantly, Watson *et al.* showed that ILF3 was able to induce the translation of antiviral cytokine IFNB1 and interferon-stimulated transcripts. In cells treated with poly(I:C), a viral dsRNA mimic, 90 kDa ILF3 remains associated with the polysomes and it is essential for the polysome association of IFNB1 transcript in a context of global protein synthesis shutdown (Watson et al., 2020). In line with these results, systematic identification of ILF3 target mRNAs by individual-nucleotide resolution CLIP (iCLIP), led to identification of several mRNAs that encode for proteins related to RNA metabolism and viral infection, the translation of which is dependent on the 90 kDa isoform of ILF3 in unstimulated HEK293 cells (Lodde et al., 2022). Taking into account the previous results, they suggest that ILF3 acts a coordinator of the antiviral response at the translational level, activating the expression of host defense mRNAs and inhibiting viral replication. Considering other physiological contexts, 90 kDa ILF3 was described to mediate the stabilization and to promote the translation of VEGF mRNA upon hypoxic conditions in human ductal adenocarcinoma cell lines (Vumbaca et al., 2008). More recently, it has been also associated with the stabilization and expression of genes encoding for the anabolic Serine-Glycine-One-Carbon (SGOC) pathway in CRC cell lines (Li et al., 2020).

These results are in concordance with a model in which ILF3 does not act as a global translational regulator, more likely acting on specific mRNAs.

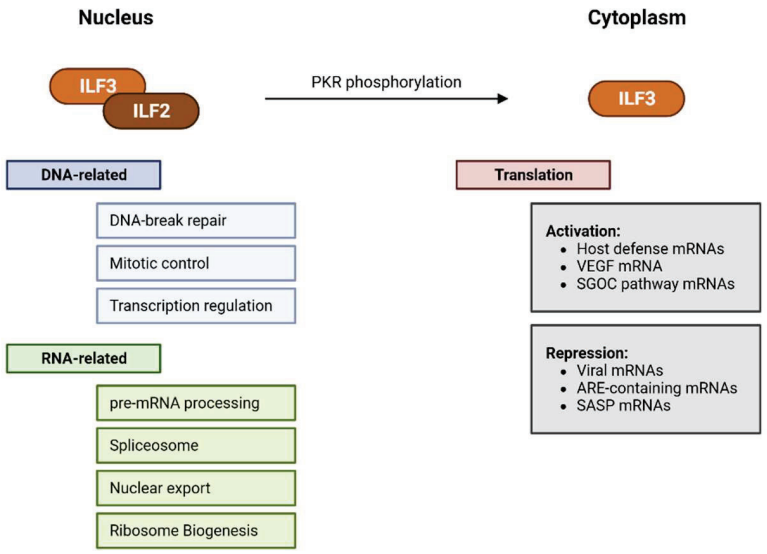

Figure I-9. ILF3 nuclear and cytoplasmic functions. ILF3 interacts with ILF2 in the nucleus and translocates to the cytoplasm after PKR phosphorylation. ILF3/ILF2 heterodimer has been associated with a number of nuclear functions. Nuclear ILF3 has been also related to RNA metabolism: pre-mRNA processing, splicing and export. Cytoplasmic ILF3 regulates positively or negatively translation of specific mRNAs and translational programs. SGOC: Serine-Glycine-One-Carbon pathway. SASP: Senesence-Associated Secretory Phenotype. Figure created with Biorender.com.

3.4 ILF3 and cancer

ILF3 proteins are involved in many cellular processes including cell cycle, immunity or differentiation, as mentioned above. Its physiological relevance is underscored by the fact that it is an essential gene required at the very first developmental stages, as the 90 kDa ILF3 -/- mice suffer from skeletal muscle weakness, respiratory failure and, eventually, perinatal death (Shi et al., 2005).

Regarding its role in pathological conditions, ILF3 has been also related to cancer progression as a result of its various regulatory functions in DNA and RNA biology. 90 kDa isoform of ILF3 was shown to be required for cervical cancer HeLa cells growth, while knockdown of 110 kDa isoform does not affect their proliferation (Guan et al., 2008). This result was contradicted years later by a study describing the role of each ILF3 isoform in several cancer contexts (R. Jia et al., 2019). Jia *et al.* showed that both

ILF3 isoforms were required for HeLa and osteosarcoma U2OS cell growth, as well as mouse embryonic fibroblasts NIH3T3 colony formation capacity. Additionally, they observed the increase in the expression of ILF3 in several tumoral tissues compared to their normal counterparts (R. Jia et al., 2019). In a breast cancer context, 90 kDa ILF3 sustains the expression of VEGF in hypoxic conditions to promote cancer growth and to induce angiogenesis *in vivo* (Vumbaca et al., 2008). *In vitro* cell growth, migration and invasion, as well as *in vivo* experiments have also correlated ILF3 expression with breast cancer development. Importantly, when comparing by immune-histochemistry (IHC) human breast cancer specimens with normal breast tissues, the aggressiveness of the tumor correlated with the nuclear, but not the cytoplasmic, expression of ILF3 (Hu et al., 2013). Moreover, in K562 erythroleukemia cells, ILF3 isoforms promote the transcription of cell growth and proliferation genes while suppressing differentiation ones, supporting a role in tumor malignancy (Wu et al., 2018). In HCC, ILF3 sustains epithelial to mesenchymal transition (EMT) by maintaining the stability of Aurora Kinase (AUKRA) mRNA and its protein expression, which plays a role in cell division (Shen et al., 2023). Finally, inhibiting the upregulation of the SGOC pathway by ILF3 with a SGOC inhibitor or by ILF3-knockdown hampered the malignant progression of CRC in patient derived organoids (PDOs) and xenografts (PDXs) (Li et al., 2020). Overall, these data confirm a pro-tumorigenic role of ILF3 in a number of tumor types.

4. Prohibitins

4.1 Prohibitins family

4.1.1 PHB1 and PHB2

Prohibitin (*PHB*), also referred to as Prohibitin 1 (*PHB1*), and Prohibitin 2 (*PHB2*) are two homologs, evolutionary conserved and ubiquitously expressed genes belonging to the prohibitins family (Tatsuta & Langer, 2017). In humans, the *PHB1* gene (chr. 17q21.33) encodes for a protein of 32 kDa, also known as BAP32. PHB2, a 37 kDa protein, can be found in the literature as BAP37 or REA and it is encoded by the *PHB2* gene (chr. 12p13.31) (ncbi.nlm.nih.gov/gene). Both PHB1 and PHB2 are also part of the SPFH

(stomatin/prohibitin/flotillin/HflKC) family of proteins that have a common SPFH domain and function as scaffolding proteins and membrane organizers (Browman et al., 2007).

Most of the studies regarding PHBs domains and structure have been carried out in yeast. Human PHB1 and PHB2 share around 50% of amino acid sequence that include the SPFH domain, also referred as PHB domain, in the middle of the protein sequence. Predictive and modeling studies have defined different N-terminal hydrophobic transmembrane domains for both prohibitins (Winter et al., 2007). In rats, the N-terminal region of PHB1 is necessary for mitochondrial import and anchor to the mitochondrial membrane (Ikonen et al., 1995). In yeast, the C-teminus of Phbs contains a coiled-coil domain, thought to be involved in the formation of multi-oligomeric complexes of Phb1/Phb2 in the mitochondrial membrane (Tatsuta et al., 2005). This domain is also conserved in human PHBs, which might have the same structural function (Winter et al., 2007). Recently, it has been described that PHB2 contains an additional LC3-interacting region (LIR) domain required to promote mitophagy upon mitochondrial depolarization in HeLa cells (Wei et al., 2017) (Figure I-10).

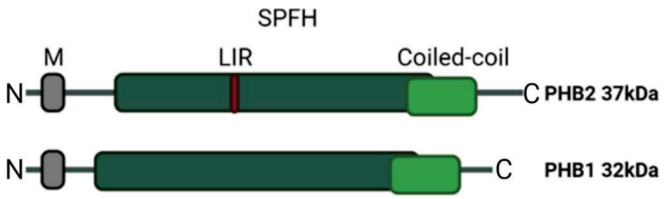

Figure I-10. PHB2 and PHB1 protein domains. M: predicted membrane binding region. SPFH domain is common to all structural proteins of the SPFH family. At the C-termini, prohibitins present a coiled-coil domain thought to be involved in the formation of multi-oligomeric complexes, the PHB complex. PHB2 presents a unique LIR motif, required for binding to LC3 autophagy protein. N- and C- indicate amino- and carboxy- termini, respectively. Figure created with BioRender.com.

4.1.2 PHB complex

PHB1 and PHB2 were originally described to form a complex binding the IgM receptor in B-lymphoma cells (Terashima et al., 1994). Posteriorly, several studies in yeast

described their mitochondrial localization in the inner mitochondrial membrane (IMM), where they assemble in a large ring complex of 1 MDa made up by multiple and alternative Phb1 and Phb2 proteins, named the PHB complex (Back et al., 2002; Nijtmans et al., 2000; Steglich et al., 1999; Tatsuta et al., 2005). Importantly, the formation of this complex stabilizes both proteins (Nijtmans et al., 2002).

4.2 PHB complex and mitochondrial functions

Prohibitins are pleiotropic proteins and their different subcellular localizations, which include the nucleus, the mitochondria and the cytoplasmic membrane, determine a wide range of cellular functions. The extra-mitochondrial roles of PHBs have been related to transcriptional functions in the nucleus and to cellular signaling cascades in the plasma membrane (Tatsuta & Langer, 2017). However, in human cells, the majority of the PHB proteins localize in the mitochondria (Osman et al., 2009), where they form a supercomplex in the IMM that include the PHB complex, the m-AAA protease subunits AFG3L2 and SPG7, the DnaJ-like chaperone DNAJC19 and IMM import translocases like TIM23, among others (Richter-Dennerlein et al., 2014). Recent studies of structural biology in bacteria have determined that the bacterial homolog of the m-AAA protease locates inside the Phbs ring complex (C. Ma et al., 2022; Qiao et al., 2022).

The functions ascribed to the PHB complex include maintenance of the mitochondrial homeostasis through regulation of mitochondrial protein synthesis and respiration, cardiolipin metabolism, mitochondrial fusion and cristae morphogenesis. It has been also related to have a role in cellular signaling in processes like mitophagy, mitochondrial unfolded protein response (mtUPR), cell proliferation and metabolic control [reviewed in (Tatsuta & Langer, 2017)] (Figure I-11).

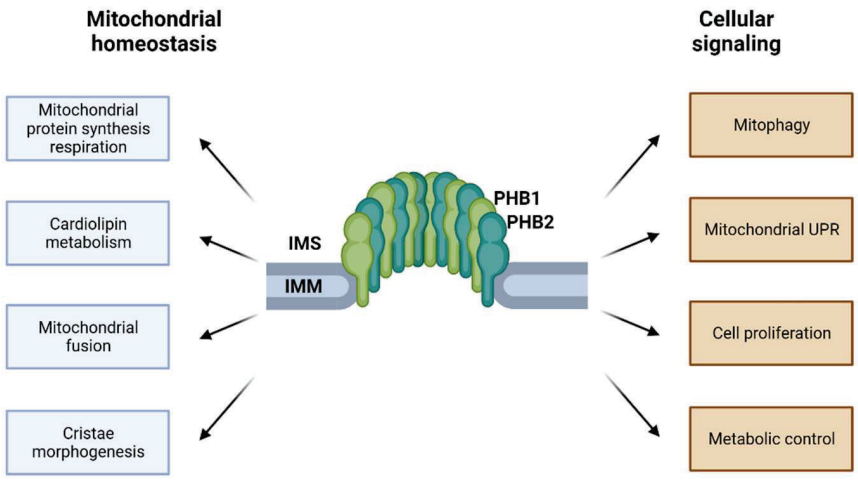

Figure I-11. PHB complex mitochondrial functions. Representation of the large ring PHB complex composed by alternating PHB1 and PHB2 proteins at the inner mitochondrial membrane (IMM). The PHB complex presents diverse roles in mitochondrial homeostasis and cellular signaling. IMS: intermembrane space. Figure adapted from Tatsuta and Langer, 2017 (Tatsuta & Langer, 2017).

4.2.1 PHB complex and mitochondrial homeostasis

Studies aiming at determining the molecular mechanisms behind the above mentioned functions have confirmed the scaffolding role of the PHB complex, although other mechanisms are emerging for mitochondrial prohibitins. Originally in yeast, the PHB complex was described to protect proteins from degradation by m-AAA protease (Steglich et al., 1999). A study carried out in mice described that PHBs protect OPA1 protein from cleavage by the metalloendopeptidase OMA1, a mechanism required for proper mitochondrial fusion. In this study, neuron specific *Phb2*-KO showed neurodegeneration and mitochondrial fragmentation, conditions that were restored to normal after *Oma1* deletion; however, physiological cristae structure and respiratory chain complex assembly were not restored (Korwitz et al., 2016). Other studies have related disturbed cristae with fatty acid metabolism and altered acylation of cardiolipin upon PHB2 knockdown in HEK293 cells (Richter-Dennerlein et al., 2014). Regarding mitochondrial synthesis of respiratory complex components, a recent publication has underscored the role of PHB/m-AAA protease complex in the maintenance of the

mitochondrial protein quality control (PQC). Kohler *et al.* has described in yeast that the PHB complex is in close proximity with the mitoribosome polypeptide exit tunnel (PTE) and determines the fate of the newly synthesized proteins to be assembled in OXPHOS complexes or to be degraded (Kohler et al., 2023).

4.2.2 PHB complex and mitochondrial signaling

Prohibitins are also key modulators of mitochondrial signaling. Their deficiency activates mitochondrial stress pathways and alters the cellular metabolic state. Importantly, PHB2 acts as a mitophagy receptor in the IMM by direct recognition of autophagosome-associated protein LC3, through a LIR domain not present in PHB1 (Wei et al., 2017). In such a way, PHB2 is essential for PINK/Parkin dependent mitophagy activation upon mitochondrial membrane depolarization or misfolded protein aggregation (Yan et al., 2020). On a different scope, PHBs have been also shown to regulate key pathways that govern global cell metabolism like mTOR and the ISR. Different studies in human cells have observed by genetic downregulation or by pharmacological inhibition with the ligand fluorizoline (FLZ) that the PHB complex sustains the mTOR pathway (Jin et al., 2020; Zhang et al., 2021). Mechanistically this might implicate the retention by PHB1 of the mTOR inhibiting protein FKBP8 in the mitochondrial membrane (Zhang et al., 2021). Another study relates the increased mobility of internal storages of Ca2+ after FLZ treatment with a decrease in global protein synthesis through two mechanisms, first, the phosphorylation of eEF2 by eEF2K, an indirect target of mTOR, and second, the phosphorylation of eIF2α (Jin et al., 2020). Regarding the latter, in HeLa cells, FLZ treatment causes the activation of the ISR through the eIF2α kinase HRI, independently from the endoplasmic reticulum stress pathway (Sánchez-Vera et al., 2023). However, how direct is the effect of the mitochondrial PHB complex over mTOR or the translational machinery is not clear yet and might be due to an indirect effect of the structural and functional mitochondrial defects caused by the deficiency of prohibitins.

4.3 Prohibitins role in nucleus and plasma membrane

Prohibitins have been also described in the nucleus or the plasma membrane with apparently different roles from the ones described in the mitochondria. However, these alternative functions seem to be specific to certain cell lines and may variate depending on the tissue and the pathophysiological context.

4.3.1 Prohibitins and nuclear functions

There are many evidence of the interaction of PHB1 with the transcription factors E2F1 and Rb *in vitro* and in human cells, interaction that leads to the inhibition of E2F-mediated transcriptional activation (S. Wang, Nath, Adlam, et al., 1999; S. Wang, Nath, Fusaro, et al., 1999). This effect appears to be indirect through the recruitment by PHB1 of the histone deacetylase HDAC1 to the target gene promoters in breast cancer and B-cell lymphoma cells (S. Wang et al., 2002). Additionally, other studies have described that PHB1 interacts and enhances the transcriptional activity of p53. Importantly, the authors show the predominant nuclear localization of PHB1 in breast cancer cells, which moves to the cytoplasm and partially to the mitochondria upon apoptotic stimulation (Fusaro et al., 2003). Moreover, PHB2 was observed to interact *in vitro* with the nuclear estrogen receptor α (ERα) transcription factor (Montano et al., 1999) and inhibit its transcriptional activity by recruitment of deacetylases, including HDAC1, in breast cancer cell lines (Kurtev et al., 2004).

4.3.2 Prohibitins at the cellular plasma membrane

The expression of PHB1 and PHB2 in the cell surface has been observed in activated T-cells (Yurugi et al., 2012) and intestinal epithelial cells after infection with a specific antigen of *Salmonella typhi* (Sharma & Qadri, 2004). Interestingly, Rajalingman *et al.* has described the interaction of PHB1 with C-RAF and the co-localization of both in the plasma membrane of HeLa cells. In this study, PHB1 depletion ablates C-RAF localization to the cell membrane and therefore its activation by Ras upon growth stimulation, underscoring an important role of PHB1 in the RAS-RAF-MEK-ERK pathway (Rajalingam et al., 2005).

Notably, the studies discerning the extra-mitochondrial roles of prohibitins focus on the individual free proteins, but do not address a potential function of the multimeric PHB complex. Moreover, given the prevalent localization of prohibitins in the mitochondria and their essential role in mitochondria homeostasis, it is difficult to dissect the nuclear and plasma membrane roles from the mitochondrial ones, which might be interconnected.

4.4 Prohibitins and cancer

4.4.1 Prohibitins expression in Cancer

Prohibitins are involved in many cancer-related processes that include tumor growth, cancer cell migration, resistance to chemotherapeutics and metastases (Yang et al., 2018). Overexpression of PHB1 has been related to cancer progression and malignancy in different tumor types that include cervical adenocarcinoma (Tsai et al., 2006), prostate adenocarcinoma (Ummanni et al., 2008), esophageal squamous cell carcinoma (Ren et al., 2010), non-small cell lung cancer (Yurugi et al., 2017) and pancreatic cancer (Zhong et al., 2015). PHB2 expression is higher in HCC samples compared to normal tissue, and it has been reported to promote HCC cell lines growth (Cheng et al., 2014). Particularly, PHB1 and PHB2 subcellular relocalization is an important hallmark in tumor development. Comparison of normal breast cells to breast cancer cells shows a significant redistribution of cellular PHB1 to the nucleus (Y. W. Chen et al., 2011). Paradoxically, sequestration of PHB2 in the cytosol by BIG3, releasing the transcriptional inhibitory effect of PHB2, enhances ERα transcriptional activity, which drives breast cancer proliferation and metastases (J. W. Kim et al., 2009). In CRC cells, intra-mitochondrial PHB1 relocates to the plasma membrane, which in turn promotes cell migration upon VEGF stimulation. This polarized expression of PHB1 correlates with poor prognosis and metastases in CRC patient samples (L.-L. Ma et al., 2017). The role of PHB1 in cell adhesion and migration had been previously described in cervical cancer HeLa cells (Rajalingam et al., 2005).

Of note, PHBs have determinant roles in resistance to chemotherapeutic regimens. Patel *et al.* have observed that PHB1 redistributes to the plasma membrane in lung adenocarcinoma A549 cells resistant to paclitaxel. In these cells, silencing of PHB1 rescues the sensitivity towards paclitaxel by activation of the intrinsic apoptosis pathway (Patel et al., 2010). Other groups have reported the role of PHB1 in resistance to staurosporine treatment in ovarian cancer cells by blocking the cell cycle in G0/G1 phase and, eventually, protecting them from apoptosis (Gregory-Bass et al., 2008). Additionally, knockdown of PHB2 in HCC cells causes an impairment in cell viability upon hypoxic conditions and chemotherapeutic treatment (Cheng et al., 2014).

4.4.2 Targeting Prohibitins in Cancer

The previous data suggest that PHBs are determinant biomarkers in cancer progression as well as interesting targets for cancer therapy, especially in drug-resistant tumors. Indeed, a number of anti-tumoral molecules have been developed to target the PHB complex, including the flavagline FL3 (Thuaud et al., 2013). The efficiency of the inhibitor FL3 has been largely proved in different tumor types. FL3 has been shown to be effective against intestinal tumorigenesis by inhibiting the Wnt/β-catenin pathway through the translocation of PHB1 to the nucleus and activation of the transcription of Axin1 (Jackson et al., 2020). A recent report has described a novel mode of action of FL3 in chronic lymphocytic leukemia (CLL) by means of disrupting the interaction of PHB with components of the translation initiation complex eIF4F, interaction that mediates the translation of MYC transcript. This study proposes for the first time an interplay of the PHB complex with components of the translational apparatus, as well as the regulation of a specific translational program by these mitochondrial proteins (Largeot et al., 2023). Fluorizoline (FLZ) was discovered as a potent inducer of apoptosis in several tumor types that targets the PHB complex (Pérez-Perarnau et al., 2014). The mechanism of action over the PHB complex at the IMM remains to be fully elucidated. However, it has been established that it activates the mitochondrial apoptotic pathway (Moncunill-Massaguer et al., 2015).To sum up, there are plenty of evidences that point out to prohibitins as promising targets in cancer therapy.

RATIONALE OF THE STUDY AND OBJECTIVES

Our group has defined that LARP1 forms a complex with the 40S ribosome to stabilize the 5'TOP mRNAs and that this complex is sensitive to mTOR pathway, whose inhibition triggers the formation of 40S-LARP1-5'TOPs complex in a translationally-repressed state. Importantly, in a cancer cell context, the 40S-LARP1-5'TOPs acts as an anabolic storage upon restrained metabolic conditions characterized by mTOR inhibition such as treatment with pharmacological inhibitors or by amino acid or serum deprivation. This reservoir of anabolic capacity can be rapidly spent by the cells to generate new ribosomes when conditions return permissive (Fuentes et al., 2021; Gentilella et al., 2017a). In other words, the presence of the TOP element confers to the transcripts a specific sensitivity to the cellular metabolic status, thus positioning the RiBi and protein synthesis translational program at the top of the translatome hierarchy. Altogether, this suggests that the mTOR / 40S-LARP1 axis could constitute a mechanism of metabolic resistance to adverse growth conditions, which might have important implications in the process of tumorigenesis and in the treatment of cancers addicted to ribosome biogenesis.

Understanding how mTOR modulates, via LARP1, the protection and translational repression of 5'TOP mRNAs, and what other molecular players are involved in this regulation would provide more mechanistic insights on how the 40S-LARP1 complex works. In this regard, the large number of functions attributed to LARP1 could depend on the nature of the interacting proteins, the composition of protein complexes and their subcellular localization. Based on that, the first objective of my doctoral project is to identify the protein constituents of the 40S-LARP1 complex, in normal growing conditions and upon mTOR inhibiting stimuli that boost the formation of this anabolic reservoir (AIM 1).

Subcellular reorganization of RNPs is a general mechanism to shape the cellular architecture and reprogram mRNA metabolism (Lécuyer et al., 2007; Panas et al., 2016). Therefore, we hypothesized that the subcellular localization of this anabolic storage would unravel unexpected metabolic compartments that the 40S-LARP1 complex might be physically assisting in both normal growing condition and under stimuli mimicking nutrient restrictions. Leaning on the 40S-LARP1 interactome defined in AIM 1, we aimed to address whether the mTOR / LARP1 axis might control the localization of this anabolic storage to specific subcellular districts. To this end, the second objective is to characterize the subcellular distribution of LARP1 and to study the dynamics of its redistribution upon mTOR inhibiting stimuli (AIM 2).

The differential composition of the protein components of an RNP complex can determine the mRNAs translational status and their subcellular localization, as well as the recognition of different RNA motifs (Baltz et al., 2012; Street et al., 2023). This premise suggests that the different partners of the 40S-LARP1 complex might confer specificity for different transcripts and/or subcellular locations. Once the 40S-LARP1 interactors were defined, we aimed to describe new regulators of 5'TOP mRNAs and to study their role in the biochemical complex formation. This will potentially lead to the identification of new targets involved in RiBi-addicted tumors. Therefore, the third objective of my doctoral thesis is to define the role of the 40S-LARP1 interactors in the regulation of 5'TOP mRNAs and in themodulation of ribosome activity (AIM 3).

OBJECTIVES:

1. To identify the protein constituents of the 40S-LARP1 complex, in normal growing conditions and upon mTOR inhibiting stimuli that boost the formation of this anabolic reservoir.

2. To characterize the subcellular distribution of LARP1 and to study the dynamics of its redistribution upon mTOR inhibiting stimuli.

3. To define the role of 40S-LARP1 interactors in the regulation of 5'TOP mRNAs, the formation of the complex and in protein synthesis.

METHODOLOGY

Cell Culture

HCT116 human colorectal carcinoma and HEK293FT human embryonic kidney cell lines were obtained from the American Type Culture Collection (ATCC). HCT116 LARP1-KO cell line was previously generated as described in (Fuentes et al., 2021). Cells were cultured in Dulbecco's modified Eagle's medium (DMEM) supplemented with 10% heat-inactivated fetal bovine serum (Sigma-Aldrich).

Reagents and Plasmids

mTOR ATP-site inhibitor TAK228 (also named Sapanisertib, INK128 or MLN0128) was purchased from MedChemExpress (Cat. #HY-13328) and dissolved in DMSO. Sodium Arsenite was purchased from Sigma (Cat. #S7400) and was dissolved in water. ISRIB (Sigma, Cat. #SML0843) was provided by the group of Dr. Joan Gil and prepared in DMSO. Doxycycline (Dox), cyclohexamide (CHX) and puromycin were purchased from Sigma (Cat. #D9891; #C7698; #P8833) and dissolved in DMSO, ethanol and water, respectively. Protease inhibitor cocktail, phosphatase inhibitor cocktails II and III were purchased from MedChemExpress (Cat. #HY-K0010; #HY-K0022; #HY-K0023). Nonidet P-40 (NP40), Triton X-100 and sodium deoxycholate monohidrate were purchased from Sigma-Aldrich (Cat. #74385; #93443; #30970). RNAse inhibitor was purchased from New England Biotechnologies (NEB; Cat. #M0307). Silencing RNAs (siRNAs) were transfected with Lipofectamine™ RNAiMAX (Thermo Scientific, Cat. #13778150). Plasmids were transfected with FuGENE® Transfection Reagent (Promega, Cat. # E2311).

Plasmid pX330 and plasmid pX458 were obtained from Addgene (Cat. #42230 and #48138) and TA Cloning™ Kit pCR2.1-TOPO from Invitrogen (Cat. # K202020) and modified as described below in CRISPR/Cas9 section. TetON pLVX-TetOne Vector (Takara, Cat. #631846), TetO-WT-L32TOP-β-Globin-MS2(12X) and TetO-MUT-L32TOP-

β-Globin-MS2(12X) (L32WT and L32MUT, respectively) were generated previously in the lab (Gentilella et al., 2017a).

CRISPR/Cas9-mediated generation of LARP1-GFP HCT116 cell lines

HCT116 cells expressing the endogenous LARP1 protein fused to a Green Fluorescent Protein (GFP) were generated by CRISPR/Cas9-based genomic editing. As depicted in Figure R-1A, in order to insert the GFP at the C-terminus of the LARP1 protein, we designed:

(1) A target-specific single guide RNA (sgRNA) directed against the boundary of the coding sequence (CDS) and 3' untranslated region (3'UTR) of *LARP1* gene (Table M-3).

(2) The targeting or donor construct, including the CDS of the enhanced GFP (eGFP) fused in frame with the last codon of LARP1 and flanked by two homology arms of ~1Kbp upstream and downstream of the sgRNA targeting region to replace by homologous recombination the locus targeted by the Cas9 cleavage (Table M-3).

$3x10^5$ parental HCT116 cells were co-transfected using FuGENE Transfection Reagent with 1.5ug of the pX330 plasmid, carrying the Cas9 coding sequence and the sgRNA, and 1.5ug of the linearized targeting plasmid, pCR2.1-TOPO carrying the donor construct. One week after transfection, GFP positive cells were selected by Fluorescent Activated Cell Sorting (FACS, BD FACSAria, BD Biosciences) and single cells were cultured to generate stable monoclonal cell lines. Subsequently, clones were analyzed for LARP1-GFP expression by western blot.

CRISPR/Cas9-mediated generation of ILF3-KO HCT116 cell lines

$3x10^5$ parental HCT116 cells were co-transfected using FuGENE Transfection Reagent with 4ug of the pX458 plasmid, carrying the Cas9 coding sequence fused to GFP and two alternative sgRNA designed to target the Exons 3 and 4 of ILF3, in order to efficiently knock-out the expression of ILF3 90 kDa and 110 kDa (Table M-3). Two days after

transfection, GFP positive cells were selected by Fluorescent Activated Cell Sorting (FACS, BD FACSAria, BD Biosciences) and single cells were cultured to generate stable monoclonal cell lines. Subsequently, clones were analyzed for ILF3 expression by western blot.

Protein Analysis

Cell protein extracts for Western blot analysis were prepared by using RIPA lysis buffer [150mM NaCl, 50mM Tris (pH 7.4), 1mM EDTA, 1% NP-40] supplemented with the protease inhibitor cocktail and phosphatase inhibitor cocktail II. Cells were incubated for lysis 10' on ice followed by centrifugation at 13,000 rpm for 10'. Protein concentrations were determined for supernatants by the BCA assay (Pierce). Twenty-five micrograms of total protein extracts was resuspended in Laemmli SDS sample buffer (LB 1X) and boiled at 95°C for 10 min. Proteins were separated on 10% SDS–polyacrylamide gels by electrophoresis or pre-cast gradient 4-20% SDS–polyacrylamide gels (Invitrogen) and transferred to polyvinylidene difluoride (PVDF) membranes (GE Healthcare Life Science). Blots were stained with amido black to confirm equal loading and transfer of proteins and then reacted with the Western blots probed with the indicated antibodies (Table M-1). Immunoblots were developed using secondary horseradish peroxidase–coupled antibodies and an enhanced chemiluminescence kit (GE Healthcare).

RNA analysis

Total cellular RNAs were isolated using TRIzol reagent (Invitrogen) according to the manufacturer's instructions. 1ug of total RNA was treated with DNaseI (NEB) to remove DNA and reverse transcription was performed using random hexamers (IDT) and M-MLV (Invitrogen). Diluted cDNA samples (1:20-1:40) were analyzed by real time quantitative PCR (RT-qPCR) using LightCycler® 480 SYBR Green I Master mix (Roche) or PrimeTime master mix (IDT). For SYBR detection, pairs of primers were used at 0.8nM final concentration and for PrimeTime detection, RNA-specific hydrolysis probes were used

at 0.125 nM and primer pairs at 0.5 nM (Table M-2). For the luciferase normalization, cells were harvested in an equal volume of cold phosphate-buffered saline (PBS), and 1/10 of the cell suspension was assayed for genomic DNA (gDNA) concentration, which we verified reflecting the cell number in the culturing conditions tested. The remaining volume of cells was centrifuged, and cell pellet was resuspended in TRIzol and spiked with an amount of Firefly Luciferase mRNA (Promega, L456A), proportional to the gDNA content, according to the ratio, 0.025 ng of Firefly mRNA per microgram of gDNA. The levels of the indicated genes were normalized to luciferase mRNA.

Polysome Profile Analysis

Distribution of mRNAs across sucrose gradients was performed as described earlier (Fumagalli et al., 2009), except for minor modifications. Briefly, $3x10^6$ HCT116 cells were plated in 100mm dish or 6 $x10^6$ cells in 150mm dish and transfected with the indicated treatment. CHX was added to the medium at 37°C for 5 min at a concentration of 100 µg/ml. Cells were washed twice with cold PBS supplemented with CHX, scraped on ice, and pelleted by centrifugation at 3000 rpm for 3' in cold. Cell pellets were resuspended in 250 µl of hypotonic lysis buffer [1.5 mM KCl, 2.5 mM MgCl2, 5 mM tris HCl (pH 7.4), 1 mM dithiothreitol (DTT), 1% sodium deoxycholate, 1% Triton X-100, and CHX (100 µg/ml)] supplemented with protease inhibitors, phosphatase inhibitors 2 and RNase inhibitor at a concentration of 100 U/ml and left in ice for 10'. Cell lysates were cleared of debris and nuclei by centrifugation for 5' at 13,000 rpm. Protein concentrations were determined by BCA assay, and equal amount of polysomal lysate (500 to 1000 µg, depending on the experiment) was loaded on 10 to 50% sucrose linear gradients generated with a BIOCOMP gradient master and containing 80 mM NaCl, 5 mM MgCl2, 20 mM tris HCl (pH 7.4), 1 mM DTT, and RNase inhibitor (10 U/ml). Gradients were centrifuged on a SW40Ti rotor for 2 hours and 55 min at 35,000 rpm. Gradients were analyzed on a BIOCOMP gradient station and collected in 13 fractions ranging from light to heavy sucrose.

For protein analysis, fractions were supplemented with SDS at a final concentration of 1% and placed for 10 min at 65°C. Protein extraction was performed by methanol-chloroform precipitation. Protein pellets were resuspended in 20ul of LB 1X and western blot analysis was performed as described above.

For RNA analysis, fractions were supplemented with SDS at a final concentration of 1% and placed for 10 min at 65°C. To each fraction was added 1 ng of firefly luciferase mRNA, followed by phenol-chloroform extraction (Ambion) and precipitation with isopropanol. Purified RNAs from each fraction were reverse-transcribed and subjected to qPCR as described above. mRNA quantification was normalized to firefly mRNA.

All sucrose gradient fractionations have been repeated at least twice in independent experiments. The profiles and RT-qPCR analyses shown in the figures are representative experiments.

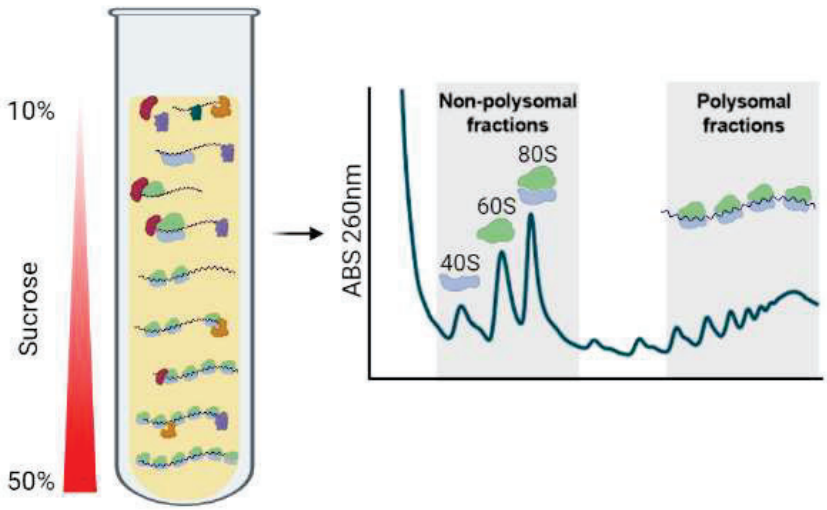

Figure M-1. Schematic representation of polysome profiling. (Left) Separation of ribonucleoprotein complexes is carried out in sucrose gradients (10-50%) by molecular weight based on the presence of ribosomes. (Right) Representation of a profile given by the RNA measure along the sucrose gradient.

Immunoprecipitation from sucrose gradients

Sucrose gradient fractions obtained as above described were pooled in non-polysomal or polysomal samples and diluted 1:2 with the same sucrose gradient buffer [80 mM NaCl, 5 mM MgCl2, 20 mM tris HCl (pH 7.4), Triton X-100 0.1%] supplemented with, 1 mM DTT, 100µg/ml CHX, RNase inhibitor (10 U/ml), 4x concentrated protease inhibitors and phosphatase inhibitors. Samples were incubated overnight at 4ºC with 50ul GFP-Trap Dynabeads (ChromTek) or Protein G Dynabeads™ (Invitrogen). Beads were washed three times with NT2 buffer [50mMTris pH7.4, 150 mM NaCl, 5 mM MgCl2, 0.1% Triton X-100] (Keene et al., 2006) and two additional washes with NT2 buffer without detergent. Half of the beads were used for protein analysis by western blot and resuspended in LB 1X. The other half was sent for protein sequencing by LC/MS-MS.

RNA-Immunoprecipitation from whole cell lysates

RNA-IP (RIP) was performed as described in (Keene et al., 2006) except for some modifications. HCT116 LARP1-GFP and LARP1-KO were plated in 150-mm dishes at $6x10^6$ cells. 24 hours later, cells were collected for t0h or treated with 250nM TAK228 for additional 24h. HEK293FT were plated in 100-mm dishes at $2.5x10^6$ cells and transfected with 2ug TetON plasmid + 2ug L32WT or L32MUT reporters using FuGENE Transfection Reagent and treated with the indicated treatments. Cells were then lysed for 10' on ice with hypotonic lysis buffer [1.5 mM KCl, 2.5 mM MgCl2, 5 mM tris HCl (pH 7.4), 1 mM dithiothreitol (DTT), 1% sodium deoxycholate, 1% Triton X-100, and CHX (100 µg/ml)] supplemented with mammalian protease inhibitors, phosphatase inhibitors and RNase inhibitor. Cell lysates were centrifuged and cleared from debris, and anti-ILF3 or normal rabbit serum IgG loaded MagnaChIP Beads (Invitrogen) were added to 500 µg of total cell extract. Samples were incubated overnight at 4ºC. Beads were washed three times with NT2 buffer [50mMTris pH7.4, 150 mM NaCl, 5 mM MgCl2, 0.1% Triton X-100]. Half of the immunoprecipitated complex was used for protein analysis and resuspended in LB 1X. The other half of the immunocomplexes isolated were first supplemented with 4ng of firefly luciferase mRNA, then processed for RNA extraction

and RT-qPCR as described above. Firefly luciferase served to normalize samples. Data is reported as anti-ILF3-immunoprecipitated mRNA subtracted from normal rabbit serum precipitated material.

Functional screening

$3x10^5$ HCT116 parental cells were transfected with the indicated siRNA (Table M-5) using Lipofectamine RNAiMax, treated with TAK228 the following day and collected after 24h. Protein and RNA analysis were performed as described above.

Protein synthetic capacity

$3x10^5$ HCT116 LARP1-GFP cells were transfected with the indicated siRNA (Table M-5) using Lipofectamine RNAiMax, treated with TAK228 the following day and collected after 24h. ISRIB was added at the same time to the siRNA and maintained during 48h. For puromycylation, culture media was supplemented with puromycin at a concentration of 1µg/ml for 30 min and then collected in cold PBS supplemented with CHX. For negative control, prior to puromycin, CHX was added to the medium for 5 min at a concentration of 100 µg/ml.

Liquid Chromatography/ Mass Spectrometry (LC/MS-MS)

Proteomic analysis was performed by UPF/CRG Proteomics Facility. IP samples were digested and then analyzed by LC/MS-MS in the Orbitrap Lumos. Samples were searched against the SwissProt human database (2021/01), using the search algorithm Mascot v2.6 (http://www.matrixscience.com/). Peptides with an FDR≤0.05 have been retained. Protein-protein interactions were scored by Significance Analysis of INTeractome (SAINT) software package to remove nonspecific interactions (Choi et al., 2011).

Protein Interactome Analysis

Gene Ontology analysis of proteins with an FDR≤0.05 was performed with DAVID (Database for Annotation, Visualization and Integrated Discovery) bioinformatics database (https://david.ncifcrf.gov).

Heatmap analysis indicating relative abundance of selected proteins from the interactome was performed with RStudio v4.1.1 (2021). Values were obtained from the Fold Enrichment scores generated by SAINT analysis for each detected protein relative to the negative control of immunoprecipitation. Normalization was performed within each protein in a range from 0 to 1, meaning 0 = no presence, 1 = maximal presence.

Network Analysis was performed with the STRING resource (https://string-db.org/). Functional and physical protein associations were considered from all the active interaction sources available (textmining, experiments, databases, co-expression, neighborhood, gene fusion and co-ocurrence). Line thickness indicates confidence, the strength of the data support. *k-means* clustering was performed on the generated network.

Immunofluorescence and imaging

HCT116 LARP1-GFP cells were seed in 10mm glass coverslips in 6 multi-well dishes at $2x10^5$. The following day cells were treated with the indicated treatments. In order to label mitochondria, MitoTracker™ Deep Red FM (Invitrogen, Cat #M46753) was used for 60min at 2X concentration. Cells were fixed with 4% PFA for 10min at room temperature, then washed with PBS supplemented with 25mM glycine and permeabilized with 0.1% Triton X-100 for 10min. For protein detection, cells were blocked with 1% bovine serum alumin (BSA) and 0.01% Triton X-100 in washing solution for 1 hour and then, incubated with the indicated antibodies (Table M-1) for 2h at room temperature. After three washes, cells were incubated with the appropriate secondary antibodies for 1 hour at room temperature, washed three times and then mounted with VECTASHIELD® antifade with DAPI (Vector Laboratories). Images were captured with

Zeiss Confocal Microscope LSM880. Images were processed with ImageJ software and co-localization analysis was performed with Intensity Correlation Analysis (ICA) plugin (Li et al., 2004) to determine cell by cell Manders Coefficient. Mander Coefficient defines the intensity of the co-localizing signal per pixel normalized by the total intensity of the signal in all pixels.

$$M_{red} = \frac{\sum_i R_{i,coloc}}{\sum_i R_i} \qquad M_{green} = \frac{\sum_i G_{i,coloc}}{\sum_i G_i}$$

$R_{i,coloc} = Ri$ if $Gi > 0$; $G_{i,coloc} = Gi$ if $Ri > 0$.
i.e. M_{red} is the sum of the intensities of red pixels that have a green component divided by the total sum of red intensities.

Figure M-2. Formula for calculation of Manders Coefficents 1 (M1) and 2 (M2).

Statistical Analysis

Data was analyzed by GraphPad Prism v8.0.2 software. Results are presented as Mean ± SD, for n=3 number of experiments despite indicated otherwise. Experimental data sets were compared by two-sampled, two-tailed Student's t-test for two data sets with normal distribution and equal variance. For multiple comparisons, sets were analyzed by 2-way ANOVA, Tukey's multiple comparison test with individual variances computed for each comparison.

Statistical significance was considered for p-values below 0.05: * p value < 0.05; ** p value < 0.01; *** p value < 0.001; **** p value < 0.0001. P-values above 0.05 were considered not statistically significant: ns = p value > 0.05

Table M-1. List of antibodies

Antibody	Host	Application	Source	Identifier
ATF4	Rabbit	WB 1:1000	CST	11815
GFP	Rabbit	WB 1:2500	Abcam	ab290
ILF3	Rabbit	WB 1:2500	Proteintech	19887-1-AP
LARP1	Rabbit	WB 1:1000	Bethyl	A302-087A-M
PABP	Rabbit	WB 1:1000	Abcam	ab21060
PHB1	Mouse	WB 1:1000	Santa Cruz	sc-377037
PHB1	Rabbit	WB 1:2500	Abcam	ab75766
PHB2	Rabbit	WB 1:1000	Abcam	ab182139
Puromycin	Mouse	WB 1:1500	Merck	MABE343
RPL5	Rabbit	WB 1:1000	Bethyl	A303-933A
RPS23	Mouse	WB 1:1000	Santa Cruz	sc-100837
RPS6	Mouse	WB 1:1000	Santa Cruz	sc-74459
p-4EBP1 (S65)	Rabbit	WB 1:1000	CST	#9451
p-eEF2 (T56)	Rabbit	WB 1:1000	CST	#2331
p-eIF2α (S51)	Rabbit	WB 1:1000	CST	#9721
p-RPS6 (S235/236)	Rabbit	WB 1:1000	CST	#2211
p-S6K (T389)	Rabbit	WB 1:1000	CST	#9205
Rabbit-HRP	Swine	WB 1:2500	Dako	P0399
Mouse-HRP	Rabbit	WB 1:2500	Dako	P0260
TrueBlot® Rabbit-HRP	Mouse	WB IP 1:2500	eBioscience	18-8816-33
TrueBlot® Mouse-HRP	Rat	WB IP 1:2500	eBioscience	18-8817-33
ILF3	Rabbit	IP 2ug/sample	Proteintech	19887-1-AP
PHB1	Rabbit	IP 2ug/sample	Abcam	ab75766
PHB2	Rabbit	IP 2ug/sample	Abcam	ab182139
Normal Rabbit Serum	Rabbit	IP 2ug/sample	CST	#2729
CANX	Mouse	IF 1:400	Santa Cruz	sc-23954
G3BP1	Mouse	IF 1:150	Santa Cruz	sc- 365338
GFP	Rabbit	IF 1:300	Abcam	ab290
TOM20	Mouse	IF 1:400	Santa Cruz	sc-17764
Rabbit-AlexaFluor™ 488	Donkey	IF 1:400	Invitrogen	A31572
Rabbit-AlexaFluor™ 555	Goat	IF 1:400	Invitrogen	A11001

Table M-2. List of oligonucleotides for RT-qPCR

Oligo	Sequence 5'-3'	Use
RPL5_Fw	GGTGTGAAGGTTGGCCTGAC	Primer
RPL5_Rv	GGCACCTGGCTGACCATCAA	Primer
RPL5_Pr	**56-FAM**/CTGGCCCGCAGGCT TCTCAATAGGTTT/**3IABkFQ**	Probe
RPL11_Fw	TCCACTGCACAGTTCGAGGG	Primer
RPL11_Rv	AAACCTGGCCTACCCAGCAC	Primer
RPL11_Pr	**56-FAM**/TATGACCCAAGCATT GGTATCTACGGCCT/**3IABkFQ**	Probe
RPS6_Fw	TCTTGACCCATGGCCGTGTC	Primer
RPS6_Rv	GCGGCGAGGCACTGTAGTAT	Primer
RPS6_Pr	**56-FAM**/CCTGTTACAGACCA AGGAGAACTGGAG/**3IABkFQ**	Probe
β-Actin_Fw	CAGGTCCAGACGCAGGATGGC	Primer
β-Actin_Rv	CTACAATGAGCTGCGTGTGGC	Primer
β-Actin_Pr	**5TexRd-XN**/CACAGCCTGGATAG CAACGTACATGG/**3IAbRQSp**	Probe
HBB_Fw	GTGAGAACTTCAGGCTCCTGG	Primer
HBB_Rv	ACCAGCCACCACTTTCTGATAG	Primer
HBB_Pr	**56-FAM**/ TGGTCTGTGTGCT GGCCCATCACTTT/**3IABkFQ**	Probe
Luciferase_Fw	ACAGATGCACATATCGAGGTG	Primer
Luciferase_Rv	GATTTGTATTCAGCCCATATCG	Primer
Luciferase_Pr	**5Cy5**/GGAATACTTCGAAA TGTCCGTTCGGTTGG/**3IAbRQSp**	Probe

Table M-3. List of oligonucleotides for CRISPR/Cas9

Oligo	Sequence 5'-3'
sgLARP1_Fw	CACCGAGTGAAAAGCTCCTTAGCCC
sgLARP1_Rv	AAACGGGCTAAGGAGCTTTTCACTC
LARP1_LeftArm_Fw	AACCCTTATGTGGTGACGCAGAC

LARP1_LeftArm_Rv	TGGTCTCACTTTCCCAAA GTCTGTGTGTTCGAGT
LARP1_RightArm_Fw	AGGTCTCTTGAAAAGCTCCTTA GCCCTGCGGCTTGAGGGGGGAA
LARP1_RightArm_Rv	AGATTCCCGCTCCACAATAAGGC
sgILF3_Ex3_Fw	CACCGTAACATGGATGTGCCCCCAG
sgILF3_Ex3_Rv	AAACCTGGGGGCACATCCATGTTAC
sgILF3_Ex4_Fw	CACCGCACATGACCAGAACCCTGCG
sgILF3_Ex4_Rv	AAACCGCAGGGTTCTGGTCATGTGC

Table M-4. List of siRNA

Oligo	Sequence 5'-3'
siLARP1 #1	GAATGGAGATGAGGATTGC
siLARP1 #2	GCGCCAGATTGAATACTACTTC
siABCF2 #1	CCTTGCATCTACAATAATCTA
siABCF2 #2	CGTTATGGCCTCATTGGTTTA
siATAD3A #1	CATCAATGAGATGGTCCACTT
siATAD3A #2	CATAGCAACAAGGAACACCAA
siILF3 #1	CCTTCCAAGATGCCCAAGAAA
siILF3 #2	CCAGAGGACGACAGTAAAGAA
siPHB #1	GCTGCCGTCCATCACAACTGA
siPHB #2	GAGTTCACAGAAGCGGTGGAA
siPLEC #1	GCACCAGTCCATCGAAGAATT
siPLEC #2	CGATGAGGAGATGAACGAGAT
siPRPF6 #1	GCGTACTTCGAGAAGAACCAT
siPRPF6 #2	CATTCCTACAGACCGACATAT
siSTAU1 #1	CCUAUAACUACAACAUGAG
siSTAU1 #2	GGAGGUGAAUGGAAGAGAAUC

RESULTS

1. Generation and characterization of the LARP1-GFP HCT116 cell line

1.1 Design and generation by CRISPR/Cas9 of a stable LARP1-GFP HCT116 cell line

Previously, our group described a specific subtype of 40S small ribosomal subunits defined by the presence of LARP1, that binds and stabilizes the 5'TOP mRNAs family (Gentilella et al., 2017a). This 40S-LARP1 complex was initially isolated by immunoprecipitation of LARP1 protein in the fraction containing the native 40S ribosome obtained by sucrose gradient ultracentrifugation. In order to characterize the protein constituents that are part of this ribonucleoprotein (RNP) complex, we aimed to improve the isolation of LARP1 immunocomplexes with the required yield and purity for Liquid Chromatography/ Mass Spectrometry (LC/MS) analysis. To this end, the colorectal cancer HCT116 cell line was genetically modified by CRISPR/Cas9 mediated homology-directed repair to express the endogenous LARP1 protein fused to a GFP tag at the C-terminus. For that, we edited the *LARP1* gene in the last coding exon so that all isoforms generated by the LARP1 genomic locus were fused to the GFP tag (Figure R-1A). After co-transfection with sgRNA - Cas9 and the targeting plasmids, single cells showing positivity for GFP signal (GFP+) were selected and isolated by FACS to generate monoclonal cell lines. These isogenic cell lines were screened by western blot to determine the stable expression of LARP1-GFP fusion protein (Figure R-1B). Most of the cell lines showed an efficient knock-in, as indicated by the increase in LARP1 molecular weight of ~30 kDa, which corresponds to the eGFP molecular weight, for both LARP1 canonical isoforms of 170 and 130 kDa. Moreover, same lysates probed against a GFP antibody showed an overlapping signal to LARP1 only on those with an increase in the molecular weight. The disappearance of the 170 and 130 kDa untagged LARP1 canonical protein isoforms, which initially could suggest a diploid knock-in targeting, could be

explained by the fact that HCT116 cells have a hemizygote expression of LARP1 protein due to a frameshift mutation in one of the two *LARP1* alleles (depmap.org/portal). Same clones were live imaged to verify the cellular distribution of the GFP signal in positive clones, which confirmed the cytoplasmic localization of LARP1 previously described by multiple studies (Burrows et al., 2010; Hong et al., 2017) (Figure R-1C).

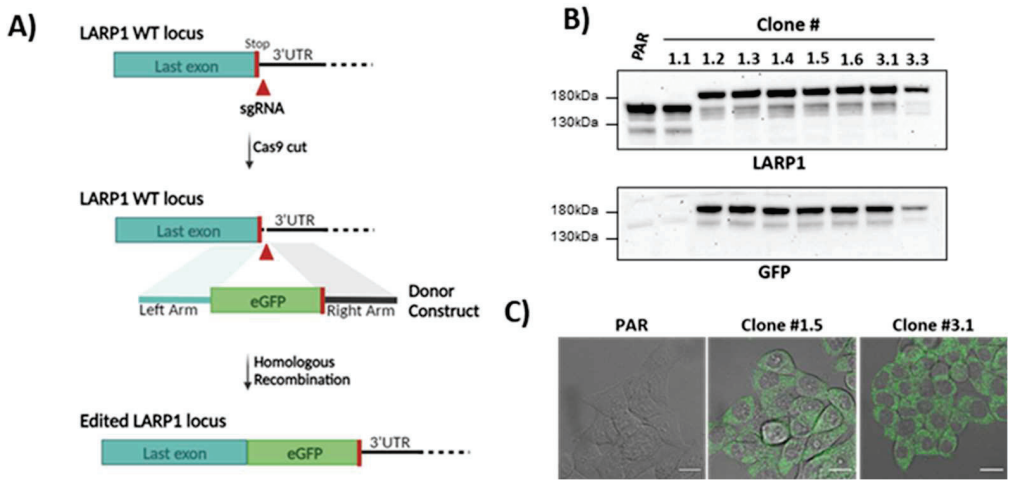

Figure R-1. Generation by CRISPR/Cas9 of stable LARP1-GFP HCT116 cell lines. **(A)** Schematic representation of the strategy followed to generate the LARP1-GFP cells by CRISPR/Cas9. sgRNA was designed to introduce a double-strand break downstream the stop codon of *LARP1* locus. Targeting construct included two homology arms of 1kb flanking the eGFP CDS, to introduce the *GFP* gene by homologous recombination. **(B)** Western blot of same amount of cellular lysates from different clones, as well as HCT116 parental (PAR) cells as a control, blotted against LARP1 and GFP. (C) Images taken by confocal microscopy of live HCT116 PAR cells and two LARP1-GFP positive clones by western blot. Superimposition of bright field and GFP (488nm) signal. Scale bar: 15µm.

1.2 Biochemical characterization of a LARP1-GFP HCT116 cell line

Once determined the stable expression of LARP1-GFP in these clones, one of them, the #3.1 – hereafter named LARP1-GFP, was selected for a further validation of its capacity to recapitulate the molecular features of the untagged endogenous LARP1. With respect to the ability of LARP1-GFP to complex with the 40S ribosome and sense the mTOR inhibition to induce the formation of the 40S-LARP1 complex (Gentilella et al., 2017a),

the clone was subjected to polysome profiling in normal growing condition or upon treatment with TAK228, an ATP-site inhibitor of mTOR kinase (Figure R-2). One of the advantages of utilizing an endogenous LARP1-GFP cell model also relies on the fact that the co-sedimentation of LARP1 with the ribosomes can be monitored by measuring at the same time the rRNA distribution (by RNA absorbance at 260nm) and the GFP signal (488nm). The rRNA and GFP profiles in Figure R-2A show that in normal growing conditions, LARP1-GFP distributes in the 40S-containing fractions, the 40S and 80S non-

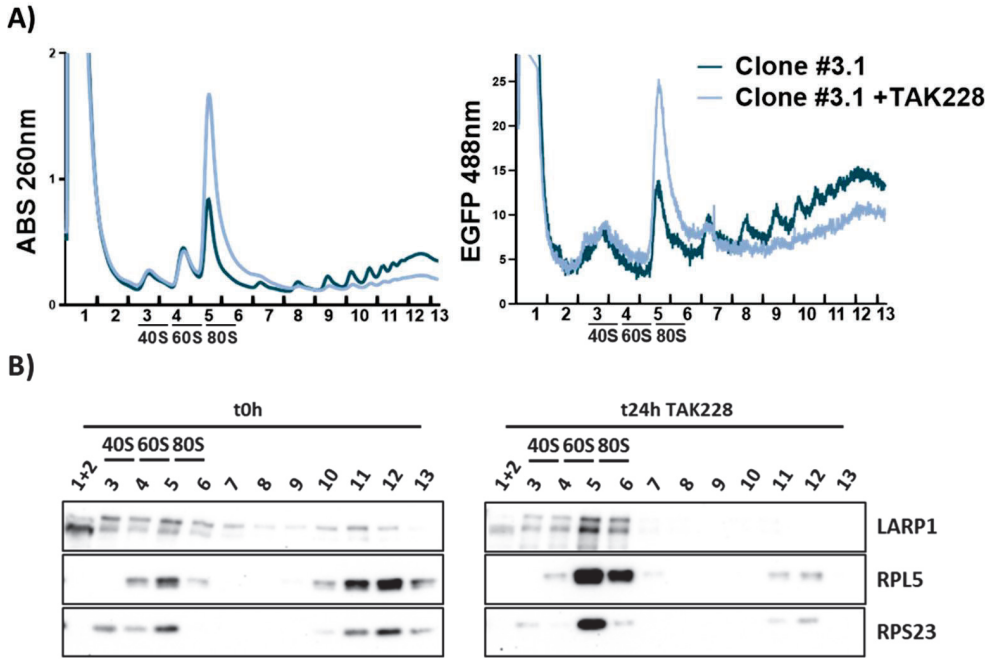

Figure R-2. LARP1-GFP fusion protein complexes with the 40S ribosome upon mTOR inhibition. Cell lysates from LARP1-GFP positive clone #3.1 collected before (t0h) and after 24 hours (t24h) of treatment with mTOR inhibitor TAK228 were subjected to polysome profiling by ultracentrifugation on a 10%-50% sucrose gradients. **(A)** (Left panel) Graphical representation of the rRNA distribution profile according to the molecular weight. Left to right: free ribosomal subunits (40S and 60S), monosomes (80S) and poly(ribo)somes. (Right panel) Profile of GFP signal distribution across the same sucrose gradient. **(B)** Same gradients were collected in 13 fractions, which were subjected to western blot against the indicated proteins. RPL5 (large 60S subunit) and RPS23 (small 40S subunit) were blotted as control of fractionation and protein precipitation.

polysomal, as well as on polysomes. The absence of GFP signal in the 60S portion of the gradient is in line with our previous findings confirming that LARP1 is a 40S interacting protein. Upon mTOR inhibition, the fusion protein was re-directed to the non-polysomal fractions, almost disappearing from the higher polysomes, as we had previously demonstrated for the untagged LARP1 (Gentilella et al., 2017a). Western blot analysis of the fractions derived from the same samples and hybridized with an anti-LARP1 antibody corroborated that the GFP signal profiling parallels LARP1 protein, as they both showed the same distribution (Figure R-2B).

With respect to the the ability of LARP1-GFP to stabilize and protect 5'TOP mRNAs upon mTOR inhibition (Fuentes et al., 2021), we measured total levels of 5'TOP (RPS6) and non-TOP (β-actin) transcripts in normal growing conditions or upon TAK228 treatment comparing HCT116 parental and LARP1-GFP knock-in cells (Figure R-3). As expected, LARP1-GFP expressing cells phenocopied the parental cells in terms of stabilization of RPS6 mRNA levels and destabilization of a non-TOP mRNA upon mTOR inhibition.

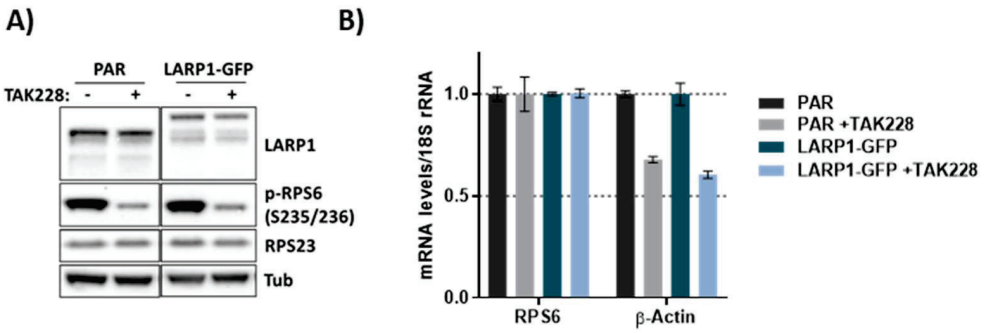

Figure R-3. LARP1-GFP cells stabilize TOP mRNAs upon mTOR inhibition. HCT116 PAR and LARP1-GFP cells (Clone #3.1) were cultured in normal growing conditions or after treatment with TAK228 for 24 hours. **(A)** Cell lysates were subjected to western blot against the indicated proteins. p-RPS6 was used as proxy of the mTOR signaling after TAK228 treatment. α-Tubulin was used as loading control. **(B)** RNA analysis by RT-qPCR of total levels of RPS6 and β-actin transcripts normalized by 18S rRNA and the normal growing condition set to 1.

1.3 Isolation of 40S-LARP1 immunocomplexes from sucrose gradients

After validation of the LARP1-GFP cell line generated, we set-up the isolation of the 40S-LARP1 complexes directly from sucrose gradient fractions in order to differentiate the composition of its protein interactome depending on the translational status. To do so, we ran a polysome profile and pooled the fractions corresponding to non-polysomal (40S-60S-80S fractions), considered as non-translating ribosomes, or polysomal fractions (10-13), as actively translating ribosomes (Figure R-4A). The immunoprecipitation with anti-GFP antibody showed the specific isolation of LARP-GFP protein with a high yield of enrichment, as indicated by the level of LARP1-GFP remaining in the post-IP unbound fraction (NB) (Figure R-4B). The co-IP efficiency was confirmed by the presence of known interactors such as ribosomal proteins of the small subunit, RPS6 and RPS23, the large subunit, RPL5, and the Poly-A Binding Protein (PABP) (Tcherkezian et al., 2014).

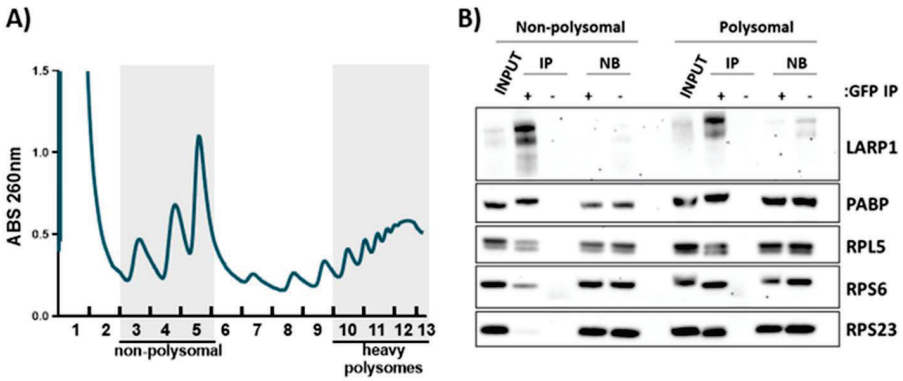

Figure R-4. 40S-LARP1 Immunoprecipitation from sucrose gradient fractions. Cell lysate from HCT116 LARP1-GFP cells cultured in normal growing conditions was subjected to polysome profiling. **(A)** Graphical representation of the profile corresponding to the RNA engaged with the different free ribosomal subunits, monosomes and polysomes. Non-polysomal fractions (40S-60S-80S) and heavy polysomes (10-13) were pooled. **(B)** Pools of non-polysomal and heavy polysomal fractions were subjected to immunoprecipitation with GFP-Trap Dynabeads and the result was resolved in a SDS-PAGE gel for western blot analysis. INPUT samples correspond to a 10% of the IP material. NB corresponds to a 10% of Non-Bound proteins.

2. The 40S-LARP1 Interactome

2.1 Experimental design

The biological function of LARP1 on 5'TOP mRNA has been largely controversial and molecular and biochemical findings have defined different abilities in terms of translational control and stability of 5'TOP mRNAs [Reviewed in (Berman et al., 2021)]. Even though many studies have described that LARP1 represses the translation of 5'TOP mRNAs (Fonseca et al., 2015; Lahr et al., 2017), LARP1 presence in the polysomal fractions (Figure R-2) opens the question of whether it might have a wider role in 5'TOP mRNAs biology. According to this, our group has shown that the knockdown of LARP1 in normal growing condition only affects the stability of 5'TOP mRNAs associated with non-polysomes while maintaining unaltered the translation of the polysomal associate (Gentilella et al., 2017a). In addition, it has been proposed that the phosphorylation status of LARP1, controlled by the mTOR pathway, determines its ability to inhibit the binding of eIF4E and cap-dependent translation of 5'TOP mRNAs (Fonseca et al., 2015; Jia et al., 2021; Philippe et al., 2018); which would be indeed accompanied by the clearance of LARP1 from the actively translating fractions (Figure R-2). However, these conclusions are based on *in vitro* studies and in absence of 40S ribosome, for which a verification in a more complex biological model is needed. In order to shed light on this matter and understand how mTOR modulates protection and translational repression of 5'TOP mRNAs, we decided to characterize the protein interactome of the 40S-LARP1 complex upon mTOR active or inactive biological contexts, as well as from non-polysomal (translationally inactive) or polysomal (translationally active) sucrose fractions.

We studied the interactome upon different mTOR inhibiting (TORi) conditions that included the pharmacological TAK228 treatment and the serum starvation (SS) as a biological approach that mimics a physiological mTOR inhibition. As observed in Figure R-5A, 24h of deprivation of serum had similar effects as TAK228 treatment in terms of global inhibition of translation, as indicated by the decrease of polysomes (left panel),

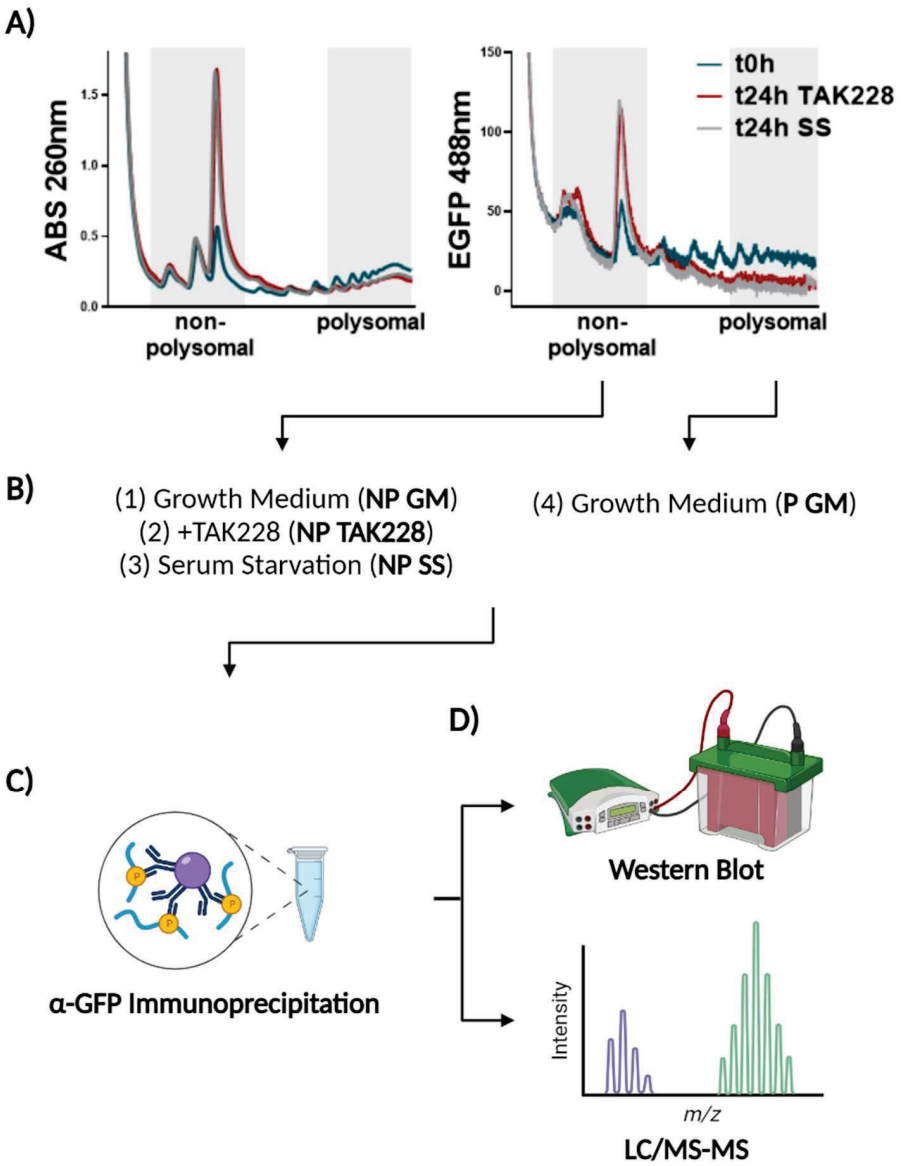

Figure R-5. Schematic representation of the IP – MS experimental workflow. (A) HCT116 LARP1-GFP cells were cultured in growth media (GM), treated with pharmacological mTORi (TAK228) or biological mTORi with serum deprivation (SS) and subjected to polysome profiling. Graphical representation of (Left panel) RNA content or (Right panel) LARP1 distribution followed by GFP signal along the sucrose gradient. **(B, C)** 40S - LARP1-GFP immunocomplexes were obtained from the indicated fractions pools by IP with anti-GFP conjugated beads (GFP-Trap Dynabeads). **(D)** Half of the sample volume was kept for Western blot analysis and half was sent for protein sequencing by LC/MS-MS.

but also with respect to the induction of the 40S-LARP1 complex formation, as seen by GFP signal accumulation in 40S-containing non-polysomal fractions (right panel). Finally, immunoprecipitation was carried out in triplicates of the samples corresponding to complexes from (1) non-polysomal fractions under normal growing conditions, (2) non-polysomal fractions following 24h treatment with TAK228, (3) non-polysomal fractions after 24h of serum starvation and (4) polysomal fractions under normal growing conditions (Figure R-5B,C). Half of the samples were utilized for protein identification by Liquid Chromatography coupled to Tandem Mass Spectrometry (LC/MS-MS) and half were analyzed by western blot (Figure R-5D; Supp. Figure S-1).

2.2 Proteomic analysis of 40S-LARP1 Interactome

The LC/MS-MS results were evaluated using SAINT (Significance Analysis of INTeractome) analysis in order to identify *bona fide* interactors, defined by a SAINT score ≥ 0.67, corresponding to a False Discovery Rate (FDR) ≤ 0.05. Almost 700 proteins were detected to interact, directly or indirectly, with LARP1, being 206 common to all experimental conditions tested (Figure R-6A). Categorization of biological processes by Gene Ontology (GO) showed that the shared proteome corresponded mainly to components of the translational machinery, including almost all ribosomal proteins, factors related to RNA processing and more surprisingly, intermediate filament organization elements (Figure R-6B). Next, we observed a high overlap in the composition of RNP complexes in the three non-polysomal conditions tested, independently of mTOR status. These were enriched in biological processes like nuclear RNA export, ribosome quality control or mitochondrial protein synthesis (Figure R-6B). Unexpectedly, we found that the polysomal 40S-LARP1 complexes were specifically constituted by players involved in stress granules (SGs) condensation, like the key axis composed by G3BPs, CAPRIN1 and USP10 (Kedersha et al., 2016). Overall, these data imply that the 40S-LARP1 complex is likely to participate to a diversity of processes involving RNA regulation and translation, but also suggest uncharacterized implications in subcellular movement and association with the mitochondria.

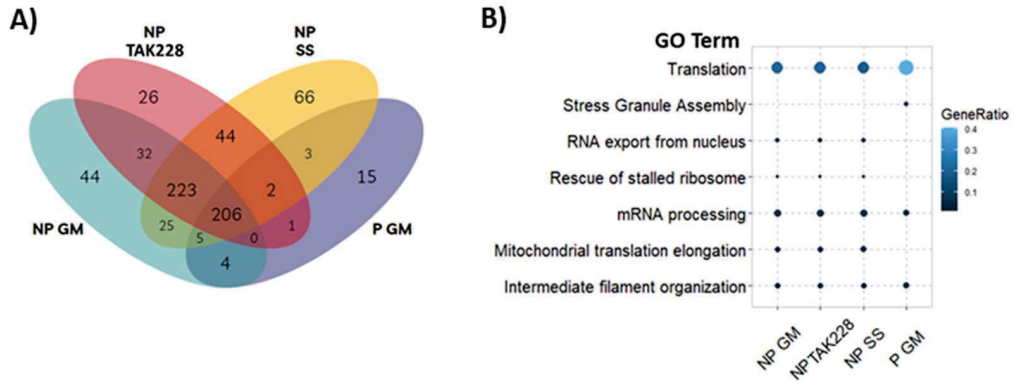

Figure R-6. 40S-LARP1 Interactome. SAINT analysis was performed from three biological replicates of immunoprecipitated 40S-LARP1 complexes under the conditions indicated in Figure R-5 to determine *bona fide* protein interactors. **(A)** Venn Diagram representation of the number of proteins (FDR≤0.05) defined for each condition. **(B)** Examples of enriched Gene Ontology Biological Processes categories are shown for each condition. Presence was scored as the gene ratio for each condition.

2.3 Selection of 40S-LARP1 interacting proteins

From the previous results, we generated a list of interactors that could potentially have a specific role in the formation of the 40S-LARP1 complex and the regulation of 5'TOP mRNAs biology (Figure R-7). To this end, we scored the proteins based on their presence, specificity and biological relevance.

First, to confirm a high probability of interaction we discarded those proteins detected by a low number of spectral counts in all the conditions, despite their high significance in terms of SAINT score. Secondly, to have an appreciation of which interactors are unique partners of the 40S-LARP1 complex, we compared our results to the global ribo-interactome described in Simsek *et al.* (Simsek et al., 2017), in which the ribosome associated proteins were identified by immunoprecipitation of a 40S or a 60S ribosomal protein. We looked for proteins that were not shared in both studies, in order to discern those interactors specific for the 40S ribosomes bound to LARP1 and not constitutive components of the translational machinery, although shared proteins were not discarded if they were considered good candidates based on other aspects.

In addition, we positively scored those partners that together are part of a specific complex, as it denotes selectivity for those networks. For instance, the CCR4-NOT complex, involved in RNA deadenylation (Collart & Panasenko, 2012); the PHB complex, related to mitochondrial function and morphology (Osman et al., 2009); the ASC-1 complex, required for ribosome quality control (Juszkiewicz et al., 2020); the heteroligomerization of ITPR components in the ER membrane (Foskett et al., 2007); or the ERLIN complex implicated in the ER-associated degradation (ERAD) pathway (Pearce et al., 2009) (Figure R-7).

Next, we gave high priority to those proteins that showed a differential enrichment among the analyzed experimental conditions, which could imply a selective role on 5'TOP mRNAs regulation or on other unidentified translational programs in which the 40S-LARP1 complex comes into play, in response to mTOR inhibition. As an example, as depicted in Figure R-7, the CNOT elements belonging to the CCR4-NOT complex, were exclusively present in polysomes associated with LARP1. Interestingly, other proteins like ILF3 and PDCD4 were enriched with the non-polysomes upon mTOR inhibition, paralleling LARP1 accumulation. In contrast, ATAD3 factors, among others, were prevalently found in non-polysomes under growing conditions.

Finally, with the aim of understanding new mechanisms underlying the relevance of the 40S-LARP1 complex in cancer biology, we considered interactors with described roles in tumorigenesis such as PRKDC (Chen et al., 2021); cancer malignancy like RRBP1 (Pan et al., 2015) and PRPF6 (Adler et al., 2014); chemotherapeutic resistance like PHB1 (Patel et al., 2010) or metastasis as PLEC (Buckup et al., 2021). Applying these selection criteria produced a curated list of 49 partners (Figure R-7).

Noticeably, further network analysis on the curated list showed the enrichment in biological processes and structures related to different stages of the mRNA life cycle and the cellular metabolism (Figure R-8). The majority of proteins had been previously described as RNA binding proteins engaged in the sequential steps of mRNA processing,

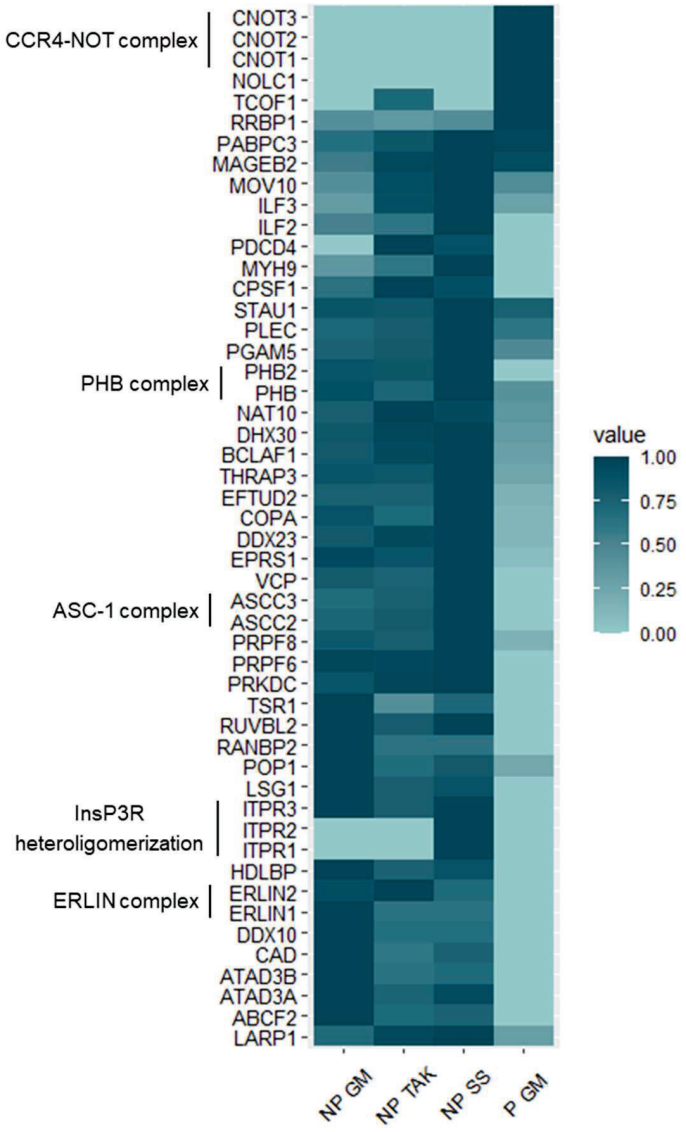

Figure R-7. Selected 40S-LARP1 interacting proteins. Interactors were selected by (1) number of spectral counts, (2) lack of presence in the Ribo-Interactome (Simsek et al., 2017), (3) presence of more than one component of specific biochemical complexes, (4) differential enrichment in the experimental conditions and (5) biological relevance in cancer. Heatmap shows the relative abundance of each protein between the samples obtained as indicated in Figure R-5. Values were obtained by normalization of Fold Enrichment scores obtained by SAINT analysis for each detected protein relative to the negative control of immunoprecipitation. Values range from 0 to 1; 0 = no presence, 1 = maximal presence.

from the nuclear events of splicing and export to the translational regulation and mRNA decay (See Discussion). Furthermore, we observed several proteins reported in the mitochondrial compartment and the endoplasmic reticulum (ER), and more interestingly, many of them are found at the interface between these two organelles with a described role in the crosstalk between the ER and the mitochondria like ITPRs and ERLINs (Cárdenas et al., 2010, 2016; Subbarayalu et al., 2023). This, together with the enrichment in factors of the ribosome biogenesis process (RiBi) were indicative of a high interconnection between the 40S-LARP1 complex and cellular anabolic pathways required for protein synthesis and energy production.

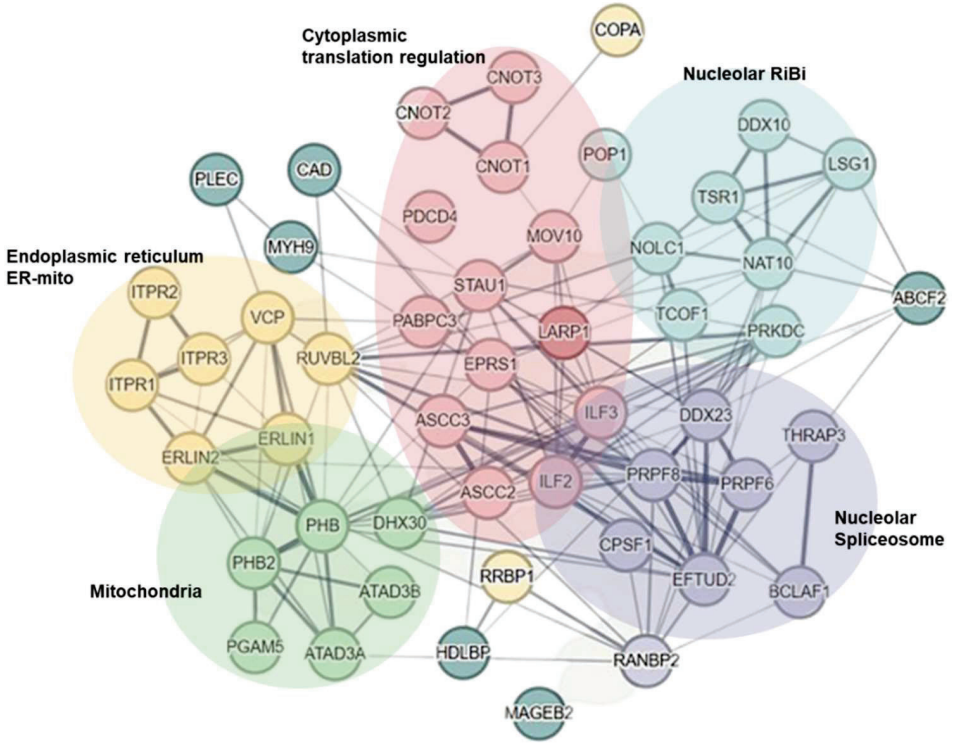

Figure R-8. STRING interaction network. Representation of interconnections between selected 40S-LARP1 interactors based on described functional and physical protein associations and clustered by biological process and subcellular compartment localization.

3. Characterization of LARP1 subcellular distribution upon mTOR inhibition

The results of the 40S-LARP1 interactome showed that the complex is not just related to the makeup of the translational machinery, but potentially also with other processes and structures. The GO biological processes (Figure R-6B) and the STRING network (Figure R-8) analyses suggest that the 40S-LARP1 complex populates different subcellular compartments, some of which might be sensitive to the status of mTOR. To test this, we imaged HCT116 cells by immunofluorescence and we stained for LARP1-GFP and markers of SGs, ER and mitochondria (Figures R-9 and R-10).

It was plausible to hypothesize that the 40S-LARP1 complex could engage with non-membrane bound RNA granules like SGs, which are sites of mRNA protection upon stress conditions (Panas et al., 2016). According to its well-accepted role as a marker of cytoplasmic SGs (Kedersha et al., 2016), we co-stained G3BP1 with LARP1-GFP. First, we observed that endogenous LARP1-GFP localization was characterized by a spread cytoplasmic distribution in puncta shaped structures, with no evident enlargement or redistribution upon the mTOR inhibiting conditions that elicit the formation of the complex (Figure R-9A). This suggests that the remarkable biochemical accumulation of the 40S-LARP1-5'TOP complex (Figures R-2 and R-5) (Fuentes et al., 2021; Gentilella et al., 2017a) is not paralleled by any evident subcellular redistribution. G3BP1 staining revealed low levels of basal expression, with a similar distribution to LARP1-GFP. A 24 hours treatment with an mTOR inhibitor or deprivation of serum did not induce the formation of any evident SGs condensates marked by G3BP1 as observed for an oxidative stress cue like sodium arsenite (SA) treatment, in which the activation of the ISR, measured by eIF2α phosphorylation, partly relocalizes LARP1 with these RNA granules (Figure R-9) (Wilbertz et al., 2019). These data suggest that the protective 40S-LARP1-5'TOP complex is not part of canonical cytoplasmic SGs.

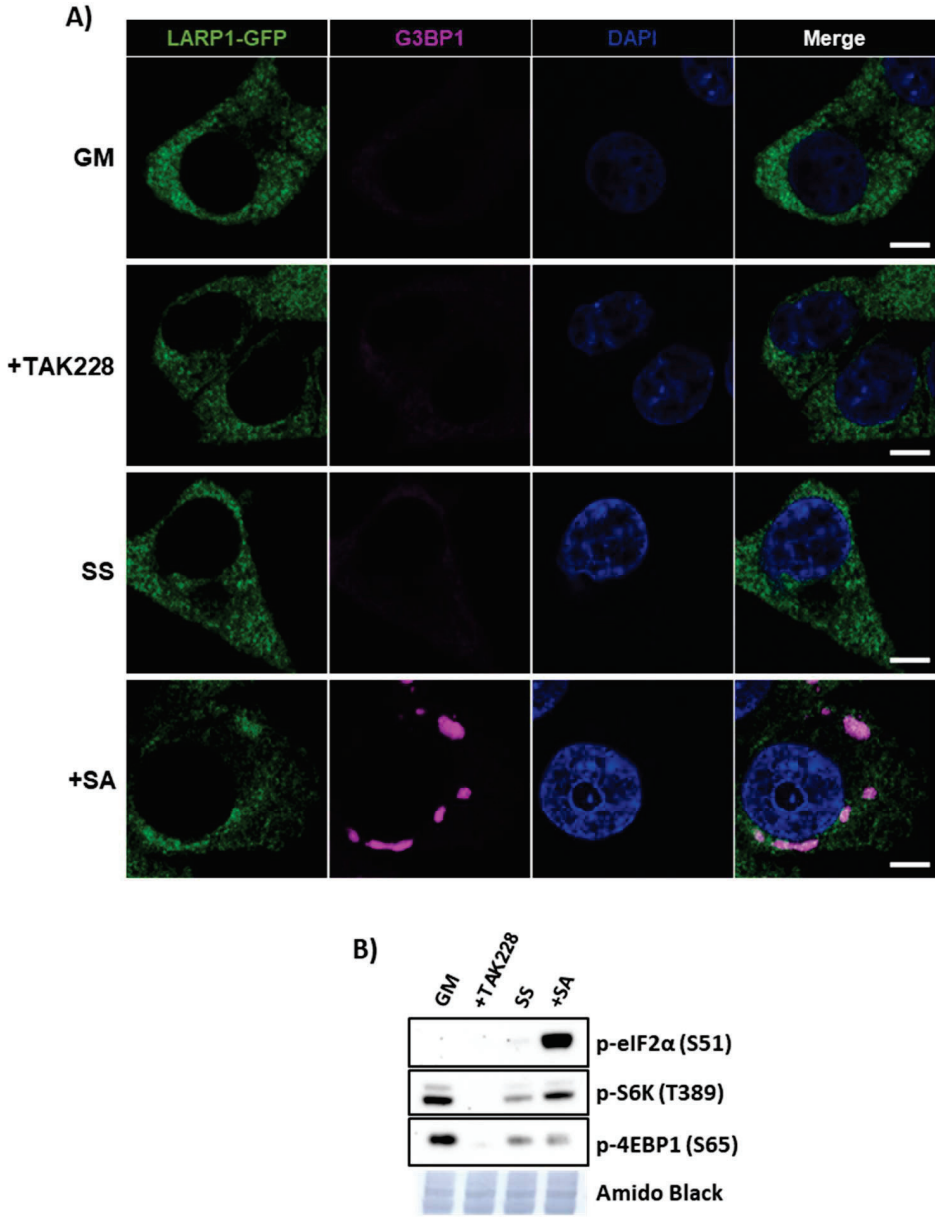

Figure R-9. mTOR inhibition does not induce the formation of stress granules. LARP1-GFP HCT116 cells cultured in growing conditions (GM), after 24h of 250nM TAK228 treatment, 24h of serum starvation (SS) or 2h of 1mM sodium arsenite (SA). **(A)** Immunofluorescence of LARP1-GFP and G3BP1. Scale bar: 5µm. **(B)** Western blot analysis of cellular lysates blotted against p-eIF2α antibody, as a redout of the activation of ISR, and p-4EBP1 and p-S6K as readouts of mTOR inhibition. Amido Black is used as loading control.

Next, we evaluated LARP1 engagement with the membrane-delimited compartments ER and mitochondria, labelled with calnexin (CANX) and TOM20, respectively (Figure R-10). Manders Coefficients of co-localization did not indicate a specific engagement to neither the ER nor the mitochondria upon normal conditions (M1 < 0.5); however, an accumulation in these structures was significant after 24 hours of mTOR inhibition, with a higher impact in response to deprivation of serum (Figure R-10B,D). These data are consistent with a widespread localization of LARP1 with respect to subcellular compartments, some of which are sensitive to the metabolic status of the cell.

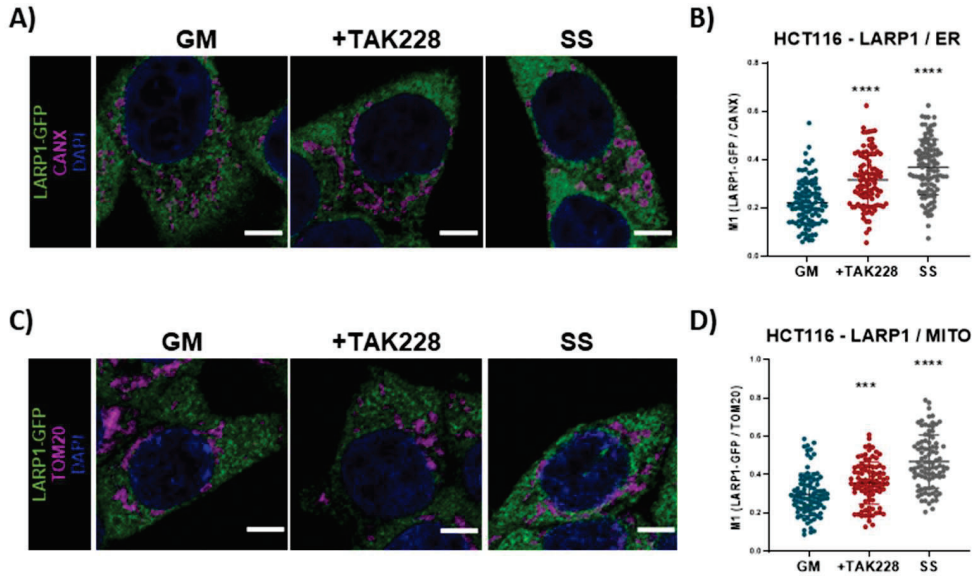

Figure R-10. LARP1 partially localizes to ER and mitochondria, redistributing upon mTOR inhibition. LARP1-GFP distribution in HCT116 cells cultured in growing conditions (GM), after 24h of 250nM TAK228 treatment or 24h of serum starvation (SS). Colocalization with **(A, B)** ER marked by CANX and **(C, D)** mitochondria with TOM20. **(B, D)** Manders Coefficients were calculated for LARP1-GFP vs subcellular organelle markers with ImageJ software (see Methodology); each dot represents a cell from different experimental replicates (n=3). Scale bar: 5µm. Statistical significance is represented as: *** p value < 0.001; **** p value < 0.0001.

4. Novel functional 40S-LARP1 interactors

4.1 Functional screening of 40S-LARP1 interactors

The definition of the 40S-LARP1 interactome suggested two main scenarios not necessarily mutually exclusive. The transcriptome bound to the 40S-LARP1 complex, defined by our group in a previous study as mainly formed by 5'TOP mRNAs (Fuentes et al., 2021), is delivered in different subcellular departments depending on the partner to which it is associated, to provide local protein synthetic capacity. A second hypothesis predicts that, despite LARP1 being a 5'TOP binding protein, other partners could confer selectivity for other *cis* motifs present on 5'TOP mRNAs (or non-TOP mRNAs) in order to deliver a specific translational program to a subcellular compartment. With the aim of describing new regulators of the 40S-LARP1 complex with a functional role in the control of 5'TOP biology, we performed a screening with selected factors to detect their capacity to stabilize 5'TOP mRNAs. We previously determined that the total levels of 5'TOPs normalized by cell number are a good readout to extrapolate the accumulation of the stability complex 40S-LARP1-5'TOPs with non-polysomes when comparing growing and TOR inhibiting conditions (Fuentes et al., 2021). Hence, we knocked-down the expression of the indicated proteins and measured total levels of RPL5 and RPL11 (TOP) and β-actin (non-TOP) transcripts (Figure R-11). Comparison with LARP1 knockdown and TAK228 treatment as controls of 5'TOP mRNAs destabilization, we observed that Interleuking Enhancer Binding Factor 3 (ILF3) and Prohibitin 1 (PHB1) were determinant in maintaining total levels of RPL5 and RPL11 mRNAs (Figure R-11A,B,D). While ILF3 downregulation phenocopies LARP1 knockdown, PHB1 downregulation only affects total 5'TOP transcripts levels under mTOR inhibition. On the other hand, neither ILF3 nor PHB1 knockdown further affected levels of the non-TOP mRNA β-actin (Figure R-11C,D), suggesting a specific role of these two proteins in 5'TOP mRNAs regulation. The results obtained on ILF3 and PHB1 gave us confidence to prioritize these two interactors for further characterization, even though the screening for the entire curated list (Figure R-7) is planned to be carried out.

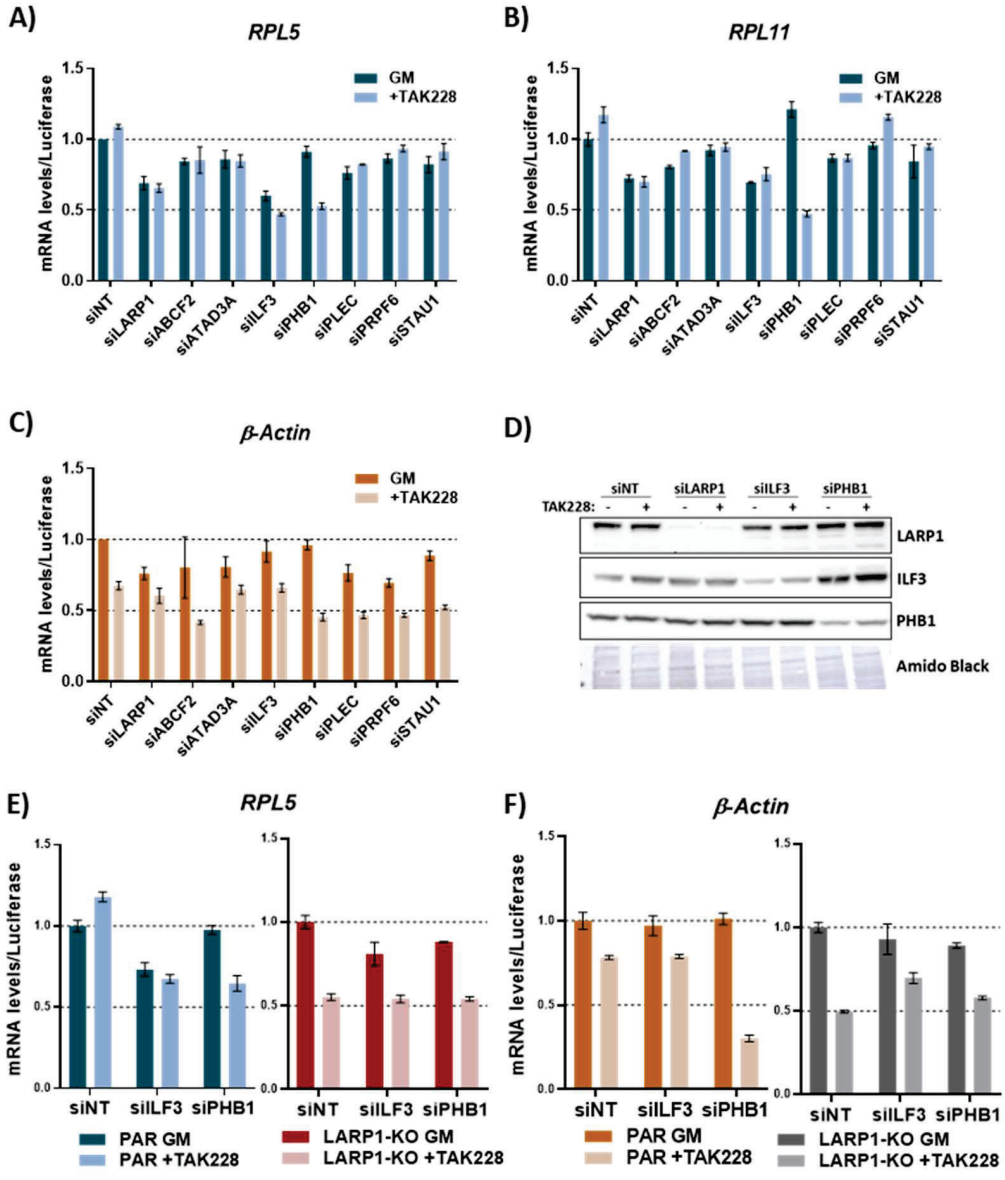

Figure R-11. Functional screening of 40S-LARP1 interactors. (A-D) HCT116 cells after knockdown and treatment with TAK228 (24h) were subjected to RT-qPCR analysis of total **(A, B)** 5'TOPs and **(C)** non-TOP transcripts relative to the number of cells (Luciferase mRNA spike in). **(D)** Same samples were subjected to western blot against LARP1, ILF3 and PHB1 proteins. Amido Black is used as loading control. **(E,F)** HCT116 PAR and LARP1-KO cells after indicated knockdown and TAK228 treatment were subjected to RT-qPCR analysis of **(E)** RPL5 and **(F)** β-Actin transcripts relative to the number of cells (Luciferase mRNA spike in). siNT stands for non-targeting siRNA.

To understand whether the effect of ILF3 and PHB1 knockdown over 5'TOP mRNAs stability was dependent on LARP1 we carried out the same experiment in HCT116 LARP1-KO cells. We observed that in LARP1-KO cells, downregulation of ILF3 expression determined only a slight reduction of total levels of RPL5 transcript in growing conditions not observed for β-actin mRNA (Figure R-11E,F), pointing to an, at least partial, LARP1-independent effect of ILF3 over 5'TOP mRNAs. A similar effect was observed for PHB1 (Figure R-11E,F). On the other hand, upon TAK228 treatment, ILF3 or PHB1 knockdown had no further effect on 5'TOP mRNAs stability (Figure R-11E), indicating that the effects of ILF3 and PHB1 knockdown under these conditions were not additional to that of LARP1 absence. These results supported that ILF3 and PHB1 might have a role in the 5'TOP stabilization operated by the 40S-LARP1 complex upon mTOR inhibition.

4.2 ILF3 and PHB1 interact distinctly with the 40S-LARP1 complex

First, we validated the presence of these new candidate regulators of the 5'TOP mRNAs in the 40S-LARP1 complex. Confirming the Mass Spectrometry data (Figure R-7), ILF3

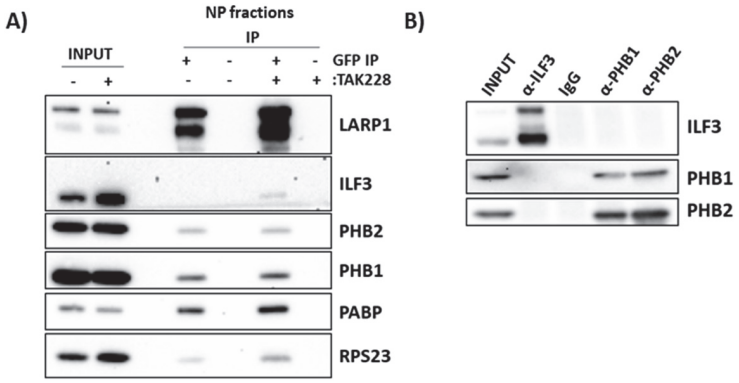

Figure R-12. Co-immunoprecipitation of ILF3 or PHB1/2 with LARP1. (A) Non-polysomal fractions from HCT116 LARP1-GFP cells without and with 24 hours of TAK228 treatment were pooled and subjected to GFP IP. The result was resolved in a SDS-PAGE gel and western blot was performed against the indicated antibodies. **(B)** Total cell lysates of HCT116 LARP1-GFP cells were subjected to immunoprecipitation against the indicated antibodies followed by western blot. INPUT corresponds to a 5% of the IPed material. IgG serves as negative control of IP.

and PHB1 showed different patterns of interaction; while ILF3 binding increased upon TORi conditions, PHB1, as well as its partner PHB2, were present in the non-polysomal complexes independently from the cellular metabolic status (Figure R-12A). Interestingly, these proteins did not co-precipitate in either normal growing conditions or mTOR inhibiting conditions (Figure R-12B; Supp. Figure S-2), indicating that they are part of distinct RNP complexes. These differences point to a model in which the 40S-LARP1 complex has a heterogeneous composition, in which the associated proteins might determine different functions, regulation of specific translatome or localization.

5. Involvement of ILF3 in the 40S-LARP1 complex

As showed above, ILF3 has been proved to be a novel partner of the 40S-LARP1 complex with a role in the stabilization of 5'TOP mRNAs. In support of this functional interconnection, metadata analysis of TCGA data showed a significant expression correlation between ILF3 and LARP1 transcripts in patients in the cohort of colorectal adenocarcinoma (COAD) (www.cbioportal.org) (Figure R-13).

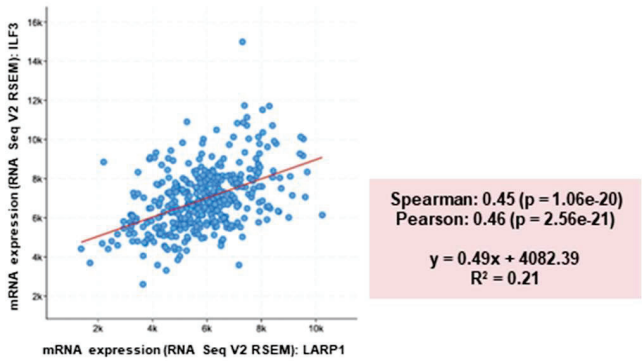

Figure R-13. Correlation of LARP1 and ILF3 transcripts expression in human colorectal cancer samples from TCGA databases (www.cBioPortal.org)

5.1 ILF3 binds to 5'TOP mRNAs in a LARP1-dependent manner

The capacity of ILF3 in phenocopying LARP1 over 5'TOP mRNA stabilization (Figure R-11) and its association with the 40S-LARP1 complex raised the possibility that ILF3 is a

new interactor of 5'TOP mRNAs. Many studies had described ILF3 as an RNA binding protein that regulates the stability and translation of several families of transcripts bearing structural motifs like AU-rich elements (Kuwano et al., 2009; Li et al., 2020; Vrakas et al., 2019). However, no previous studies have identified the 5'TOP mRNAs as ILF3 targets. To characterize the specificity of ILF3 for this family of mRNAs, we took advantage of the TetO-WT-L32TOP-β-Globin-MS2(12X) reporter plasmid constituted by the 5'TOP element from the ribosomal protein L32 (L32WT) followed by the β-globin coding sequence, and a control reporter plasmid in which a set of mutations in the 5'TOP element ablates the TOP regulation (L32MUT). As expected, we observed that doxycycline treatment induced similar levels of expression of L32WT and L32MUT reporter mRNAs in HEK293 cells in normal growing conditions and that mTOR inhibition increased the stability of the L32WT transcript only (Figure R-14A). Under these experimental conditions, RNA immunoprecipitation (RIP) of ILF3 was carried out in hypotonic lysis buffer in order to use the same experimental setting employed for 40S-LARP1 complex isolation (Figure R-12). The results of the RIP showed the capacity of ILF3 to bind LARP1 in another cellular context (Figure R-14B), and that ILF3 was able to immunoprecipitate 5'TOP as well as the non-TOP mRNAs (Figure R-14C). Importantly, treatment with TAK228 increased the accumulation of only L32WT reporter in the ILF3 immunocomplexes (Figure R-14C), in line with the induction of the 40S-LARP1-5'TOP mRNAs complex formation. A similar result is obtained by calculating the enrichment over the input (Supp. Figure S-3).

To evaluate the role of LARP1 in the interaction between ILF3 and 5'TOP mRNAs, we immunoprecipitated ILF3 from HCT116 LARP1-GFP cells and measured 5'TOP mRNAs levels. As observed in Figure R-15B, ILF3 significantly increased its binding to RP mRNAs after TAK228 treatment, while β-Actin transcript levels were barely detectable. In contrast, this accumulation upon mTOR inhibition was lost or reduced in HCT116 LARP1-KO cells (Figure R-15B; Supp. Figure S-4), suggesting that the increased interaction of 5'TOP with ILF3 in conditions of mTOR inhibition is LARP1-dependent. Considering that ILF3 knockdown recapitulates LARP1 knockdown with respect to the levels of 5'TOP

mRNAs (Figure R-11), these data suggest that ILF3 is a functional component of the 40S-LARP1-5'TOP complex particularly upon mTOR inhibition.

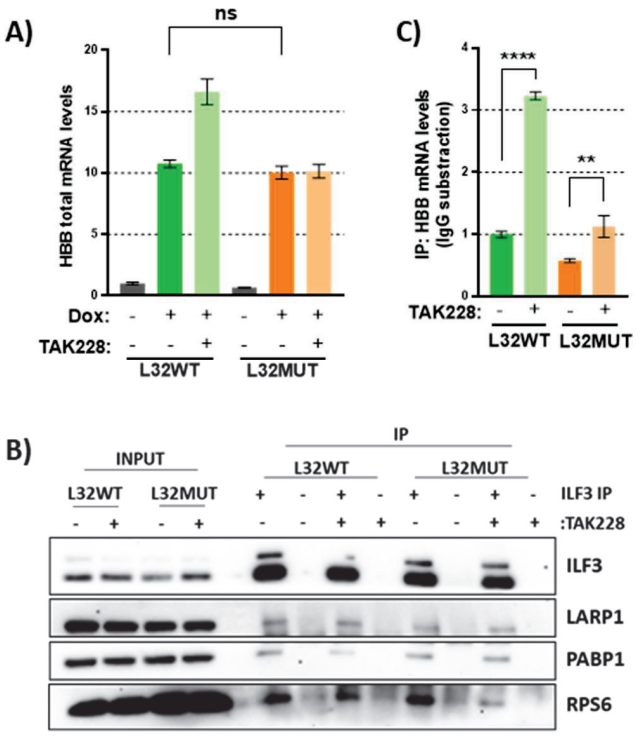

Figure R-14. ILF3 stabilize 5'TOP mRNAs upon mTOR inhibition. HEK293 cells were transfected with TetO-WT-L32TOP-β-Globin-MS2(12X) (L32WT) or TetO-MUT-L32TOP-β-Globin-MS2(12X) (L32MUT), treated with doxycycline (Dox) for 48h, with the last 24h in presence of the TAK228 where indicated. **(A)** Total β-Globin transcript levels were determined by RT-qPCR and normalized to number of cells (Luciferase spike-in). **(B,C)** RNA IP of ILF3 from polysomal lysates. **(B)** 50% of the ILF3 immunocomplexes were resolved by Western Blot to assay ILF3, LARP1, PABP and RPS6. INPUT samples corresponded to 5% of the material subjected to IP. **(C)** The remaining 50% of RIP reactions were subjected to RT-qPCR to measure β-Globin transcript levels normalized to total amount of IP material (Luciferase spike-in). Statistical significance is represented as: ns= p value > 0.05; ** p value < 0.01; **** p value < 0.0001

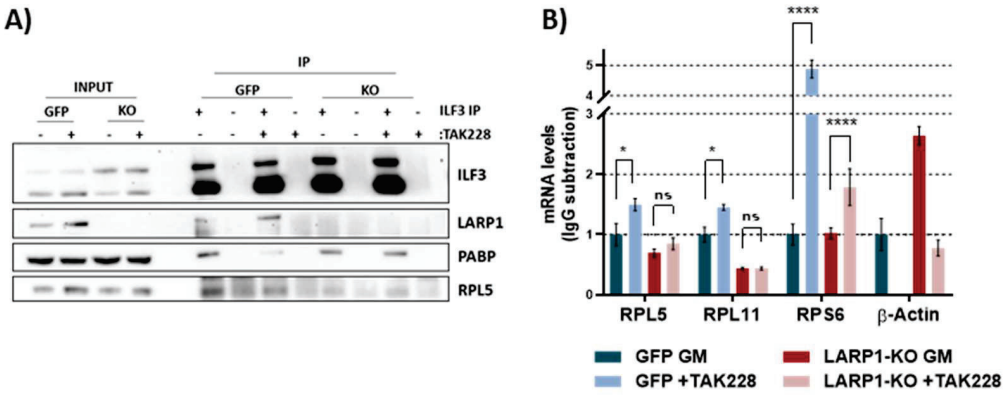

Figure R-15. ILF3 stabilizes RP mRNAs upon TORi in a LARP1-dependent manner. RNA IP of ILF3 from polysomal lysates of HCT116 LARP1-GFP or LARP1-KO cells obtained from growing cells or cells treated with TAK228 for 24h. **(A)** 50% of the ILF3 immunocomplexes were resolved by Western Blot to assay LARP1, PABP, RPL5 and ILF3. INPUT samples corresponded to 5% of the material subjected to IP. **(B))** The remaining 50% of RIP reactions were subjected to RT-qPCR to measure RP transcripts or β-Actin mRNA levels normalized to total amount of IP material (Luciferase spike-in). Statistical significance is represented as: ns= p value > 0.05; * p value < 0.05; **** p value < 0.0001.

5.2 Exploring the role of ILF3 in the 40S-LARP1-5'TOP mRNAs stabilization complex

Given that that ILF3 knockdown reduces the total RP mRNAs levels (Figure R-11) and that the increased interaction between ILF3 and 5'TOP mRNAs upon mTOR inhibition is LARP1-dependent (Figure R-15), we sought to investigate the role of ILF3 in the 40S-LARP1-5'TOP mRNAs stability complex. Our first approach to study the functional role of ILF3 was to characterize whether it participates in the formation of the 40S-LARP1-5'TOP mRNAs stability complex upon mTOR inhibition. Many studies had previously described the interaction of ILF3 with the translational machinery (Pfeifer et al., 2008; Watson et al., 2020). However little is known about how the association of ILF3 with ribosomes could change upon mTOR inhibiting conditions, when the formation of the 40S-LARP1-5'TOP complex is induced. To do so, we measured by western blot ILF3 co-sedimentation with ribosomes after polysome profile fractionation (Figure R-16). ILF3 appeared with both translating and non-translating ribosomes and, interestingly, upon

mTOR inhibition it mostly accumulated within the monosome fractions in a fashion similar to LARP1 (Figure R-16B).

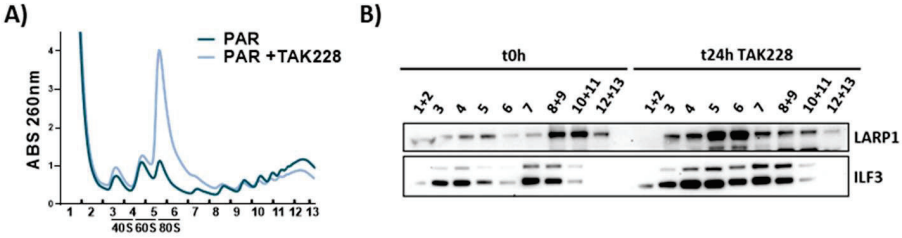

Figure R-16. ILF3 co-sedimentation with ribosomes upon mTOR inhibition. Cell lysates from PAR or LARP1-KO cells collected before (t0h) and after 24 hours (t24h) of treatment with TAK228 were subjected to polysome profiling by ultracentrifugation on a 10%-50% sucrose gradients. (A) Graphical representation of rRNA content. (B) Same gradients were collected in 13 fractions, which were subjected to western blot against LARP1 and ILF3 protein.

Taking into account the similar pattern followed by LARP1 and ILF3 in co-sedimentation in a polysome profile after inhibition of mTOR, we asked whether it was dependent on LARP1 and the formation of the 40S-LARP1 complex upon mTOR inhibition. To test so, we performed the same experiment as above comparing PAR and LARP1-KO cells (Figure R-17). The ILF3 redistribution appeared to be LARP1-independent as LARP1-KO cells showed a similar co-sedimentation pattern of ILF3 as parental cells (Figure R-17D).

In view of the fact that ILF3 does not require LARP1 to interact with the translational machinery, however it increases its association with 5'TOP mRNAs in mTOR inhibiting conditions (Figures R-14 and R-15), we sought to investigate whether ILF3 might be controlling the accumulation of 5'TOPs with the 40S-LARP1 complex upon mTOR inhibition. Indeed, a recent study has defined ILF3 as a novel mTORC1 regulator, needed for signal transduction after amino acid deprivation (Yan et al., 2023). To address this question, we performed polysome profile analysis to determine the effect of ILF3 knockdown in the distribution of LARP1-GFP and 5'TOP mRNAs upon mTOR inhibition (Figure R-18).

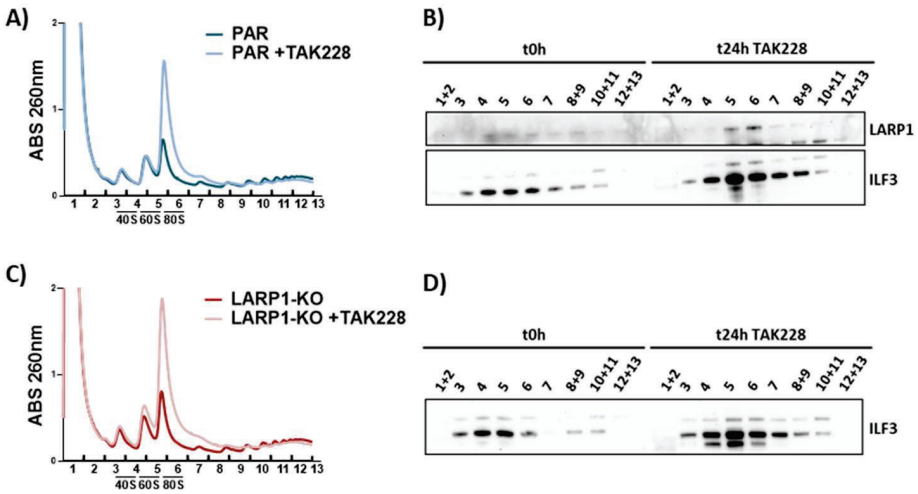

Figure R-17. ILF3 co-sedimentation with ribosomes in LARP1-KO cells. Cell lysates from PAR or LARP1-KO cells collected before (t0h) and after 24 hours (t24h) of treatment with TAK228 were analyzed as in Figure R-16. (A, B) PAR cells (A) Graphical representation of rRNA content (B) Same gradients were collected in 13 fractions, which were subjected to western blot against LARP1 and ILF3 protein. (C,D) same as A,B in LARP1-KO cells.

Analysis of sucrose gradient ultracentrifugation of cell lysates revealed that the knockdown of ILF3 did not alter significantly the mean polysome size nor the non-polysomes in both conditions (Figure R-18A – upper panel). With regard to the LARP1 distribution, as marked by the GFP signal, it almost overlapped in all conditions, with an expected reduction in polysomes and an increase in 40S and 80S fractions upon TAK228 treatment (Figure R-18A - bottom panel). The effect of ILF3 knockdown were only limited to a shallow decrease of GFP signal in the 40S ribosomes in TOR inhibiting condition. Paralleling LARP1 distribution, as previously observed in our laboratory (Fuentes et al., 2021), a 24h TAK228 treatment induced the decrease of every mRNAs (5'TOP and non-TOP) associated with the polysomal fractions as an effect of the reduction of global translation. However, this was accompanied by the accumulation of only the 5'TOP mRNAs, RPL5 and RPS6 transcripts (Figure R-18B-D) in the 40S-containing non-polysomal fractions. In the same condition the ILF3 knockdown impaired the accumulation of RPL5 transcript with the 40S ribosomes, effect that was only minimal

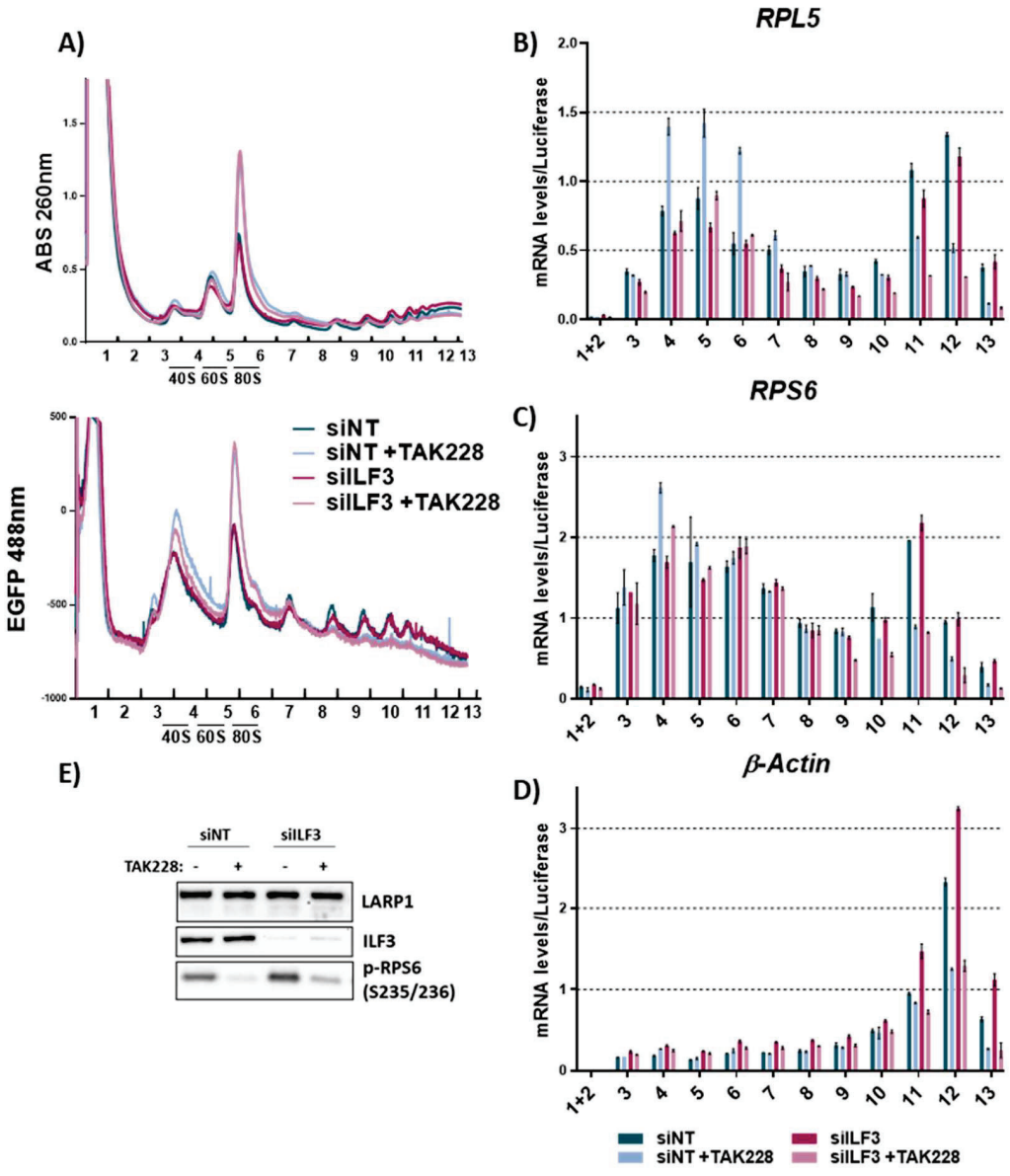

Figure R-18. ILF3 does not affect LARP1 redistribution to non-polysomes upon TORi. LARP1-GFP cells were transfected with siRNAs: siNT -non targeting- or siILF3 for 48h and maintained in growing conditions or treated with TAK228 for the last 24h. **(A-D)** Cell lysates were subjected to polysome profiling. (A) Graphical representation of (upper panel) rRNA content or (bottom panel) GFP distribution. **(B)** RPL5 **(C)** RPS6 and **(D)** β-Actin mRNAs were measured by RT-qPCR in each fraction. **(E)** Cell lysates were subjected to western blot and blotted against the indicated proteins.

for RPS6 mRNA (Figure R-18B,C). As expected, β-actin transcript does not accumulate in non-polysome fractions and is not dependent on ILF3 expression (Figure R-18D). In order to overcome the potential effect of the remaining ILF3 in the cells, which could mask the observations of ILF3 function, we sought to generate ILF3-KO cells by CRISPR/Cas9. Unfortunately, no viable HCT116 ILF3-KO clones were produced (Supp. Figure S-5), suggesting that ILF3 is indeed an essential gene. Together, these data support a model in which, under unfavorable growth conditions, a non-identified pool of ILF3 binds the 40S-LARP1 complex and regulates the accumulation of at least RPL5 5'TOP mRNAs with the non polysomes. However, further studies will be necessary to confirm at what extent ILF3 is implicated in the redistribution of 5'TOP mRNAs with the protective 40S-LARP1 complex upon mTOR inhibiting conditions.

Additionally, the apparent mild increase in the polysome size after ILF3 knockdown (Figure R-18A), which had been observed in previous studies explaining ILF3 as a global translational repressor (Pfeifer et al., 2008), led us to characterize the role of ILF3 in global protein synthesis (Figure R-19). Nevertheless, ILF3 knockdown reduced puromycin incorporation into newly synthesized proteins (Figure R-19), indicating a reduction in translation.

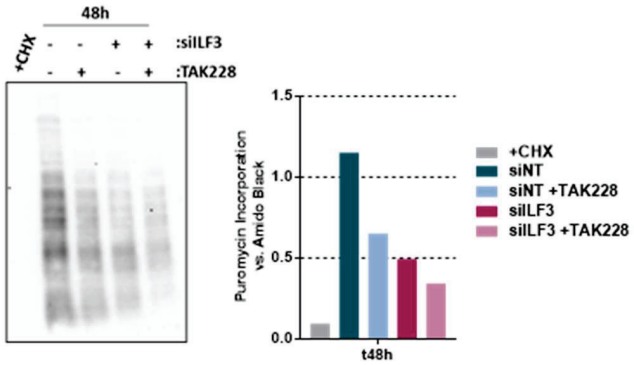

Figure R-19. ILF3 expression and global protein synthesis. HCT116 cells were treated as in Figure R-11. Protein synthesis rate measured by incorporation of puromycin into total protein (see Methodology). (Left) Western Blot blotted against Puromycin. (Right) Quantifiaction of puromycin incorporation versus amido black staining. Cycloheximide (CHX) treatment at 100ug/ul during the puromycin labeling served as a negative control of incorporation.

6. PHB1 and the 40S-LARP1 complex

6.1 PHB1 association with the translational machinery and its impact on 5'TOPs translation

The discovery of the association of prohibitins with the 40S-LARP1 complex was initially unexpected as it had not been previously associated with the cytoplasmic translational machinery. As for ILF3, we decided to better understand the distribution of prohibitins with ribosomes and how they respond to inhibition of mTOR by polysome profiling (Figure R-20). We observed that in growing conditions both PHB1 and PHB2 are mainly present in the non-polysomal fractions, with almost no presence in the fractions free of ribosomes (1+2). Surprisingly, after TAK228 treatment, a condition that reduces total polysome levels (Figure R-20A), PHBs populated mostly the small polysomes fractions (6 to 9) (Figure R-20B). These data, together with the association of LARP1 and PHB1 in the non-polysomes (Figure R-12A) corroborate a previously uncharacterized interaction of prohibitins with the cytoplasmic ribosomes, and present a new scenario, in which a LARP1 interacting protein redistributes with polysomes upon mTOR inhibition.

We had observed that knockdown of PHB1 destabilized the total levels of 5'TOP mRNAs only upon mTOR inhibiting conditions (Figure R-11), suggesting a potential role of PHB1 in the 40S-LARP1 stabilization complex. In order to study the formation of the 40S-LARP1 complex, we carried out polysome profiling experiments after PHB1 downregulation and studied LARP1-GFP and 5'TOP mRNAs distribution (Figure R-21). Unexpectedly, an effective PHB1 knockdown (Figure R-21E) in growth conditions, which did not have an effect at the total levels of 5'TOP mRNAs (Figure R-11), induced an increase of the 80S ribosome peak along with LARP1-GFP and RP mRNAs (Figure R-21A,B,C), redistribution that could not be observed for the non-TOP mRNA β-actin (Figure R-21D). When treating with the mTOR inhibitor upon PHB1 knockdown, we observed the expected reduction in polysome levels, but cells failed to accumulate LARP1-GFP protein in the 40S fraction as observed in siNT transfected cells (Figure R-21A) as well as the 5'TOP mRNAs RPL5 and

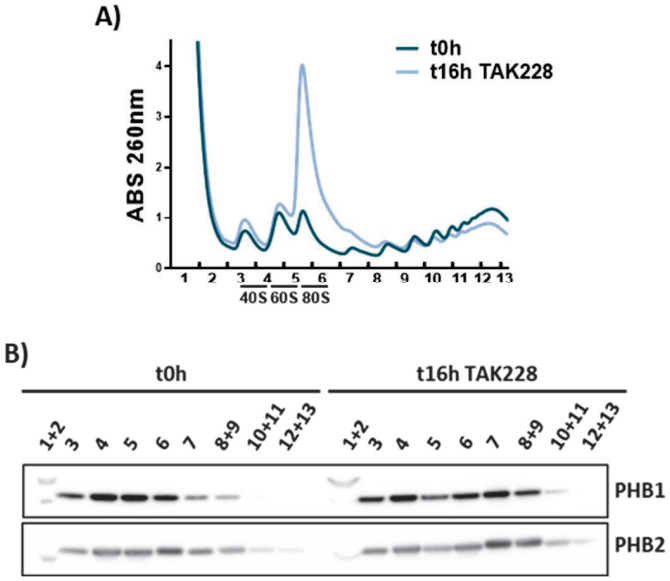

Figure R-20. Prohibitins associate with the translational machinery. Cell lysates from HCT116 PAR cells collected before (t0h) and after 16 hours (t16h) of treatment with TAK228 were subjected to polysome profiling by ultracentrifugation on a 10%-50% sucrose gradients. **(A)** Graphical representation of rRNA content. **(B)** Same gradients were collected in 13 fractions, which were subjected to western blot against PHB1 and PHB2 proteins.

RPS6 (Figure R-21B,C). The non-TOP mRNA β-Actin was not affected by PHB1 knockdown (Figure R-21D). Moreover, the distribution with the translational machinery of RPL5 and RPS6 in condition of PHB1 knockdown and mTOR inhibition did not mirror the strong reduction observed in the total levels of the same transcripts (Figure R-11). This suggests that at least with respect to the 5'TOP mRNAs levels upon low mTOR signaling, PHB1 might utilize other mechanisms not involving the translational machinery, and that its presence within the 40S-LARP1 complex might have other roles not yet identified (see Discussion). Overall, these data indicate that PHB1, and its partner PHB2, associate with the translational machinery mostly with non-polysomes, where the interaction with the 40S-LARP1 complex has been identified by Mass Spectrometry.

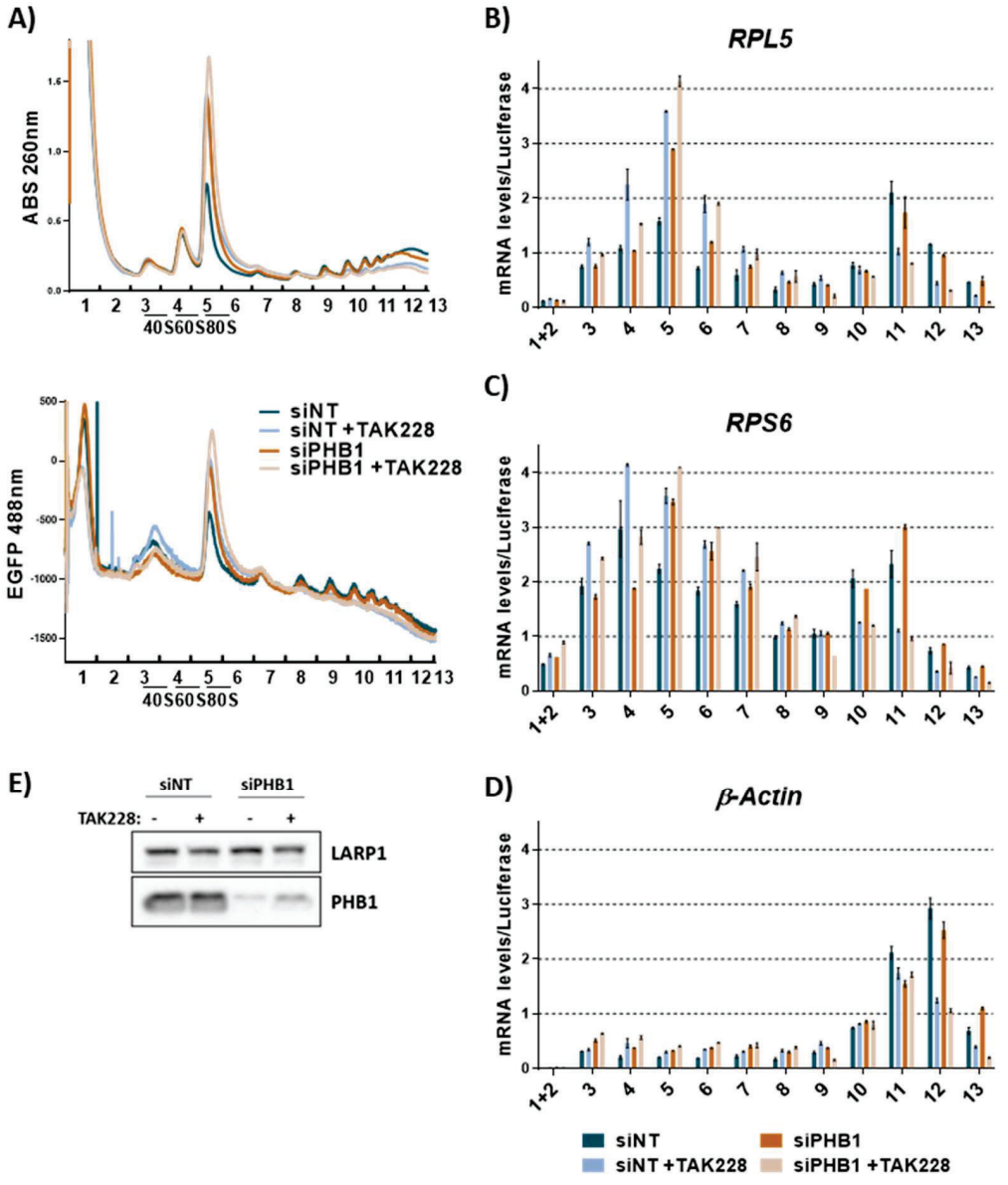

Figure R-21. PHB1 knockdown drives LARP1 and RP mRNAs accumulation in monosomes. LARP1-GFP cells were transfected with siRNAs: siNT -non targeting- or siPHB1 for 48h and maintained in growing conditions or treated with TAK228 for the last 24h. **(A-D)** Cell lysates were subjected to polysome profiling. **(A)** Graphical representation of rRNA content (upper panel) or GFP distribution (bottom panel). **(B)** RPL5 **(C)** RPS6 and **(D)** β-Actin mRNAs were measured by RT-qPCR in each fraction. **(E)** Cell lysates were subjected to western blot and blotted against LARP1 and PHB1 proteins.

Given that PHB1 knockdown increased the accumulation of LARP1 in the 80S fractions upon growing conditions and in order to decipher the potential role of PHB1-LARP1 interaction in translation beyond 5'TOP levels, we studied the protein synthesis capacity of HCT116 cells (Figure R-22). First, we measured puromycylation of proteins, as a readout of ribosome activity, after PHB1 depletion in parental cells. This showed that PHB1 knockdown reduces global protein synthesis. Of note, this effect was reproduced in LARP1-KO cells (Figure R-22A), indicating that PHB1 role on global protein synthesis is LARP1-independent. The inhibition of the PHB complex has been previously described to reduce translation through the activation of the ISR (Jin et al., 2020) and inhibition of the mTOR pathway (Zhang et al., 2021). Accordingly, we observed that in parental cells, PHB1 knockdown activates the ISR, as observed by the increase in the levels of ISR effector ATF4, and inhibits the mTOR pathway, as indicated by the phosphorylation of 4E-BP1. Surprisingly, LARP1-KO cells further increased ISR (Figure R-22B). In order to test the possibility that the ISR is driving the inhibition of global translation, we used the ISR inhibitor ISRIB to block the inhibition of translation initiation by p-eIF2α (Figure R-22C,D). Increasing concentrations of ISRIB show efficient block of ISR after siPHB1, as observed by the decreasing levels ATF4 (Figure R-22D,F). Nevertheless, global translation was not rescued in these conditions (Figure R-22C), meaning that the ISR is not mediating the defect observed after PHB1 depletion. Counterintuitively, total translation decreased after PHB1 knockdown while total polysome levels were not affected (Figure R-21A – upper panel), which could be explained by a decrease in the translational elongation rate of the ribosomes. To test this hypothesis, we measured elongation factor eEF2 phosphorylation as a marker of elongation blockade (Gismondi et al., 2014) and observed that PHB1 knockdown increased p-eEF2 levels (Figure R-22B), pointing to an impairment in the elongation rates. Importantly, mTOR signaling regulates the translation elongation step (Gentilella et al., 2015). These data points to a role for PHB1 in translational elongation, however, whether this is a direct effect of its engagement with the translation machinery or a general effect through the activation of stress pathways still needs to be addressed. Furthermore, it remains to be

determined the link between the destabilization of 5'TOP mRNAs upon mTOR inhibition after PHB1 knockdown, the induction of the accumulation in the 80S monosomes and the defect in global translation, which will be key to understand the role of PHB1 in the 40S-LARP1 complex.

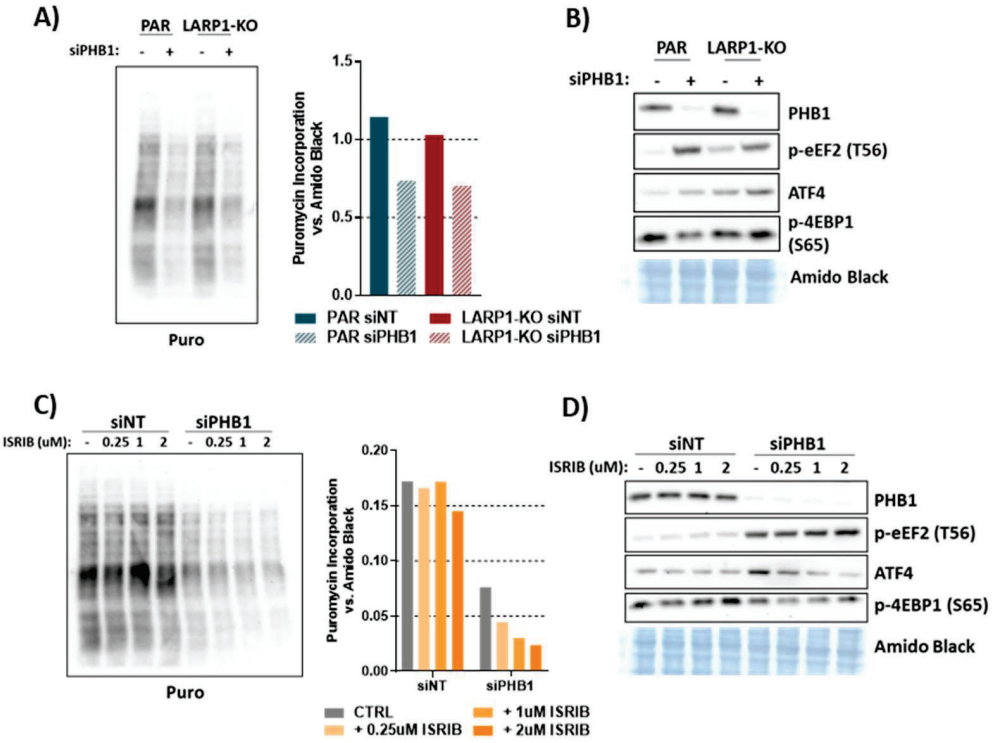

Figure R-22. PHB1 knockdown decreases global protein synthesis and reduces translational elongation. (A,B) LARP1-GFP and LARP1 KO cells were transfected with siNT -non targeting- or siPHB1 for 48h and maintained in growing conditions. **(A)** Protein synthesis rate measured by incorporation of puromycin into total protein. Western Blot probed against Puromycin antibody (left) and quantificatified versus total protein stained with Amido Black (right). **(B)** Total levels of indicated proteins were measured by Western Blot. **(C,D)** LARP1-GFP cells were transfected with siNT or siPHB1 for 48h and maintained in growing conditions or treated with increasing concentrations of ISRIB for the whole experiment (see Methodology). **(C)** Protein synthesis rate measured by incorporation of puromycin as in A. **(D)** Total levels of indicated proteins were measured by Western Blot. Amido Black was used as loading control.

6.2 Characterization of PHB1 and LARP1 at the mitochondria

PHB1 is predominantly a mitochondrial protein; however, it has been also located in the plasma membrane and in the nucleus, which determines its molecular function (Tatsuta & Langer, 2017). As its subcellular distribution can vary also depending on the cellular type, we first analyzed by immunofluorescence the localization of PHB1 in HCT116 cells and its colocalization with LARP1. By labelling the mitochondria with MitoTracker™, we determined on one hand that in our cell model PHB1 is largely confined to mitochondria and that LARP1-GFP and PHB1 colocalize in this cellular compartment, raising the possibility that this is where they interact (Figure R-23).

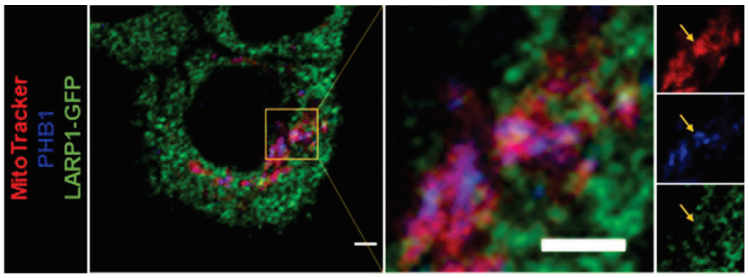

Figure R-23. PHB1 and LARP1 co-localization in the mitochondria. Immunofluorescence of PHB1 and LARP1-GFP in HCT116 cells cultured in normal growth media and labelled for 1h with MitoTracker™ Deep Red. Scale bar: 1µm.

The mitochondrial PHB complex is located in the inner mitochondrial membrane (IMM) and has been widely related to scaffolding functions (Osman et al., 2009). As a membrane organizer, we hypothesized that PHB1 might act as a molecular tether of the 40S-LARP1 complex to the mitochondrial compartment. To test this, we measured the colocalization of LARP1 to the mitochondria as previously shown (Figure R-10) upon PHB1 depletion (Figure R-24). Immunofluorescence analysis showed that PHB1 knockdown does not reduce the fraction of LARP1 colocalizing with TOM20. On the contrary, we observed a significant increase in the Manders Coefficient upon PHB1 knockdown (Figure R-24B). These results indicate that the fraction of LARP1 localizing to the mitochondria in any of the condition tested does not depend on PHB1 as a

tethering factor. However, this result does not exclude that the interaction of PHB1 and LARP1 might occur in this cellular district.

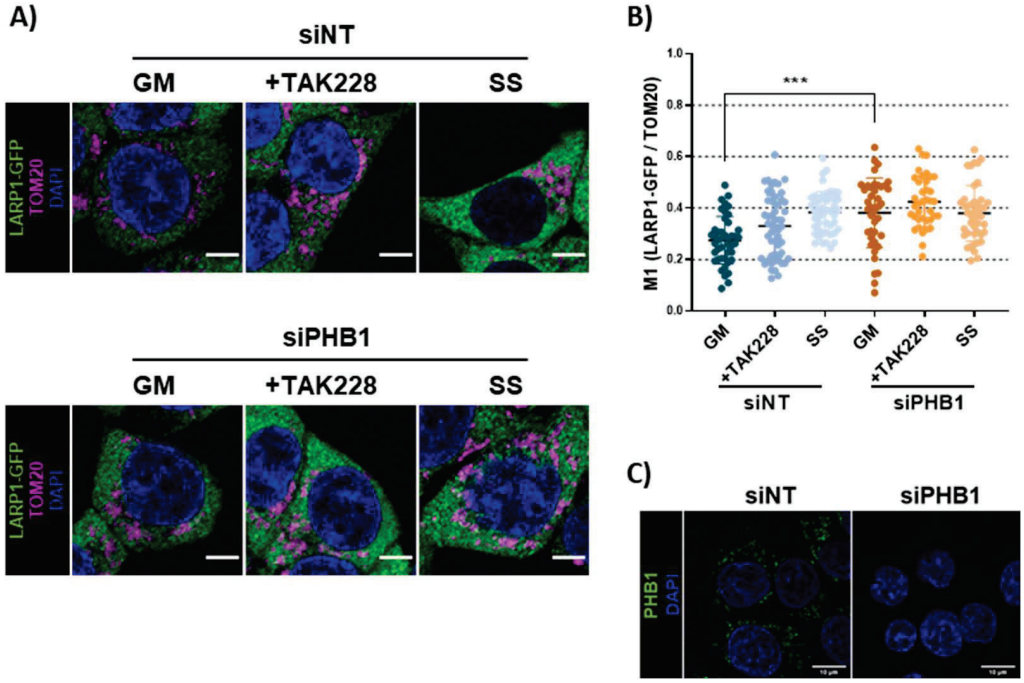

Figure R-24. PHB1 does not act as a mitochondrial tether for LARP1. LARP1-GFP HCT116 were transfected with siNT -non targeting- or siPHB1 for 48h and maintained in growing conditions (GM), treated with TAK228 or deprived for serum (SS) for the last 24h. **(A)** Colocalization with mitochondria marked with TOM20. Scale bar: 5µm. **(B)** Manders Coefficients were calculated for LARP1-GFP vs TOM20 with ImageJ software; each dot represents a cell. **(C)** Immunofluorescence of PHB1. Scale bar 10 µm.Statistical significance is represented as: *** p value < 0.001.

SUPPLEMENTARY FIGURES

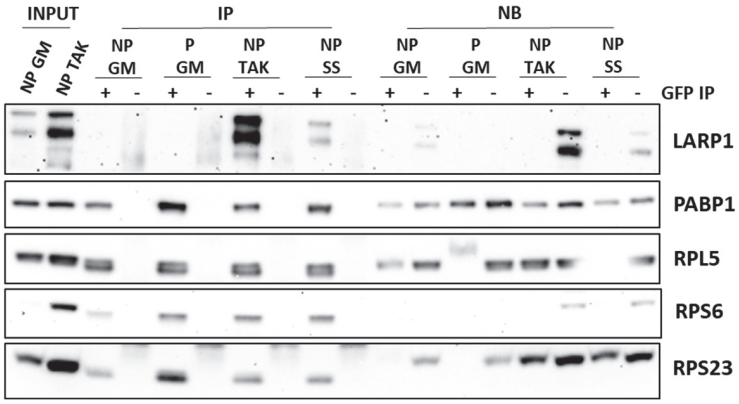

Supp. Figure S-1. LARP1 Immunoprecipitation from sucrose gradient fractions for LC-MS/MS. Cell lysates from HCT116 LARP1-GFP cells cultured in normal growing conditions (GM), 24h treatment with 250µM TAK228 (TAK) or 24h serum starvation (SS) were subjected to polysome profiling. Fractions were pooled in non-polysomes (NP) and heavy polysomes (P). Pools of non-polysomes and heavy polysomal fractions were subjected to immunoprecipitation with GFP-Trap Dynabeads and then resolved by western blot analysis. INPUT samples correspond to a 10% of the IP material. NB corresponds to a 10% of Non-Bound proteins.

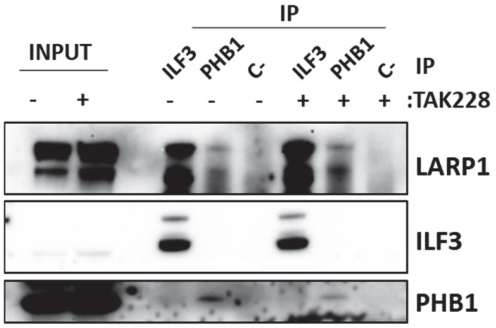

Supp. Figure S-2. ILF3 and PHB1 co-immunoprecipitation. Related to Figure R-12. Total cell lysates of HCT116 LARP1-GFP cells were subjected to immunoprecipitation against the indicated antibodies followed by western blot. INPUT corresponds to a 5% of the immunoprecipitated material. IgG (C-) serves as negative control of IP.

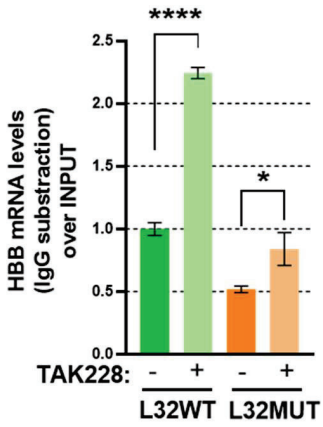

Supp. Figure S-3. ILF3 stabilize 5'TOP mRNAs upon mTOR inhibition. Same experiment from Figure R-14 represented as HBB mRNA in the ILF3 immunocomplexes over total levels of the mRNA in the INPUT sample. Statistical significance is represented as: * p value < 0.05; **** p value < 0.0001

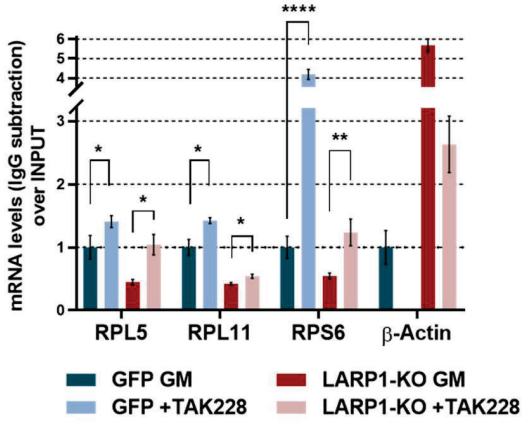

Supp. Figure S-4. ILF3 stabilizes RP mRNAs upon TORi in a LARP1-dependent manner. Same experiment as in Figure R-15 represented as IPed mRNAs over total levels of the same mRNAs in the INPUT sample. Statistical significance is represented as: * p value < 0.05; ** p value < 0.01; **** p value < 0.0001

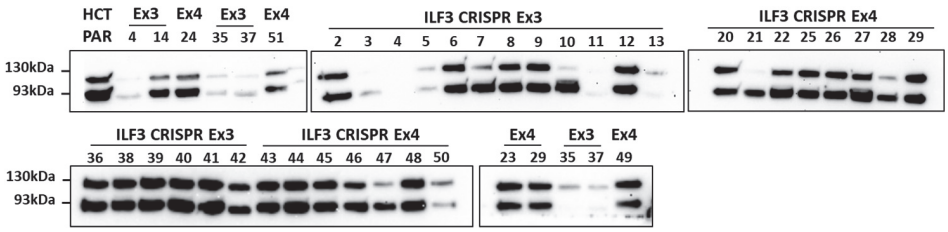

Supp. Figure S-5. Generation of ILF3 CRISPR/Cas9 knock-out. Western Blot against ILF3 of cellular lysates from monoclonal cell lines obtained after CRISPR/Cas9 gene editing on ILF3 locus.

DISCUSSION

Cancer cells undergo a transformative process, acquiring distinct features pivotal for the progression of neoplastic growth and tumor malignancy. Among these “Hallmarks of Cancer”, the maintenance of a proliferative signaling and reprogramming of the cellular metabolism are of paramount importance to ensure uncontrolled cellular growth, proliferation as well as high levels of energy production (Hanahan & Weinberg, 2011). In order to sustain it, many tumor types, such as sporadic colorectal cancer, rely on the hyperactivation of the protein synthesis and its machinery, specifically ribosomes, to perpetuate these processes (Pelletier et al., 2018). Importantly, beyond the mere hyperproduction of ribosomes, cancer cells exhibit plasticity and adaptability to unfavorable conditions imposed by the tumor microenvironment or chemotherapeutic treatments. In this context, the 40S-LARP1 complex assumes a pivotal role by conferring a metabolic advantage to cancer cells in conditions characterized by chronic mTOR inhibition. This establishes a priority in the production of ribosomal proteins and components of the translational machinery to rapidly restore the cellular protein synthetic capacity, a decisive step in RiBi-addicted cancers (Fuentes et al., 2021).

This thesis investigates the composition of the 40S-LARP1 complex and its subcellular localization in response to metabolic constraints leading to mTOR inhibition. Our study has expanded the repertoire of processes in which the 40S-LARP1 complex can play a role, by the discovery of partners involved in nuclear events that include ribosome biogenesis and pre-mRNA processing. Additionally, the complex demonstrates cytoplasmic localization to subcellular compartments such as the endoplasmic reticulum (ER) and the mitochondria. Furthermore, we have identified two novel regulators of 5’TOP mRNAs biology, namely Interleukin Enhancer Factor 3 (ILF3) and Prohibitin 1 (PHB1). Altogether, these results provide a global molecular definition of the 40S-LARP1 complex that will help to better understand the role and the processes

occurring in tumors addicted to the production of ribosomes, opening a window on their potential vulnerabilities.

LARP1-GFP HCT116 cells constitute a valuable tool for characterization of the 40S-LARP1 complex

In order to generate a tool that allows a more efficient characterization of the 40S-LARP1 complex protein composition, first, we have successfully generated by CRISPR/Cas9 a colorectal cancer HCT116 cell line stably expressing an endogenous version of the LARP1 protein tagged with GFP (Figure R-1). We have corroborated that the addition of a GFP moiety at the C-terminus of LARP1 does not affect the ability of LARP1-GFP to form the 40S-LARP1 complex (Figure R-2) and to stabilize the levels of 5'TOP mRNAs as a response to the inhibition of the mTOR pathway (Figure R-3). Notably, the LARP1-GFP HCT116 cell line constitutes an invaluable tool for the analysis of LARP1 protein distribution in polysome profile experiments right during gradient fractionation (Figure R-2), as well as for immunoprecipitation of LARP1 directly from sucrose fractions, which allows for a high-yield analysis of non-translating and translationally-active 40S-LARP1 complexes (Figure R-4).

The 40S-LARP1 complex composition changes according to the mTOR and translational status

The analysis of the 40S-LARP1 interactome revealed almost 700 proteins making contacts with the complex in the different conditions tested. As expected, proteins that immunoprecipitated with LARP1 in all conditions included the protein synthetic machinery and the increased ratio in the polysomal fractions, meaning actively translating ribosomes, confirmed the power of the analysis (Figure R-6). With the objective of understanding how the 40S-LARP1 complex can turn on and off the ribosome biogenesis process as a function of the mTOR pathway, we focused our analysis on the determination of the differential composition of the complex in the experimental conditions tested.

On one hand, the comparison between non-polysomal and polysomal 40S-LARP1 complexes revealed substantial differences in composition and enrichment within specific pathways (Figures R-6). The predominant category of proteins in the polysomal 40S-LARP1 complex was associated with the process of translation, accounting for 40% of the interactors, followed by the category of proteins involved in "mRNA processing". Within the latter, our analysis identified several components of the CCR4-NOT complex, such as CNOT1, CNOT2 or CNOT3 exclusively present in polysomal complexes (Figure R-7). Surprisingly, this finding opposes to the established association of the CCR4-NOT complex with RNA decay through deadenylation of the poly-A (Collart & Panasenko, 2012). Indeed, a recent study has described that LARP1, in complex with PABP, protects mRNAs from degradation by preventing the deadenylation activity of the CCR4-NOT complex (Park et al., 2023). Nevertheless, the CCR4-NOT complex also associates with actively translating ribosomes as part of the protein quality control mechanism (Collart & Panasenko, 2012), which could be one of the plausible explanations for its association with LARP1. However, more evidence on the alternative roles of the CNOT proteins in post-transcriptional regulation are emerging. Indeed, depletion of CNOT1 leads to translational repression of ER-targeted mRNAs, and to the upregulation of others, suggesting a role in specific translational programs (Gillen et al., 2021).

Another primary objective of the interactome analysis was to determine how mTOR inhibition could affect the composition of the 40S-LARP1 complex. Although we did not observe any enriched biological process in the set of proteins of non-polysomes sample for each experimental condition, the analysis on the relative abundance of each protein across the samples showed relevant differences in the composition of the 40S-LARP1 complex (Figure R-7). Of note, some of the groups of proteins, such as ribosomal proteins, that are known to increase its binding to the 40S-LARP1 complex upon TORi conditions (Figures R-12A and S-1) did not increase in the SAINT analysis, pointing to a suboptimal sensitivity of the quantitative power of the analysis. However, for targets such as LARP1, ILF3 or PHBs, the relative quantification was confirmed (Figures R-7 and R-12A). Potential negative regulators of the mTOR/40S-LARP1 complex axis would be

expected to be among those proteins enriched upon TAK228 treatment and serum starvation. For instance, the tumor suppressor PDCD4, a target of S6K1, is known to inhibit translation initiation by binding to eIF4A helicase and displacing the eIF4G scaffold protein from the translation initiation complex (Suzuki et al., 2008).

Overall, these data confirm that the 40S-LARP1 interactome represent a mosaic of proteins, which composition changes depending on the mTOR and the translation status of the cell, that could amplify the repertoire of function depending on the specific combination. Further analyses on the role of these interactors within the complex are imperative for a comprehensive understanding of the mTOR / LARP1 / 5'TOP mRNAs regulation.

The 40S-LARP1 complex is dynamic and might drive local translation

Interestingly, the identification within the 40S-LARP1 interactome of components of the intermediate filament organization (Figure R-6) aligns with the observations from the study by Burrows *et al.*. In their investigation, knockdown of LARP1 in HeLa cells altered the distribution of β- and γ-actin impacting cell migration dynamics (Burrows et al., 2010). Most importantly, in our study, we have confirmed that the LARP1 engaged with the translational machinery interacts with cytoskeleton proteins. One plausible interpretation is that these structural elements allow for the repositioning of LARP1, and potentially the entire 40S-LARP1 complex, across the different subcellular compartments, event that we have observed after mTOR inhibition (Figures R-9 and R-10).

In specific subsets of translationally silenced mRNAs, the protein constituents of the RNP complexes promote their accumulation within cytoplasmic RNA granules, which are non-membrane bound compartments, like stress granules (SGs) or processing bodies (PBs) (Anderson & Kedersha, 2006, 2009). Intriguingly, we observed the presence of stress granules structural elements, like G3BP1, CAPRIN1 and USP10, in polysomal complexes under growing conditions, a biochemical context not

conventionally associated with such structures. Notably, we validated this observation and confirmed the absence of SGs condensates upon mTOR inhibition, as marked by the co-localization with the SG marker G3BP1 (Figures R-6B and R-9). These data suggest that the biochemical accumulation of the 40S-LARP1-5'TOP complex(es) upon mTOR inhibition is not paralleled by evident physical aggregation of LARP1 in any sort of condensates and/or that we could be facing a different RNP structure that does not correspond to canonical SGs. Moreover, the complex could respond to alternative stressful conditions like oxidative stress, independently from the mTOR pathway, as observed upon Sodium Arsenite (Figure R-9) (Wilbertz et al., 2019).

Furthermore, RNA localization is recognized to play an important role in many cellular functions and architecture, for instance, there are many evidence that mRNA localization controls the targeted synthesis of protein within specific cellular compartments, nucleating localized cellular machineries (Lécuyer et al., 2007). This phenomenon, named as local translation, has been previously observed for RP mRNAs in cell protrusions during migration, a process coordinated by the RBP LARP6 (Dermit et al., 2020), as well as in neuronal axons (Fusco et al., 2021; Shigeoka et al., 2019). The redistribution of the LARP1 protein to the ER and the mitochondria upon mTOR inhibition (Figure R-10) may represent one such event, strategically positioning the translational machinery where it will be needed once the conditions become permissive and mTOR pathway is reactivated. Of note, the ER and the mitochondria form highly interconnected structures through the mitochondrial associated membranes (MAMs), that have been described as signaling hubs for stress-activated pathways and cellular processes involved in cancer (Carreras-Sureda et al., 2018; Doghman-Bouguerra & Lalli, 2019). This could imply that the 40S-LARP1 complex is relocalized upon mTOR inhibiting conditions in such structures as a target of such stress pathways, which might regulate its translational status, protein or RNA composition

Considerations about the 40S-LARP1 complex: a heterogeneous RNP complex at different stages of the mRNA life cycle?

Analysis of the interaction network of selected 40S-LARP1 binders showed clustering in specific processes of the RNA and cellular metabolism (Figure R-8). Multiple proteins, identified across conditions, emerged as key regulators of mRNAs biology. In this regard, RNA Binding Proteins (RBPs) orchestrate mRNA processing, transport, stability, translation and degradation, through the recognition of specific *cis*-regulatory elements within transcripts and the formation of RNP functional units (Baltz et al., 2012; Dreyfuss et al., 2002).

Nuclear mRNA processing of transcribed pre-mRNAs involves splicing, capping, 3' end processing, as well as some post-transcriptional modifications. Among the LARP1-associated interactors identified in non-polysomal fractions, we could find proteins involved in pre-mRNA stability such as BCLAF1 and THRAP3 (Bracken et al., 2008) along with components of the splicing machinery such as PRPF8 and PRPF6, heterogeneous nuclear RNPs (hnRNPs) or small nucleolar RNPs (snRNPs) (Wan et al., 2020). Other catalytic proteins involved in mRNA processing included CPSF1, important for polyadenylation at the 3'end (Zhao et al., 1999) or NAT10 an mRNA acetyltransferase (Arango et al., 2018) were also identified. Nuclear export of mRNA, a subsequent step in its life cycle, is carried out by exportins and other associated factors such as RANBP2 (Vetter et al., 1999), found in the 40S-LARP1 interactome. Another nuclear process highly enriched in our MS results was RiBi. TCOF1 and NOLC1 form a platform that regulates RNA PolI, in charge of rRNA production (Werner et al., 2015); NAT10 acetylates rRNA (Suzuki et al., 2014) and POP1 is implicated in rRNA maturation (Goldfarb & Cech, 2017). Furthermore, LSG1 is involved in 60S ribosome biogenesis and export to the cytoplasmic compartment (Kallstrom et al., 2003) (Figures R-7 and R-8). The presence of a high number of nuclear proteins within our study was initially unexpected taking into account that the complexes were isolated from cytoplasmic lysates subjected to polysome profiling. Although a suboptimal isolation of pure

cytoplasmic lysates cannot be discarded, it does not seem to be the case, due to the presence of a great number of nuclear proteins related to RNA-specific events as well as certain partners paired in their functions such as BCLAF1 and THRAP3 (Bracken et al., 2008) or TCOF1 and NOLC1 (Werner et al., 2015). Among the mentioned proteins, the majority have been uniquely described to reside in the nucleus; however, BCLAF1 cytoplasmic localization increases in rectal cancer compared to non-neoplastic tissues (Brown et al., 2016). This could set a scenario in which the cytoplasmic localization of nuclear proteins concedes uncharacterized roles to these proteins. Furthermore, the coordination between the cytoplasmic and the nuclear events is essential for the process of RiBi (See Introduction). The presence of proteins related to the nuclear-cytoplasmic trafficking such as RANBP2, could suggest the implication of the 40S-LARP1 complex in the coordination of this compartmentalization between the transcription and the translation processes.

Cytoplasmic mRNAs are part of several RNP complexes that govern their localization, translational status and degradation. As already mentioned, one of the most prevalent group of proteins found in every condition of the 40S-LARP1 interactome was the cytoplasmic translational machinery, including RPs, eIFs and eEFs (Figure R-6). RNA localization, as well as storage within RNA granules, influence local translation and mRNA half-life. For instance, Staufen (STAU1), an RBP associated with RNA and microtubules in the ER, has been described in RNA-transporting granules in neurons (Kanai et al., 2004). The presence of components of SGs like G3BP1 and CAPRIN1 (Kedersha et al., 2016), also underscored the involvement of the 40S-LARP1 complex in the protection of mRNAs. Finally, proteins associated with mRNA decay pathways, such as components of the RNA exosome (EXOSC10, EXOSC6) (Van Dijk et al., 2007), were also part of the interactome. Moreover, translational inhibitors linked to the miRNA degradation pathway, such as MOV10 (Kenny et al., 2014), were found enriched in the mTOR inhibited non-polysomal samples (Figures R-7 and R-8).

A recent study has developed a tool for analyzing the cellular RBP interactome at distinct stages of the mRNA life cycle. It underscores the complexity of RBPs with multiple simultaneous or context-dependent subcellular localizations to execute different functions, emphasizing the intricate crosstalk between different stages and processes. Notably, they observed how the context can modify the RNP complex composition as

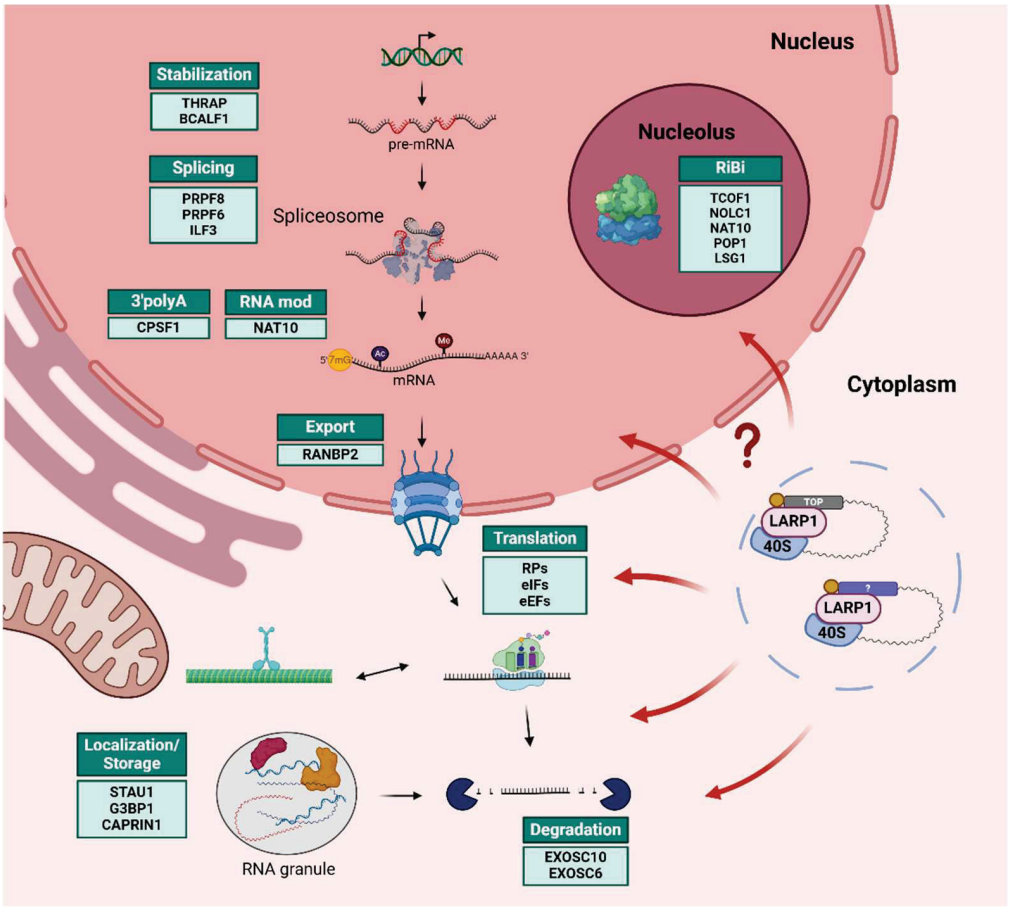

Figure D-1. The partners of the 40S-LARP1 complex engage in all the stages of the mRNA life cycle. Protein interactors of the 40S-LARP1 complex detected in the different experimental conditions were clustered in specific processes of the RNA metabolism. The 40S-LARP1 complex might carry the 5'TOP mRNAs and potentially others through the sequential stages of the mRNA life. Additionally, the protein interactors in charge of subcellular localization might be related to the transport to the structures like the mitochondria and the ER. Green boxes indicate process and selected interactors of the 40S-LARP1 complex. Created with Biorender.com.

well as the recognition and binding to distinct *cis* RNA motifs by the same RBP (Street et al., 2023). In a similar way, we have observed for ILF3 and PHB1, as 40S-LARP1 partners, distinct patterns of stabilization of 5'TOP mRNAs and association to the complex. The absence of co-precipitation of ILF3 and PHB1 suggests potential engagement of the 40S-LARP1 in different complexes (Figures R-11, R-12 and S-2). This hypothesis is supported by the widespread subcellular localization of LARP1 and its modification upon TORi (Figures R-9 and R-11), which might be dependent on the specific partners of the 40S-LARP1 complex. Taken together, this information substantiates the view that the 40S-LARP1 complex serves as the core of distinct heterogeneous RNP complexes, depicting LARP1 as a functional *trans*-acting factor that regulates 5'TOP mRNAs, and potentially other transcripts, at different stages of the mRNA life cycle (Figure D-1). However, further in-depth characterization is needed to validate these unexplored roles and to understand whether the mTOR pathway can regulate the engagement of the 40S-LARP1 complex throughout the stages of the mRNA life cycle.

ILF3 emerges as a novel regulator of 5'TOP mRNA within the 40S-LARP1 complex

The definition of the 40S-LARP1 protein interactome provided a comprehensive overview of the cellular pathways and localizations associated with the functionality of the complex on a broader scale. Following this, our focus shifted towards identifying new functional partners of the 40S-LARP1 complex that might drive selectivity for specific translational programs and/or subcellular localizations. In a first round of analysis of the selected hits, we described two interactors - ILF3 and PHB1 - whose knockdown selectively impacted the levels of RP mRNAs. The investigation of the role of ILF3 in 5'TOP mRNAs stability and the formation of the complex upon mTOR inhibition showed a similar effect to that of LARP1. First, we observed that the downregulation of ILF3 led to a decrease in the total levels of RPL5 and RPL11 transcripts, both in normal growing conditions and following mTOR inhibition (Figure R-11). Furthermore, ILF3

demonstrated the ability to bind endogenous as well as reporter 5'TOP mRNAs in both conditions, with an increased interaction observed specifically upon mTOR inhibition in a LARP1 dependent manner (Figures R-14 and R-15). This was in line with the increased accumulation of ILF3 protein with non-polysomes and its interaction with the 40S-LARP1 complex upon TAK228 treatment (Figures R-12 and R-16). Of note, the interaction with endogenous abundant non-TOP mRNAs such as β-Actin strongly decreased under TOR inhibition (Figure R-15B). Taken together, these results show that ILF3 appears to have a general role over 5'TOP mRNAs biology and that the inhibition of mTOR confers to ILF3 the ability to bind and accumulate with the 40S-LARP1-5'TOP mRNAs complex. In order to test the putative role of ILF3 in the formation of the 40S-LARP1 complex we observed that the downregulation of ILF3 expression did not affect LARP1 accumulation with the non-polysomes upon mTOR inhibition. Notably, the stabilization of RPL5 mRNA with the complex upon the same conditions was impaired (Figure R-18). Conversely, another 5'TOP mRNAs, such as RPS6 (Figure R-18C) or RPL11 (data not shown) transcripts, did not show the same unequivocal pattern. This opens the possibility of a model in which ILF3 plays a role in the accumulation of 5'TOP mRNAs with the 40S-LARP1 complex under unfavorable growth conditions (Figure D-2). However, further studies will be needed to confirm whether the increased interaction of LARP1 with 5'TOP mRNAs in TORi conditions is dependent on ILF3 presence. Finally, we characterized the role of ILF3 in sustaining global protein synthesis (Figure R-19), contradicting the polysome levels (Figure R-18A), a fact that could be explained by a decrease in the elongation rate.

Additionally, ILF3 has been previously described as a protein primarily localized in the nucleus, involved in transcription (Wu et al., 2018), but also in splicing and RNA export (Chen et al., 2004; Gwizdek et al., 2004; Zhou et al., 2002). The cytoplasmic localization of ILF3 has been reported in response to stress conditions such as viral infection and following phosphorylation by PKR (Harashima et al., 2010). Given the predominantly nuclear localization of ILF3 in HCT116 cells (data not shown), this might open the possibility that its role in the maintenance of total 5'TOP mRNAs levels in normal

conditions could be also ascribed to its nuclear functions. Moreover, this hypothesis is supported by the fact that ILF3 knockdown in growing conditions leads to a decrease of total 5'TOP mRNA levels (Figure R-11), while their polysomal levels are maintained (Figure R-18). Conversely, inhibition of the mTOR kinase may induce post-translational modifications in the ILF3 protein, as observed for other mTOR phopsho-targets in the same condition, potentially affecting its subcellular localization to the cytoplasm and its accumulation with the 40S-LARP1 complex. To test this possibility, proximity ligation assays (PLA) experiments will determine the localization of the interaction between ILF3 and LARP1, and whether to ascertain its dependency on the mTOR pathway status.

The role in translation is one of the main cytoplasmic functions attributed to ILF3 [reviewed in (Castella et al., 2015)]. Several studies have highlighted the regulation by ILF3 of distinct translational programs, such as the activation of translation of VEGF mRNA upon hypoxia (Vumbaca et al., 2008) and the repression of ARE-containing mRNAs or the SASP-related transcripts (Kuwano et al., 2009; Tominaga-Yamanaka et al., 2012). This specificity of ILF3 suggests that it could confer to the 40S-LARP1 complex selectivity for a subset of transcripts. A comprehensive analysis of the transcriptome bound by the 40S-LARP1 complex with and without the assistance of ILF3 will be indispensable to address this question. Analysis of common features among these transcripts, such as *cis* elements, will aid in defining novel subsets of 5'TOP mRNAs and non-TOP mRNAs.

PHB1 regulates global translation and 5'TOP mRNAs

Prohibitins, PHB1 and PHB2, were selected as promising hits of the 40S-LARP1 interactome due to their unexpected relation with the cytoplasmic translational machinery and their mitochondrial localization. The specific interaction of both PHBs with the 40S-LARP1 complex and with the translational machinery was confirmed. While their binding to the 40S-LARP1 complex was not affected by mTOR inhibition, their distribution along a polysome gradient revealed a partial shift towards the lighter polysomes (Figures R-12 and R-20). In concordance with a reduced translational

elongation following mTOR inhibition (Gentilella et al., 2015), this might indicate that PHBs, potentially in association with the 40S-LARP1 complex, accumulate in stalled or slowly translating polysomes. Another scenario that might justify this result, is PHB1 stimulating the selective translation of a specific population of mRNAs with a short coding sequence under mTOR inhibition. Either way, the analysis in a LARP1 KO genetic setting will elucidate the involvement of the 40S-LARP1 complex in these processes.

Concerning their role in the 5'TOP biology, and different from ILF3, the downregulation of PHB1 expression selectively reduced the total levels of RP mRNAs only in conditions of mTOR inhibition (Figure R-11). The analysis of the polysome distribution of these mRNAs showed that in normal growing conditions, PHB1 knockdown induced the accumulation of RP mRNAs in the 80S containing fractions together with LARP1 protein,. Upon mTOR inhibition this accumulation was maintained accompanied by the decrease in the polysome-associated mRNAs similar to the controls and by a concomitant decrease of 5'TOPs and LARP1 from the 40S fractions (Figure R-21). Discrepancies in total levels of 5'TOP mRNAs between the two analyses may be attributed to alternative lysing methods, TRIzol or hypotonic lysis buffer respectively, extracting RNA from different subcellular compartments with different efficiencies. This still must be investigated. Interestingly, regarding the formation of the 40S-LARP1 complex, PHB1 knockdown exhibited an opposite effect on LARP1 complexation with the 40S compared to the 80S, decreasing the accumulation of LARP1 in the 40S fractions. Concomitantly, global protein synthesis and specifically the elongation step were impaired (Figure R-22). Together, this observation is compatible with a defect in the recycling of elongating ribosomes loaded with LARP1 and 5'TOP mRNAs to 40S ribosomes, with the accumulation in the 80S an indication of elongation slowdown. Discerning the role of PHB1 as direct interactor of the translational machinery compared to its effect on mTOR signaling pathway would be critical to interpret these results. Additionally, to discern whether these functions are specific to PHB1 or attributable to the PHB complex, these findings should be validated in a PHB2 knockdown context.

The presence of a number of mitochondrial proteins and the re-localization of LARP1 to the mitochondria upon mTOR inhibition prompted us to investigate whether the interaction with PHB1 extended to these organelles. We observe that LARP1 and PHB1 co-localize in the mitochondria in normal conditions (Figure R-23). Surprisingly, PHB1 knockdown induced a small but significant increase in the accumulation of LARP1 within the mitochondria, probably due to the downregulation of the mTOR pathway or to a defect in mitochondrial structure (Osman et al., 2009), rather than as a direct effect on the 40S-LARP1 complex. The functional role of PHB1 as part of the 40S-LARP1 complex still remains elusive. We had previously characterized that the 40S-LARP1 complex also protects cytoplasmic mRNAs encoding for mitochondrial components of the OXPHOS machinery and the mitochondrial ribosome (Fuentes et al., 2021; Gentilella et al., 2017).

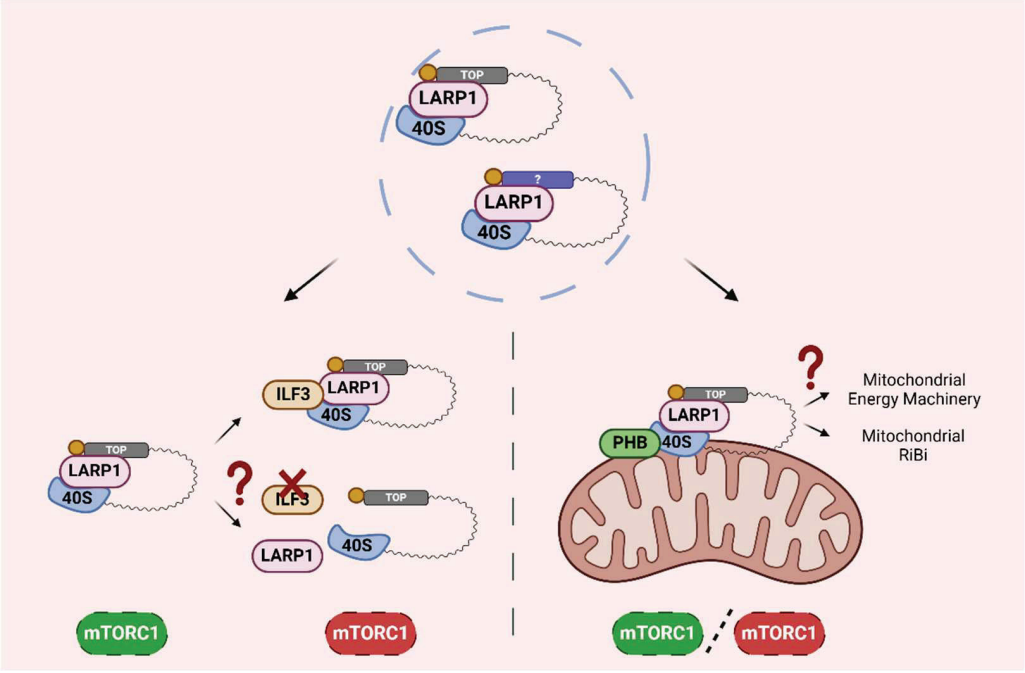

Figure D-2. The 40S-LARP1 complex forms alternative RNP complexes. ILF3 forms the complex upon mTOR inhibition, conditions in which ILF3 might play a role in the accumulation of 5'TOP mRNAs with the 40S-LARP1 complex. On the other hand, PHB1 interacts with LARP1, and potentially the 40S-LARP1 complex, in the mitochondria, which might be implicated in the regulation of the mitochondrial translational program. Created with BioRender.com

Importantly, the PHB complex has been described as a mitochondrial chaperone that regulates the OXPHOS complexes formation at the translational level (Kohler et al., 2023). This could indicate that PHB1 might be implicated in the 40S-LARP1 complex regulation of the mitochondrial translational program (Figure D-2). In a similar way to ILF3, in order to define this translatome, which might include OXPHOS and mitochondrial RPs (MRPs) mRNAs, a characterization by RIP-seq of the 40S-LARP1 complex in conditions of PHB1 depletion would shed light on this.

New implications in Cancer

Several lines of investigation in our laboratory are pointing at the role of the 40S-LARP1 complex as an anabolic asset that cancer cells can utilize to resist adverse growth condition. Specifically, the advantage that the 40S-LARP1 complex confers to cancer cells resides in the protection of the protein synthetic machinery upon stress conditions converging on mTOR inhibition. The depletion of LARP1 protein deprives the capacity of cancer cells to restore ribosome biogenesis and to resume growth upon cessation of the mTOR inhibition treatment (Fuentes et al., 2021). The central role of LARP1 for translation of 5'TOP mRNAs during the recovery from unfavorable conditions categorizes the 40S-LARP1 complex as a subset of cancer-related ribosome, often referred as onco-ribosome. In this doctoral thesis, we have determined that the 40S-LARP1 complex has a heterogeneous protein composition. The different architecture of the ribosome associated proteins (RAPs) contributes to ribosome heterogeneity, influencing the specificity for certain translational programs and subcellular localizations (Genuth & Barna, 2018). Defining the transcriptomes regulated by the 40S-LARP1 sub-complexes, as in the case of ILF3 and PHB1, will disclose new biological pathways that are fed by this reservoir, providing a more complete scenario of the mechanisms involved in the recovery of cancer cells from unfavorable conditions. The identification of novel regulators of the 40S-LARP1 complex would be critical to unravel new vulnerabilities of this anabolic storage in tumors. To date,no chemical components attacking LARP1 or the 40S-LARP1 complex have been developed, thus making of this

study a comprehensive resource of information on this avenue. Indeed, here we have identified two novel regulators of 5'TOP mRNAs and one of them, PHB1 (and the PHB complex), has been proved to be a target of a set of drugs, like FL3 or fluorizoline (FLZ). The mechanisms of action are still controversial. However, their effects recapitulate the downregulation of either PHB1 or PHB2 (Pérez-Perarnau et al., 2014; Thuaud et al., 2013). Importantly, the knockdown of PHB1 decreases the levels of 5'TOP mRNAs only upon mTOR inhibition, conditions of formation of the complex (Figure R-11). It would be of interest to determine whether FL3 or FLZ treatment yield similar effects and prevent re-growth of cancer cells after the release of mTOR inhibition, akin to the impact observed with LARP1 depletion. Such investigations could pave the way for novel therapeutic approaches in the treatment of ribosome biogenesis addicted tumors, such as Colorectal Cancer.

CONCLUSIONS

1. HCT116 cells expressing an endogenous LARP1-GFP protein are a valuable tool for the characterization of the interactome of the 40S-LARP1 complex and to follow LARP1 co-sedimentation with ribosomes in real-time with a dropwise resolution.

2. The 40S-LARP1 complex composition changes according to the translational status and the mTOR pathway.

3. The 40S-LARP1 complex interacts with proteins related to a diversity of processes involving RNA regulation and translation, as well as cellular anabolic pathways required for protein synthesis and energy production.

4. LARP1 has a widespread localization largely cytoplasmatic, and upon mTOR inhibition part of it re-distributes to the endoplasmic reticulum and the mitochondria.

5. The accumulation of the 40S-LARP1 anabolic storage observed in biochemical fractionations, is not organized in canonical stress granules upon mTOR inhibition.

6. ILF3 expression sustain total levels of RP mRNAs upon normal conditions and mTOR inhibition, whilst PHB1 only upon mTOR inhibition.

7. ILF3 and PHB1 partner with the 40S-LARP1 complex in distinct RNPs.

8. ILF3 binds to 5'TOP mRNAs and this association increases upon mTOR inhibition in a LARP1-dependent manner.

9. PHB1 interacts with the translational machinery and the 40S-LARP1 complex and its deficiency impacts translation elongation upon normal growth conditions and mTOR inhibition.

10. PHB1 and LARP1 co-localize in the mitochondria.

REFERENCES

Adler, A. S., McCleland, M. L., Yee, S., Yaylaoglu, M., Hussain, S., Cosino, E., Quinones, G., Modrusan, Z., Seshagiri, S., Torres, E., Chopra, V. S., Haley, B., Zhang, Z., Blackwood, E. M., Singh, M., Junttila, M., Stephan, J. P., Liu, J., Pau, G., … Firestein, R. (2014). An integrative analysis of colon cancer identifies an essential function for PRPF6 in tumor growth. *Genes and Development*, *28*(10), 1068–1084. https://doi.org/10.1101/gad.237206.113

Anderson, P., & Kedersha, N. (2006). RNA granules. In *Journal of Cell Biology* (Vol. 172, Issue 6, pp. 803–808). https://doi.org/10.1083/jcb.200512082

Anderson, P., & Kedersha, N. (2009). RNA granules: Post-transcriptional and epigenetic modulators of gene expression. In *Nature Reviews Molecular Cell Biology* (Vol. 10, Issue 6, pp. 430–436). https://doi.org/10.1038/nrm2694

Aoki, K., Adachi, S., Homoto, M., Kusano, H., Koike, K., & Natsume, T. (2013). LARP1 specifically recognizes the 3′ terminus of poly(A) mRNA. *FEBS Letters*, *587*(14), 2173–2178. https://doi.org/10.1016/j.febslet.2013.05.035

Arabi, A., Wu, S., Ridderstråle, K., Bierhoff, H., Shiue, C., Fatyol, K., Fahlén, S., Hydbring, P., Söderberg, O., Grummt, I., Larsson, L. G., & Wright, A. P. H. (2005). c-Myc associates with ribosomal DNA and activates RNA polymerase I transcription. *Nature Cell Biology*, *7*(3), 303–310. https://doi.org/10.1038/ncb1225

Arango, D., Sturgill, D., Alhusaini, N., Dillman, A. A., Sweet, T. J., Hanson, G., Hosogane, M., Sinclair, W. R., Nanan, K. K., Mandler, M. D., Fox, S. D., Zengeya, T. T., Andresson, T., Meier, J. L., Coller, J., & Oberdoerffer, S. (2018). Acetylation of Cytidine in mRNA Promotes Translation Efficiency. *Cell*, *175*(7), 1872-1886.e24. https://doi.org/10.1016/j.cell.2018.10.030

Avni, D., Shama, S., Loreni, F., & Meyuhas, O. (1994). Vertebrate mRNAs with a 5′-Terminal Pyrimidine Tract Are Candidates for Translational Repression in Quiescent Cells: Characterization of the Translational cis -Regulatory Element . *Molecular and Cellular Biology*, *14*(6), 3822–3833. https://doi.org/10.1128/mcb.14.6.3822-3833.1994

Back, J. W., Sanz, M. A., de Jong, L., de Koning, L. J., Nijtmans, L. G. J., de Koster, C. G., Grivell, L. A., van der Spek, H., & Muijsers, A. O. (2002). A structure for the yeast prohibitin complex: Structure prediction and evidence from chemical crosslinking and mass spectrometry. *Protein Science*, *11*(10), 2471–2478. https://doi.org/10.1110/ps.0212602

Baltz, A. G., Munschauer, M., Schwanhäusser, B., Vasile, A., Murakawa, Y., Schueler, M., Youngs, N., Penfold-Brown, D., Drew, K., Milek, M., Wyler, E., Bonneau, R., Selbach,

M., Dieterich, C., & Landthaler, M. (2012). The mRNA-Bound Proteome and Its Global Occupancy Profile on Protein-Coding Transcripts. *Molecular Cell*, *46*(5), 674–690. https://doi.org/10.1016/j.molcel.2012.05.021

Barna, M., Pusic, A., Zollo, O., Costa, M., Kondrashov, N., Rego, E., Rao, P. H., & Ruggero, D. (2008). Suppression of Myc oncogenic activity by ribosomal protein haploinsufficiency. *Nature*, *456*(7224), 971–975. https://doi.org/10.1038/nature07449

Ben-Sahra, I., Howell, J., Asara, J., & Manning, B. (2013). Stimulation of de Novo Pyrimidine Synthesis by Growth Signaling Through mTOR and S6K1. *Science*, *339*(6125), 1323–1328. https://doi.org/10.1126/science.1228771

Ben-Sahra, I., Hoxhaj, G., Ricoult, S., Asara, J., & Manning, B. (2016). mTORC1 induces purine synthesis through control of the mitochondrial tetrahydrofolate cycle. *Science*, *351*(6274), 728–733. https://doi.org/10.1126/science.aac5681

Ben-Shem, A., Garreau de Loubresse, N., Melnikov, S., Jenner, L., Yusupova, G., & Yusupov, M. (2011). The Structure of the Eukaryotic Ribosome at 3.0 Å Resolution. *Science*, *334*(6062), 1524–1529. https://doi.org/10.1126/science.1205438

Berman, A. J., Thoreen, C. C., Dedeic, Z., Chettle, J., Roux, P. P., & Blagden, S. P. (2021). Controversies around the function of LARP1. *RNA Biology*, *18*(2), 207–217. https://doi.org/10.1080/15476286.2020.1733787

Biever, A., Glock, C., Tushev, G., Ciirdaeva, E., Dalmay, T., Langer, J. D., & Schuman, E. M. (2020). Monosomes actively translate synaptic mRNAs in neuronal processes. *Science*, *367*(6477). https://doi.org/10.1126/science.aay4991

Blagden, S. P., Gatt, M. K., Archambault, V., Lada, K., Ichihara, K., Lilley, K. S., Inoue, Y. H., & Glover, D. M. (2009). Drosophila Larp associates with poly(A)-binding protein and is required for male fertility and syncytial embryo development. *Developmental Biology*, *334*(1), 186–197. https://doi.org/10.1016/j.ydbio.2009.07.016

Boon, K., Caron, H. N., Van Asperen, R., Valentijn, L., Hermus, M. C., Van Sluis, P., Roobeek, I., Weis, I., Voûte, P. A., Schwab, M., & Versteeg, R. (2001). N-myc enhances the expression of a large set of genes functioning in ribosome biogenesis and protein synthesis. *EMBO Journal*, *20*(6), 1383–1393. https://doi.org/10.1093/emboj/20.6.1383

Bousquet-Antonelli, C., & Deragon, J. M. (2009). A comprehensive analysis of the La-motif protein superfamily. *RNA*, *15*(5), 750–764. https://doi.org/10.1261/rna.1478709

Bracken, C. P., Wall, S. J., Barré, B., Panov, K. I., Ajuh, P. M., & Perkins, N. D. (2008). Regulation of cyclin D1 RNA stability by SNIP1. *Cancer Research*, *68*(18), 7621–7628. https://doi.org/10.1158/0008-5472.CAN-08-1217

Browman, D. T., Hoegg, M. B., & Robbins, S. M. (2007). The SPFH domain-containing proteins: more than lipid raft markers. *Trends in Cell Biology*, *17*(8), 394–402. https://doi.org/10.1016/j.tcb.2007.06.005

Brown, G. T., Cash, B., Alnabulsi, A., Samuel, L. M., & Murray, G. I. (2016). The expression and prognostic significance of bcl-2-associated transcription factor 1 in rectal cancer following neoadjuvant therapy. *Histopathology*, *68*(4), 556–566. https://doi.org/10.1111/his.12780

Brugarolas, J., Lei, K., Hurley, R. L., Manning, B. D., Reiling, J. H., Hafen, E., Witters, L. A., Ellisen, L. W., & Kaelin, W. G. (2004). Regulation of mTOR function in response to hypoxia by REDD1 and the TSC1/TSC2 tumor suppressor complex. *Genes and Development*, *18*(23), 2893–2904. https://doi.org/10.1101/gad.1256804

Buckup, M., Rice, M. A., Hsu, E. C., Garcia-Marques, F., Liu, S., Aslan, M., Bermudez, A., Huang, J., Pitteri, S. J., & Stoyanova, T. (2021). Plectin is a regulator of prostate cancer growth and metastasis. *Oncogene*, *40*(3), 663–676. https://doi.org/10.1038/s41388-020-01557-9

Burger, K., Mühl, B., Harasim, T., Rohrmoser, M., Malamoussi, A., Orban, M., Kellner, M., Gruber-Eber, A., Kremmer, E., Hölzel, M., & Eick, D. (2010). Chemotherapeutic drugs inhibit ribosome biogenesis at various levels. *Journal of Biological Chemistry*, *285*(16), 12416–12425. https://doi.org/10.1074/jbc.M109.074211

Burrows, C., Abd Latip, N., Lam, S. J., Carpenter, L., Sawicka, K., Tzolovsky, G., Gabra, H., Bushell, M., Glover, D. M., Willis, A. E., & Blagden, S. P. (2010). The RNA binding protein Larp1 regulates cell division, apoptosis and cell migration. *Nucleic Acids Research*, *38*(16), 5542–5553. https://doi.org/10.1093/nar/gkq294

Bustelo, X. R., & Dosil, M. (2018). Ribosome biogenesis and cancer: basic and translational challenges. In *Current Opinion in Genetics and Development* (Vol. 48, pp. 22–29). Elsevier Ltd. https://doi.org/10.1016/j.gde.2017.10.003

Bywater, M. J., Poortinga, G., Sanij, E., Hein, N., Peck, A., Cullinane, C., Wall, M., Cluse, L., Drygin, D., Anderes, K., Huser, N., Proffitt, C., Bliesath, J., Haddach, M., Schwaebe, M. K., Ryckman, D. M., Rice, W. G., Schmitt, C., Lowe, S. W., … Hannan, R. D. (2012). Inhibition of RNA Polymerase I as a Therapeutic Strategy to Promote Cancer-Specific Activation of p53. *Cancer Cell*, *22*(1), 51–65. https://doi.org/10.1016/j.ccr.2012.05.019

Cárdenas, C., Miller, R. A., Smith, I., Bui, T., Molgó, J., Müller, M., Vais, H., Cheung, K. H., Yang, J., Parker, I., Thompson, C. B., Birnbaum, M. J., Hallows, K. R., & Foskett, J. K. (2010). Essential Regulation of Cell Bioenergetics by Constitutive InsP3 Receptor

Ca2+ Transfer to Mitochondria. *Cell*, *142*(2), 270–283. https://doi.org/10.1016/j.cell.2010.06.007

Cárdenas, C., Müller, M., McNeal, A., Lovy, A., Jaňa, F., Bustos, G., Urra, F., Smith, N., Molgó, J., Diehl, J. A., Ridky, T. W., & Foskett, J. K. (2016). Selective Vulnerability of Cancer Cells by Inhibition of Ca2+ Transfer from Endoplasmic Reticulum to Mitochondria. *Cell Reports*, *14*(10), 2313–2324. https://doi.org/10.1016/j.celrep.2016.02.030

Carreras-Sureda, A., Pihán, P., & Hetz, C. (2018). Calcium signaling at the endoplasmic reticulum: fine-tuning stress responses. In *Cell Calcium* (Vol. 70, pp. 24–31). Elsevier Ltd. https://doi.org/10.1016/j.ceca.2017.08.004

Castella, S., Bernard, R., Corno, M., Fradin, A., & Larcher, J. C. (2015). Ilf3 and NF90 functions in RNA biology. In *Wiley Interdisciplinary Reviews: RNA* (Vol. 6, Issue 2, pp. 243–256). https://doi.org/10.1002/wrna.1270

Chan, J. C., Hannan, K. M., Riddell, K., Yee Ng, P., Peck, A., Lee, R. S., Hung, S., Astle, M. V, Bywater, M., Wall, M., Poortinga, G., Jastrzebski, K., Sheppard, K. E., Hemmings, B. A., Hall, M. N., Johnstone, R. W., McArthur, G. A., Hannan, R. D., & Pearson, R. B. (2011). AKT Promotes rRNA Synthesis and Cooperates with c-MYC to Stimulate Ribosome Biogenesis in Cancer. *Science Signalling*, *4*(188). https://doi.org/10.1126/scisignal.2001754

Charitou, T., Srihari, S., Lynn, M. A., Jarboui, M. A., Fasterius, E., Moldovan, M., Shirasawa, S., Tsunoda, T., Ueffing, M., Xie, J., Xin, J., Wang, X., Proud, C. G., Boldt, K., Al-Khalili Szigyarto, C., Kolch, W., & Lynn, D. J. (2019). Transcriptional and metabolic rewiring of colorectal cancer cells expressing the oncogenic KRASG13D mutation. *British Journal of Cancer*, *121*(1), 37–50. https://doi.org/10.1038/s41416-019-0477-7

Chaumet, A., Castella, S., Gasmi, L., Fradin, A., Clodic, G., Bolbach, G., Poulhe, R., Denoulet, P., & Larcher, J. C. (2013). Proteomic analysis of interleukin enhancer binding factor 3 (Ilf3) and nuclear factor 90 (NF90) interactome. *Biochimie*, *95*(6), 1146–1157. https://doi.org/10.1016/j.biochi.2013.01.004

Chauvin, C., Koka, V., Nouschi, A., Mieulet, V., Hoareau-Aveilla, C., Dreazen, A., Cagnard, N., Carpentier, W., Kiss, T., Meyuhas, O., & Pende, M. (2014). Ribosomal protein S6 kinase activity controls the ribosome biogenesis transcriptional program. *Oncogene*, *33*(4), 474–483. https://doi.org/10.1038/onc.2012.606

Cheng, J., Gao, F., Chen, X., Wu, J., Xing, C., Lv, Z., Xu, W., Xie, Q., Wu, L., Ye, S., Xie, H., Zheng, S., & Zhou, L. (2014). Prohibitin-2 promotes hepatocellular carcinoma malignancy progression in hypoxia based on a label-free quantitative proteomics strategy. *Molecular Carcinogenesis*, *53*(10), 820–832. https://doi.org/10.1002/mc.22040

Chen, T., Brownawell, A. M., & Macara, I. G. (2004). Nucleocytoplasmic Shuttling of JAZ, a New Cargo Protein for Exportin-5. *Molecular and Cellular Biology*, *24*(15), 6608–6619. https://doi.org/10.1128/mcb.24.15.6608-6619.2004

Chen, Y., Li, Y., Xiong, J., Lan, B., Wang, X., Liu, J., Lin, J., Fei, Z., Zheng, X., & Chen, C. (2021). Role of PRKDC in cancer initiation, progression, and treatment. *Cancer Cell International*, *21*(1). https://doi.org/10.1186/s12935-021-02229-8

Chen, Y. W., Chou, H. C., Lyu, P. C., Yin, H. S., Huang, F. L., Chang, W. S. W., Fan, C. Y., Tu, I. F., Lai, T. C., Lin, S. T., Lu, Y. C., Wu, C. L., Huang, S. H., & Chan, H. L. (2011). Mitochondrial proteomics analysis of tumorigenic and metastatic breast cancer markers. *Functional and Integrative Genomics*, *11*(2), 225–239. https://doi.org/10.1007/s10142-011-0210-y

Choi, H., Larsen, B., Lin, Z. Y., Breitkreutz, A., Mellacheruvu, D., Fermin, D., Qin, Z. S., Tyers, M., Gingras, A. C., & Nesvizhskii, A. I. (2011). SAINT: Probabilistic scoring of affinity purificationg-mass spectrometry data. *Nature Methods*, *8*(1), 70–73. https://doi.org/10.1038/nmeth.1541

Collart, M. A., & Panasenko, O. O. (2012). The Ccr4-Not complex. *Gene*, *492*(1), 42–53. https://doi.org/10.1016/j.gene.2011.09.033

Corthésy, B., & Kao, P. N. (1994). Purification by DNA affinity chromatography of two polypeptides that contact the NF-AT DNA binding site in the interleukin 2 promoter. *Journal of Biological Chemistry*, *269*(32), 20682–20690. https://doi.org/10.1016/s0021-9258(17)32047-1

Damgaard, C. K., & Lykke-Andersen, J. (2011). Translational coregulation of 5'TOP mRNAs by TIA-1 and TIAR. *Genes and Development*, *25*(19), 2057–2068. https://doi.org/10.1101/gad.17355911

Dermit, M., Dodel, M., Lee, F. C. Y., Azman, M. S., Schwenzer, H., Jones, J. L., Blagden, S. P., Ule, J., & Mardakheh, F. K. (2020). Subcellular mRNA Localization Regulates Ribosome Biogenesis in Migrating Cells. *Developmental Cell*, *55*(3), 298-313.e10. https://doi.org/10.1016/j.devcel.2020.10.006

Dienstmann, R., Rodon, J., Serra, V., & Tabernero, J. (2014). Picking the point of inhibition: A comparative review of PI3K/AKT/mTOR pathway inhibitors. *Molecular Cancer Therapeutics*, *13*(5), 1021–1031. https://doi.org/10.1158/1535-7163.MCT-13-0639

Doghman-Bouguerra, M., & Lalli, E. (2019). ER-mitochondria interactions: Both strength and weakness within cancer cells. *Biochimica et Biophysica Acta (BBA) - Molecular Cell Research*, *1866*(4), 650–662. https://doi.org/10.1016/j.bbamcr.2019.01.009

Domostegui, A., Peddigari, S., Mercer, C. A., Iannizzotto, F., Rodriguez, M. L., Garcia-Cajide, M., Amador, V., Diepstraten, S. T., Kelly, G. L., Salazar, R., Kozma, S. C.,

Kusnadi, E. P., Kang, J., Gentilella, A., Pearson, R. B., Thomas, G., & Pelletier, J. (2021). Impaired ribosome biogenesis checkpoint activation induces p53-dependent MCL-1 degradation and MYC-driven lymphoma death. *Blood*, *137*(24), 3351–3364. https://doi.org/10.1182/blood.2020007452

Donati, G., Peddigari, S., Mercer, C. A., & Thomas, G. (2013). 5S Ribosomal RNA Is an Essential Component of a Nascent Ribosomal Precursor Complex that Regulates the Hdm2-p53 Checkpoint. *Cell Reports*, *4*(1), 87–98. https://doi.org/10.1016/j.celrep.2013.05.045

Dorrello, N., Peschiaroli, A., Guardavaccaro, D., Colburn, N., Sherman, N., & Pagano, M. (2006). S6K1- and bTRCP-Mediated Degradation of PDCD4 Promotes Protein Translation and Cell Growth. *Science*, *314*(5798), 467–471.

Dreyfuss, G., Kim, V. N., & Kataoka, N. (2002). Messenger-RNA-binding proteins and the messages they carry. *Nature Reviews Molecular Cell Biology*, *3*(3), 195–205. https://doi.org/10.1038/nrm760

Emmott, E., Jovanovic, M., & Slavov, N. (2019). Ribosome Stoichiometry: From Form to Function. *Trends in Biochemical Sciences*, *44*(2), 95–109. https://doi.org/10.1016/j.tibs.2018.10.009

Farley, K. I., & Baserga, S. J. (2016). Probing the mechanisms underlying human diseases in making ribosomes. *Biochemical Society Transactions*, *44*(4), 1035–1044. https://doi.org/10.1042/BST20160064

Farooq, Z., Kusuma, F., Burke, P., Dufour, C. R., Lee, D., Tabatabaei, N., Toboz, P., Radovani, E., Greenblatt, J. F., Rehman, J., Class, J., Khoutorsky, A., Fonseca, B. D., Richner, J. M., Mercier, E., Bourque, G., Giguère, V., Subramaniam, A. R., Han, J., & Tahmasebi, S. (2022). The amino acid sensor GCN2 suppresses terminal oligopyrimidine (TOP) mRNA translation via La-related protein 1 (LARP1). *Journal of Biological Chemistry*, *298*(9). https://doi.org/10.1016/j.jbc.2022.102277

Feng, Z., Hu, W., De Stanchina, E., Teresky, A. K., Jin, S., Lowe, S., & Levine, A. J. (2007). The regulation of AMPK β1, TSC2, and PTEN expression by p53: Stress, cell and tissue specificity, and the role of these gene products in modulating the IGF-1-AKT-mTOR pathways. *Cancer Research*, *67*(7), 3043–3053. https://doi.org/10.1158/0008-5472.CAN-06-4149

Fonseca, B. D., Zakaria, C., Jia, J. J., Graber, T. E., Svitkin, Y., Tahmasebi, S., Healy, D., Hoang, H. D., Jensen, J. M., Diao, I. T., Lussier, A., Dajadian, C., Padmanabhan, N., Wang, W., Matta-Camacho, E., Hearnden, J., Smith, E. M., Tsukumo, Y., Yanagiya, A., … Damgaard, C. K. (2015). La-related protein 1 (LARP1) represses terminal oligopyrimidine (TOP) mRNA translation downstream of mTOR complex 1 (mTORC1). *Journal of Biological Chemistry*, *290*(26), 15996–16020. https://doi.org/10.1074/jbc.M114.621730

Foskett, J. K., White, C., Cheung, K.-H., & Mak, D.-O. D. (2007). Inositol Trisphosphate Receptor Ca 2 Release Channels. *Physiology Review*, *87*, 593–658. https://doi.org/doi:10.1152/physrev.00035.2006.

Fuentes, P., Pelletier, J., Martinez-Herráez, C., Diez-Obrero, V., Iannizzotto, F., Rubio, T., Garcia-Cajide, M., Menoyo, S., Moreno, V., Salazar, R., Tauler, A., & Gentilella, A. (2021). The 40S-LARP1 complex reprograms the cellular translatome upon mTOR inhibition to preserve the protein synthetic capacity. *Science Advances*, *7*, 9275.

Fumagalli, S., Di Cara, A., Neb-Gulati, A., Natt, F., Schwemberger, S., Hall, J., Babcock, G. F., Bernardi, R., Pandolfi, P. P., & Thomas, G. (2009). Absence of nucleolar disruption after impairment of 40S ribosome biogenesis reveals an rpL11-translationdependent mechanism of p53 induction. *Nature Cell Biology*, *11*(4), 501–508. https://doi.org/10.1038/ncb1858

Fusaro, G., Dasgupta, P., Rastogi, S., Joshi, B., & Chellappan, S. (2003). Prohibitin Induces the Transcriptional Activity of p53 and Is Exported from the Nucleus upon Apoptotic Signaling. *Journal of Biological Chemistry*, *278*(48), 47853–47861. https://doi.org/10.1074/jbc.M305171200

Fusco, C. M., Desch, K., Dörrbaum, A. R., Wang, M., Staab, A., Chan, I. C. W., Vail, E., Villeri, V., Langer, J. D., & Schuman, E. M. (2021). Neuronal ribosomes exhibit dynamic and context-dependent exchange of ribosomal proteins. *Nature Communications*, *12*(1). https://doi.org/10.1038/s41467-021-26365-x

Garcia-Echeverria, C. (2011). Blocking the mTOR pathway: A drug discovery perspective. *Biochemical Society Transactions*, *39*(2), 451–455. https://doi.org/10.1042/BST0390451

Gentilella, A., Kozma, S. C., & Thomas, G. (2015). A liaison between mTOR signaling, ribosome biogenesis and cancer. *Biochimica et Biophysica Acta - Gene Regulatory Mechanisms*, *1849*(7), 812–820. https://doi.org/10.1016/j.bbagrm.2015.02.005

Gentilella, A., Morón-Duran, F. D., Fuentes, P., Rocha, G. Z., Riaño-Canalias, F., Pelletier, J., Ruiz, M., Turón, G., Castaño, J., Tauler, A., Bueno, C., Menéndez, P., Kozma, S. C., & Thomas, G. (2017a). Autogenous Control of 5'TOP mRNA Stability by 40S Ribosomes. *Molecular Cell*, *67*(1), 55-70.e4. https://doi.org/10.1016/j.molcel.2017.06.005

Gentilella, A., Morón-Duran, F. D., Fuentes, P., Rocha, G. Z., Riaño-Canalias, F., Pelletier, J., Ruiz, M., Turón, G., Castaño, J., Tauler, A., Bueno, C., Menéndez, P., Kozma, S. C., & Thomas, G. (2017b). Autogenous Control of 5'TOP mRNA Stability by 40S Ribosomes. *Molecular Cell*, *67*(1), 55-70.e4. https://doi.org/10.1016/j.molcel.2017.06.005

Genuth, N. R., & Barna, M. (2018). The Discovery of Ribosome Heterogeneity and Its Implications for Gene Regulation and Organismal Life. *Molecular Cell*, *71*(3), 364–374. https://doi.org/10.1016/j.molcel.2018.07.018

Gillen, S. L., Giacomelli, C., Hodge, K., Zanivan, S., Bushell, M., & Wilczynska, A. (2021). Differential regulation of mRNA fate by the human Ccr4-Not complex is driven by coding sequence composition and mRNA localization. *Genome Biology*, *22*(1). https://doi.org/10.1186/s13059-021-02494-w

Gingras, A.-C., Kennedy, S. G., O'leary, M. A., Sonenberg, N., & Hay, N. (1998). 4E-BP1, a repressor of mRNA translation, is phosphorylated and inactivated by the Akt(PKB) signaling pathway. *Genes and Development*, *12*, 502–513.

Gismondi, A., Caldarola, S., Lisi, G., Juli, G., Chellini, L., Iadevaia, V., Proud, C. G., & Loreni, F. (2014). Ribosomal stress activates eEF2K-eEF2 pathway causing translation elongation inhibition and recruitment of Terminal Oligopyrimidine (TOP) mRNAs on polysomes. *Nucleic Acids Research*, *42*(10), 12668–12680. https://doi.org/10.1093/nar/gku996

Goldfarb, K. C., & Cech, T. R. (2017). Targeted CRISPR disruption reveals a role for RNase MRP RNA in human preribosomal RNA processing. *Genes and Development*, *31*(1), 59–71. https://doi.org/10.1101/gad.286963.116

Gomez-Roman, N., Grandori, C., Eisenman, R. N., & White, R. J. (2003). Direct activation of RNA polymerase III transcription by c-Myc. *Nature*, *421*(6920), 290–294. https://doi.org/10.1038/nature01327.

Grandori, C., Gomez-Roman, N., Felton-Edkins, Z. A., Ngouenet, C., Galloway, D. A., Eisenman, R. N., & White, R. J. (2005). c-Myc binds to human ribosomal DNA and stimulates transcription of rRNA genes by RNA polymerase I. *Nature Cell Biology*, *7*(3), 311–318. https://doi.org/10.1038/ncb1224

Granneman, S., & Baserga, S. J. (2004). Ribosome biogenesis: Of knobs and RNA processing. *Experimental Cell Research*, *296*(1), 43–50. https://doi.org/10.1016/j.yexcr.2004.03.016

Green, R., & Noller, H. F. (1997). Ribosomes and Translation. *Annu. Rev. Biochem*, *66*, 679–716.

Gregory-Bass, R. C., Olatinwo, M., Xu, W., Matthews, R., Stiles, J. K., Thomas, K., Liu, D., Tsang, B., & Thompson, W. E. (2008). Prohibitin silencing reverses stabilization of mitochondrial integrity and chemoresistance in ovarian cancer cells by increasing their sensitivity to apoptosis. *International Journal of Cancer*, *122*(9), 1923–1930. https://doi.org/10.1002/ijc.23351

Guan, D., Altan-Bonnet, N., Parrott, A. M., Arrigo, C. J., Li, Q., Khaleduzzaman, M., Li, H., Lee, C.-G., Pe'ery, T., & Mathews, M. B. (2008). Nuclear Factor 45 (NF45) Is a

Regulatory Subunit of Complexes with NF90/110 Involved in Mitotic Control. *Molecular and Cellular Biology*, *28*(14), 4629–4641. https://doi.org/10.1128/mcb.00120-08

Gwinn, D. M., Shackelford, D. B., Egan, D. F., Mihaylova, M. M., Mery, A., Vasquez, D. S., Turk, B. E., & Shaw, R. J. (2008). AMPK Phosphorylation of Raptor Mediates a Metabolic Checkpoint. *Molecular Cell*, *30*(2), 214–226. https://doi.org/10.1016/j.molcel.2008.03.003

Gwizdek, C., Ossareh-Nazari, B., Brownawell, A. M., Evers, S., Macara, I. G., & Dargemont, C. (2004). Minihelix-containing RNAs Mediate Exportin-5-dependent Nuclear Export of the Double-stranded RNA-binding Protein ILF3. *Journal of Biological Chemistry*, *279*(2), 884–891. https://doi.org/10.1074/jbc.M306808200

Hanahan, D., & Weinberg, R. A. (2011). Hallmarks of cancer: The next generation. In *Cell* (Vol. 144, Issue 5, pp. 646–674). https://doi.org/10.1016/j.cell.2011.02.013

Haneke, K., Schott, J., Lindner, D., Hollensen, A. K., Damgaard, C. K., Mongis, C., Knop, M., Palm, W., Ruggieri, A., & Stoecklin, G. (2020). CDK1 couples proliferation with protein synthesis. *Journal of Cell Biology*, *219*(3). https://doi.org/10.1083/jcb.201906147

Hannan, K. M., Brandenburger, Y., Jenkins, A., Sharkey, K., Cavanaugh, A., Rothblum, L., Moss, T., Poortinga, G., McArthur, G. A., Pearson, R. B., & Hannan, R. D. (2003). mTOR-Dependent Regulation of Ribosomal Gene Transcription Requires S6K1 and Is Mediated by Phosphorylation of the Carboxy-Terminal Activation Domain of the Nucleolar Transcription Factor UBF†. *Molecular and Cellular Biology*, *23*(23), 8862–8877. https://doi.org/10.1128/mcb.23.23.8862-8877.2003

Hara, K., Maruki, Y., Long, X., Yoshino, K.-I., Oshiro, N., Hidayat, S., Tokunaga, C., Avruch, J., & Yonezawa, K. (2002). Raptor, a Binding Partner of Target of Rapamycin (TOR), Mediates TOR Action. *Cell*, *110*, 177–189.

Harashima, A., Guettouche, T., & Barber, G. N. (2010). Phosphorylation of the NFAR proteins by the dsRNA-dependent protein kinase PKR constitutes a novel mechanism of translational regulation and cellular defense. *Genes and Development*, *24*(23), 2640–2653. https://doi.org/10.1101/gad.1965010

Hong, S., Freeberg, M. A., Han, T., Kamath, A., Yao, Y., Fukuda, T., Suzuki, T., Kim, J. K., & Inoki, K. (2017). LARP1 functions as a molecular switch for mTORC1-mediated translation of an essential class of mRNAs. *ELife*, *6*(e25237). https://doi.org/10.7554/eLife.25237.001

Hopkins, T. G., Mura, M., Al-Ashtal, H. A., Lahr, R. M., Abd-Latip, N., Sweeney, K., Lu, H., Weir, J., El-Bahrawy, M., Steel, J. H., Ghaem-Maghami, S., Aboagye, E. O., Berman, A. J., & Blagden, S. P. (2016). The RNA-binding protein LARP1 is a post-

transcriptional regulator of survival and tumorigenesis in ovarian cancer. *Nucleic Acids Research*, *44*(3), 1227–1246. https://doi.org/10.1093/nar/gkv1515

Hsieh, A. C., Liu, Y., Edlind, M. P., Ingolia, N. T., Janes, M. R., Sher, A., Shi, E. Y., Stumpf, C. R., Christensen, C., Bonham, M. J., Wang, S., Ren, P., Martin, M., Jessen, K., Feldman, M. E., Weissman, J. S., Shokat, K. M., Rommel, C., & Ruggero, D. (2012). The translational landscape of mTOR signalling steers cancer initiation and metastasis. *Nature*, *485*(7396), 55–61. https://doi.org/10.1038/nature10912

Hsu, P. P., Kang, S. A., Rameseder, J., Zhang, Y., Ottina, K. A., Lim, D., Peterson, T. R., Choi, Y., Gray, N. S., Yaffe, M. B., Marto, J. A., & Sabatini, D. M. (2011). The mTOR-regulated phosphoproteome reveals a mechanism of mTORC1-mediated inhibition of growth factor signaling. *Science*, *332*(6035), 1317–1322. https://doi.org/10.1126/science.1199498

Hu, Q., Lu, Y. Y., Noh, H., Hong, S., Dong, Z., Ding, H. F., Su, S. B., & Huang, S. (2013). Interleukin enhancer-binding factor 3 promotes breast tumor progression by regulating sustained urokinase-type plasminogen activator expression. *Oncogene*, *32*(34), 3933–3943. https://doi.org/10.1038/onc.2012.414

Ikonen, E., Fiedler, K., Parton, R. G., & Simons, K. (1995). Prohibitin, an antiproliferative protein, is localized to mitochondria. *FEBS Letters*, *358*(3), 273–277. https://doi.org/10.1016/0014-5793(94)01444-6

Inoki, K., Li, Y., Xu, T., & Guan, K. L. (2003). Rheb GTpase is a direct target of TSC2 GAP activity and regulates mTOR signaling. *Genes and Development*, *17*(15), 1829–1834. https://doi.org/10.1101/gad.1110003

Inoki, K., Li, Y., Zhu, T., Wu, J., & Guan, K. L. (2002). TSC2 is phosphorylated and inhibited by Akt and suppresses mTOR signalling. *Nature Cell Biology*, *4*(9), 648–657. https://doi.org/10.1038/ncb839

Inoki, K., Ouyang, H., Zhu, T., Lindvall, C., Wang, Y., Zhang, X., Yang, Q., Bennett, C., Harada, Y., Stankunas, K., Wang, C. yu, He, X., MacDougald, O. A., You, M., Williams, B. O., & Guan, K. L. (2006). TSC2 Integrates Wnt and Energy Signals via a Coordinated Phosphorylation by AMPK and GSK3 to Regulate Cell Growth. *Cell*, *126*(5), 955–968. https://doi.org/10.1016/j.cell.2006.06.055

Inoki, K., Zhu, T., & Guan, K.-L. (2003). TSC2 Mediates Cellular Energy Response to Control Cell Growth and Survival. *Cell*, *115*, 577–590.

Jacinto, E., Loewith, R., Schmidt, A., Lin, S., Rüegg, M. A., Hall, A., & Hall, M. N. (2004). Mammalian TOR complex 2 controls the actin cytoskeleton and is rapamycin insensitive. *Nature Cell Biology*, *6*(11), 1122–1128. https://doi.org/10.1038/ncb1183

Jackson, D. N., Alula, K. M., Delgado-Deida, Y., Tabti, R., Turner, K., Wang, X., Venuprasad, K., Souza, R. F., Desaubry, L., & Theiss, A. L. (2020). The synthetic small molecule FL3 combats intestinal tumorigenesis via axin1-mediated inhibition of Wnt/b-catenin signaling. *Cancer Research*, *80*(17), 3519–3529. https://doi.org/10.1158/0008-5472.CAN-20-0216

Jefferies, H., Fumagalli, S., Dennis, P. B., Reinhard, C., Pearson, R. B., Thomas, G., & Miescher, F. (1997). Rapamycin suppresses 5TOP mRNA translation through inhibition of p70S6K. *The EMBO Journal*, *16*(12), 3693–3704.

Jefferies, H., Reinhard, C., Kozma, S. C., & Thomas, G. (1994). Rapamycin selectively represses translation of the "polypyrimidine tract" mRNA family. *Proc. Natl. Acad. Sci. USA*, *91*, 4441–4445.

Jia, J. J., Lahr, R. M., Solgaard, M. T., Moraes, B. J., Pointet, R., Yang, A. D., Celucci, G., Graber, T. E., Hoang, H. D., Niklaus, M. R., Pena, I. A., Hollensen, A. K., Smith, E. M., Chaker-Margot, M., Anton, L., Dajadian, C., Livingstone, M., Hearnden, J., Wang, X. D., … Fonseca, B. D. (2021). MTORC1 promotes TOP mRNA translation through site-specific phosphorylation of LARP1. *Nucleic Acids Research*, *49*(6), 3461–3489. https://doi.org/10.1093/nar/gkaa1239

Jia, R., Ajiro, M., Yu, L., Mccoy, P., & Zheng, Z.-M. (2019). Oncogenic splicing factor SRSF3 regulates ILF3 alternative splicing to promote cancer cell proliferation and transformation. *RNA*, *25*, 630–644. https://doi.org/10.1261/rna

Jin, X., Xie, J., Zabolocki, M., Wang, X., Jiang, T., Wang, D., Désaubry, L., Bardy, C., & Proud, C. G. (2020). The prohibitin-binding compound fluorizoline affects multiple components of the translational machinery and inhibits protein synthesis. *Journal of Biological Chemistry*, *295*(29), 9855–9867. https://doi.org/10.1074/jbc.ra120.012979

Juszkiewicz, S., Speldewinde, S. H., Wan, L., Svejstrup, J. Q., & Hegde, R. S. (2020). The ASC-1 Complex Disassembles Collided Ribosomes. *Molecular Cell*, *79*(4), 603-614.e8. https://doi.org/10.1016/j.molcel.2020.06.006

Kallstrom, G., Hedges, J., & Johnson, A. (2003). The Putative GTPases Nog1p and Lsg1p Are Required for 60S Ribosomal Subunit Biogenesis and Are Localized to the Nucleus and Cytoplasm, Respectively. *Molecular and Cellular Biology*, *23*(12), 4344–4355. https://doi.org/10.1128/mcb.23.12.4344-4355.2003

Kampen, K. R., Sulima, S. O., Verbelen, B., Girardi, T., Vereecke, S., Rinaldi, G., Verbeeck, J., Op de Beeck, J., Uyttebroeck, A., Meijerink, J. P. P., Moorman, A. V., Harrison, C. J., Spincemaille, P., Cools, J., Cassiman, D., Fendt, S. M., Vermeersch, P., & De Keersmaecker, K. (2019). The ribosomal RPL10 R98S mutation drives IRES-dependent BCL-2 translation in T-ALL. *Leukemia*, *33*(2), 319–332. https://doi.org/10.1038/s41375-018-0176-z

Kanai, Y., Dohmae, N., & Hirokawa, N. (2004). Kinesin Transports RNA: Isolation and Characterization of an RNA-Transporting Granule. *Neuron*, *43*, 513–525.

Kang, J., Brajanovski, N., Chan, K. T., Xuan, J., Pearson, R. B., & Sanij, E. (2021). Ribosomal proteins and human diseases: molecular mechanisms and targeted therapy. *Signal Transduction and Targeted Therapy*, *6*(1). https://doi.org/10.1038/s41392-021-00728-8

Kantidakis, T., Ramsbottom, B. A., Birch, J. L., Dowding, S. N., & White, R. J. (2010). mTOR associates with TFIIIC, is found at tRNA and 5S rRNA genes, and targets their repressor Maf1. *Proceedings of the National Academy of Sciences of the United States of America*, *107*(26), 11823–11828. https://doi.org/10.1073/pnas.1005188107

Kato, M., Goto, Y., Matsushita, R., Kurozumi, A., Fukumoto, I., Nishikawa, R., Sakamoto, S., Enokida, H., Nakagawa, M., Ichikawa, T., & Seki, N. (2015). MicroRNA-26a/b directly regulate La-related protein 1 and inhibit cancer cell invasion in prostate cancer. *International Journal of Oncology*, *47*(2), 710–718. https://doi.org/10.3892/ijo.2015.3043

Kedersha, N., Panas, M. D., Achorn, C. A., Lyons, S., Tisdale, S., Hickman, T., Thomas, M., Lieberman, J., McInerney, G. M., Ivanov, P., & Anderson, P. (2016). G3BP-Caprin1-USP10 complexes mediate stress granule condensation and associate with 40S subunits. *Journal of Cell Biology*, *212*(7), 845–860. https://doi.org/10.1083/jcb.201508028

Keene, J. D., Komisarow, J. M., & Friedersdorf, M. B. (2006). RIP-Chip: The isolation and identification of mRNAs, microRNAs and protein components of ribonucleoprotein complexes from cell extracts. *Nature Protocols*, *1*(1), 302–307. https://doi.org/10.1038/nprot.2006.47

Kenny, P. J., Zhou, H., Kim, M., Skariah, G., Khetani, R. S., Drnevich, J., Arcila, M. L., Kosik, K. S., & Ceman, S. (2014). MOV10 and FMRP Regulate AGO2 Association with MicroRNA Recognition Elements. *Cell Reports*, *9*(5), 1729–1741. https://doi.org/10.1016/j.celrep.2014.10.054

Kiesler, P., Haynes, P. A., Shi, L., Kao, P. N., Wysocki, V. H., & Vercelli, D. (2010). NF45 and NF90 regulate HS4-dependent interleukin-13 transcription in T cells. *Journal of Biological Chemistry*, *285*(11), 8256–8267. https://doi.org/10.1074/jbc.M109.041004

Kim, D. H., Sarbassov, D. D., Ali, S. M., King, J. E., Latek, R. R., Erdjument-Bromage, H., Tempst, P., & Sabatini, D. M. (2002). mTOR Interacts with Raptor to Form a Nutrient-Sensitive Complex that Signals to the Cell Growth. *Cell*, *110*, 163–175.

Kim, E., Goraksha-Hicks, P., Li, L., Neufeld, T. P., & Guan, K. L. (2008). Regulation of TORC1 by Rag GTPases in nutrient response. *Nature Cell Biology*, *10*(8), 935–945. https://doi.org/10.1038/ncb1753

Kim, J. W., Akiyama, M., Park, J. H., Lin, M. L., Shimo, A., Ueki, T., Daigo, Y., Tsunoda, T., Nishidate, T., Nakamura, Y., & Katagiri, T. (2009). Activation of an estrogen/estrogen receptor signaling by BIG3 through its inhibitory effect on nuclear transport of PHB2/REA in breast cancer. *Cancer Science*, *100*(8), 1468–1478. https://doi.org/10.1111/j.1349-7006.2009.01209.x

Kohler, A., Carlström, A., Nolte, H., Kohler, V., Jung, S. jun, Sridhara, S., Tatsuta, T., Berndtsson, J., Langer, T., & Ott, M. (2023). Early fate decision for mitochondrially encoded proteins by a molecular triage. *Molecular Cell*, *83*(19), 3470-3484.e8. https://doi.org/10.1016/j.molcel.2023.09.001

Korwitz, A., Merkwirth, C., Richter-Dennerlein, R., Tröder, S. E., Sprenger, H. G., Quirós, P. M., López-Otín, C., Rugarli, E. I., & Langer, T. (2016). Loss of OMA1 delays neurodegeneration by preventing stress-induced OPA1 processing in mitochondria. *Journal of Cell Biology*, *212*(2), 157–166. https://doi.org/10.1083/jcb.201507022

Kressler, D., Hurt, E., & Baßler, J. (2017). A Puzzle of Life: Crafting Ribosomal Subunits. *Trends in Biochemical Sciences*, *42*(8), 640–654. https://doi.org/10.1016/j.tibs.2017.05.005

Kurtev, V., Margueron, R., Kroboth, K., Ogris, E., Cavailles, V., & Seiser, C. (2004). Transcriptional regulation by the repressor of estrogen receptor activity via recruitment of histone deacetylases. *Journal of Biological Chemistry*, *279*(23), 24834–24843. https://doi.org/10.1074/jbc.M312300200

Kuwano, Y., Pullmann, R., Marasa, B. S., Abdelmohsen, K., Lee, E. K., Yang, X., Martindale, J. L., Zhan, M., & Gorospe, M. (2009). NF90 selectively represses the translation of target mRNAs bearing an AU-rich signature motif. *Nucleic Acids Research*, *38*(1), 225–238. https://doi.org/10.1093/nar/gkp861

Lafita-Navarro, M. C., Kim, M., Borenstein-Auerbach, N., Venkateswaran, N., Hao, Y. H., Ray, R., Brabletz, T., Scaglioni, P. P., Shay, J. W., & Conacci-Sorrell, M. (2018). The aryl hydrocarbon receptor regulates nucleolar activity and protein synthesis in MYC-expressing cells. *Genes and Development*, *32*(19–20), 1303–1308. https://doi.org/10.1101/GAD.313007.118

Lahr, R. M., Fonseca, B. D., Ciotti, G. E., Al-Ashtal, H. A., Jia, J.-J., Niklaus, M. R., Blagden, S. P., Alain, T., & Berman, A. J. (2017). La-related protein 1 (LARP1) binds the mRNA cap, blocking eIF4F assembly on TOP mRNAs. *ELife*, *6*(e24146). https://doi.org/10.7554/eLife.24146.001

Lahr, R. M., Mack, S. M., Héroux, A., Blagden, S. P., Bousquet-Antonelli, C., Deragon, J. M., & Berman, A. J. (2015). The La-related protein 1-specific domain repurposes HEAT-like repeats to directly bind a 5'TOP sequence. *Nucleic Acids Research*, *43*(16), 8077–8088. https://doi.org/10.1093/nar/gkv748

Largeot, A., Klapp, V., Viry, E., Gonder, S., Fernandez Botana, I., Blomme, A., Benzarti, M., Pierson, S., Duculty, C., Marttila, P., Wierz, M., Gargiulo, E., Pagano, G., An, N., El Hachem, N., Perez Hernandez, D., Chakraborty, S., Ysebaert, L., François, J. H., … Moussay, E. (2023). Inhibition of MYC translation through targeting of the newly identified PHB-eIF4F complex as a therapeutic strategy in CLL. *Blood*, *141*(26), 3166–3183. https://doi.org/10.1182/blood.2022017839

Lecompte, O., Ripp, R., Thierry, J.-C., Moras, D., & Poch, O. (2002). Comparative analysis of ribosomal proteins in complete genomes: an example of reductive evolution at the domain scale. *Nucleic Acids Research*, *30*(24), 5382–5390.

Lécuyer, E., Yoshida, H., Parthasarathy, N., Alm, C., Babak, T., Cerovina, T., Hughes, T. R., Tomancak, P., & Krause, H. M. (2007). Global Analysis of mRNA Localization Reveals a Prominent Role in Organizing Cellular Architecture and Function. *Cell*, *131*(1), 174–187. https://doi.org/10.1016/j.cell.2007.08.003

Lee, D. F., Kuo, H. P., Chen, C. Te, Hsu, J. M., Chou, C. K., Wei, Y., Sun, H. L., Li, L. Y., Ping, B., Huang, W. C., He, X., Hung, J. Y., Lai, C. C., Ding, Q., Su, J. L., Yang, J. Y., Sahin, A. A., Hortobagyi, G. N., Tsai, F. J., … Hung, M. C. (2007). IKKβ Suppression of TSC1 Links Inflammation and Tumor Angiogenesis via the mTOR Pathway. *Cell*, *130*(3), 440–455. https://doi.org/10.1016/j.cell.2007.05.058

Lempiäinen, H., & Shore, D. (2009). Growth control and ribosome biogenesis. *Current Opinion in Cell Biology*, *21*(6), 855–863. https://doi.org/10.1016/j.ceb.2009.09.002

Li, K., Wu, J. lin, Qin, B., Fan, Z., Tang, Q., Lu, W., Zhang, H., Xing, F., Meng, M., Zou, S., Wei, W., Chen, H., Cai, J., Wang, H., Zhang, H., Cai, J., Fang, L., Bian, X., Chen, C., … Lee, M. H. (2020). ILF3 is a substrate of SPOP for regulating serine biosynthesis in colorectal cancer. *Cell Research*, *30*(2), 163–178. https://doi.org/10.1038/s41422-019-0257-1

Li, Q., Lau, A., Morris, T. J., Guo, L., Fordyce, C. B., & Stanley, E. F. (2004). A Syntaxin 1, Gαo, and N-Type Calcium Channel Complex at a Presynaptic Nerve Terminal: Analysis by Quantitative Immunocolocalization. *Journal of Neuroscience*, *24*(16), 4070–4081. https://doi.org/10.1523/JNEUROSCI.0346-04.2004

Lodde, V., Floris, M., Munk, R., Martindale, J. L., Piredda, D., Napodano, C. M. P., Cucca, F., Uzzau, S., Abdelmohsen, K., Gorospe, M., Noh, J. H., & Idda, M. L. (2022). Systematic identification of NF90 target RNAs by iCLIP analysis. *Scientific Reports*, *12*(1). https://doi.org/10.1038/s41598-021-04101-1

Ma, C., Wang, C., Luo, D., Yan, L., Yang, W., Li, N., & Gao, N. (2022). Structural insights into the membrane microdomain organization by SPFH family proteins. *Cell Research*, *32*(2), 176–189. https://doi.org/10.1038/s41422-021-00598-3

Ma, L., Chen, Z., Erdjument-Bromage, H., Tempst, P., & Pandolfi, P. P. (2005). Phosphorylation and functional inactivation of TSC2 by Erk: Implications for tuberous sclerosis and cancer pathogenesis. *Cell*, *121*(2), 179–193. https://doi.org/10.1016/j.cell.2005.02.031

Ma, L.-L., Shen, L., Tong, G.-H., Tang, N., Luo, Y., Guo, L.-L., Hu, C.-T., Huang, Y.-X., Huang, G., Jing, F.-Y., Liu, C., Li, Z.-Y., Zhou, N., Yan, Q.-W., Lei, Y., Zhu, S.-J., Cheng, Z.-Q., Cao, G.-W., Deng, Y.-J., & Ding, Y.-Q. (2017). Prohibitin, relocated to the front ends, can control the migration directionality of colorectal cancer cells. *Oncotarget*, *8*(44), 76340–76356. www.impactjournals.com/oncotarget

Manning, B. D., Tee, A. R., Logsdon, M. N., Blenis, J., & Cantley, L. C. (2002). Identification of the Tuberous Sclerosis Complex-2 Tumor Suppressor Gene Product Tuberin as a Target of the Phosphoinositide 3-Kinase/Akt Pathway. *Molecular Cell*, *10*, 151–162.

Mao, B., Zhang, Q., Ma, L., Zhao, D. S., Zhao, P., & Yan, P. (2022). Overview of Research into mTOR Inhibitors. In *Molecules* (Vol. 27, Issue 16). MDPI. https://doi.org/10.3390/molecules27165295

Marcel, V., Ghayad, S. E., Belin, S., Therizols, G., Morel, A. P., Solano-Gonzàlez, E., Vendrell, J. A., Hacot, S., Mertani, H. C., Albaret, M. A., Bourdon, J. C., Jordan, L., Thompson, A., Tafer, Y., Cong, R., Bouvet, P., Saurin, J. C., Catez, F., Prats, A. C., … Diaz, J. J. (2013). P53 Acts as a Safeguard of Translational Control by Regulating Fibrillarin and rRNA Methylation in Cancer. *Cancer Cell*, *24*(3), 318–330. https://doi.org/10.1016/j.ccr.2013.08.013

Masuda, K., Kuwano, Y., Nishida, K., Rokutan, K., & Imoto, I. (2013). NF90 in posttranscriptional gene regulation and microRNA biogenesis. *International Journal of Molecular Sciences*, *14*(8), 17111–17121. https://doi.org/10.3390/ijms140817111

Mattijssen, S., Kozlov, G., Gaidamakov, S., Ranjan, A., Fonseca, B. D., Gehring, K., & Maraia, R. J. (2021). The isolated La-module of LARP1 mediates 3’ poly(A) protection and mRNA stabilization, dependent on its intrinsic PAM2 binding to PABPC1. *RNA Biology*, *18*(2), 275–289. https://doi.org/10.1080/15476286.2020.1860376

Mayer, C., & Grummt, I. (2006). Ribosome biogenesis and cell growth: mTOR coordinates transcription by all three classes of nuclear RNA polymerases. *Oncogene*, *25*(48), 6384–6391. https://doi.org/10.1038/sj.onc.1209883

Mayer, C., Zhao, J., Yuan, X., & Grummt, I. (2004). mTOR-dependent activation of the transcription factor TIF-IA links rRNA synthesis to nutrient availability. *Genes and Development*, *18*(4), 423–434. https://doi.org/10.1101/gad.285504

Meyuhas, O. (2000). Synthesis of the translational apparatus is regulated at the translational level. *Eur. J. Biochem*, *267*.

Moncunill-Massaguer, C., Saura-Esteller, J., Pérez-Perarnau, A., Palmeri, C. M., Núñez-Vázquez, S., Cosialls, A. M., González-Gironès, D. M., Pomares, H., Korwitz, A., Preciado, S., Albericio, F., Lavilla, R., Pons, G., Langer, T., Iglesias-Serret, D., & Gil, J. (2015). A novel prohibitin-binding compound induces the mitochondrial apoptotic pathway through NOXA and BIM upregulation. *Oncotarget*, *6*(39), 41750–41765.

Montano, M. M., Ekena, K., Delage-Mourroux, R., Chang, W., Martini, P., & Katzenellenbogen, B. S. (1999). An estrogen receptor-selective coregulator that potentiates the effectiveness of antiestrogens and represses the activity of estrogens. *Proceedings of the National Academy of Sciences of the United States of America*, *96*(12), 6947–6952. https://doi.org/10.1073/pnas.96.12.6947

Mura, M., Hopkins, T. G., Michael, T., Abd-Latip, N., Weir, J., Aboagye, E., Mauri, F., Jameson, C., Sturge, J., Gabra, H., Bushell, M., Willis, A. E., Curry, E., & Blagden, S. P. (2015). LARP1 post-transcriptionally regulates mTOR and contributes to cancer progression. *Oncogene*, *34*(39), 5025–5036. https://doi.org/10.1038/onc.2014.428

Muzny, D. M., Bainbridge, M. N., Chang, K., Dinh, H. H., Drummond, J. A., Fowler, G., Kovar, C. L., Lewis, L. R., Morgan, M. B., Newsham, I. F., Reid, J. G., Santibanez, J., Shinbrot, E., Trevino, L. R., Wu, Y. Q., Wang, M., Gunaratne, P., Donehower, L. A., Creighton, C. J., … Thomson., E. (2012). Comprehensive molecular characterization of human colon and rectal cancer. *Nature*, *487*(7407), 330–337. https://doi.org/10.1038/nature11252

Nait Slimane, S., Marcel, V., Fenouil, T., Catez, F., Saurin, J. C., Bouvet, P., Diaz, J. J., & Mertani, H. C. (2020). Ribosome Biogenesis Alterations in Colorectal Cancer. *Cells*, *9*(11). https://doi.org/10.3390/cells9112361

Nakadai, T., Fukuda, A., Shimada, M., Nishimura, K., & Hisatake, K. (2015). The RNA binding complexes NF45-NF90 and NF45-NF110 associate dynamically with the c-fos gene and function as transcriptional coactivators. *Journal of Biological Chemistry*, *290*(44), 26832–26845. https://doi.org/10.1074/jbc.M115.688317

Narla, A., & Ebert, B. L. (2010). Ribosomopathies: Human disorders of ribosome dysfunction. *Blood*, *115*(16), 3196–3205. https://doi.org/10.1182/blood-2009-10-178129

Nijtmans, L. G. J., Artal Sanz, M., Grivell, L. A., & Coates, P. J. (2002). The mitochondrial PHB complex: roles in mitochondrial respiratory complex assembly, ageing and degenerative disease. *Cellular and Molecular Life Sciences*, *59*, 143–151.

Nijtmans, L. G. J., De Jong, L., Sanz, M. A., Coates, P. J., Berden, J. A., Back, J. W., Muijsers, A. O., Van Der Spek, H., & Grivell, L. A. (2000). Prohibitins act as a membrane-bound chaperone for the stabilization of mitochondrial proteins. *EMBO Journal*, *19*(11), 2444–2451. https://doi.org/10.1093/emboj/19.11.2444

Nojima, H., Tokunaga, C., Eguchi, S., Oshiro, N., Hidayat, S., Yoshino, K. I., Hara, K., Tanaka, N., Avruch, J., & Yonezawa, K. (2003). The mammalian target of rapamycin (mTOR) partner, raptor, binds the mTOR substrates p70 S6 kinase and 4E-BP1 through their TOR signaling (TOS) motif. *Journal of Biological Chemistry*, *278*(18), 15461–15464. https://doi.org/10.1074/jbc.C200665200

Nykamp, K., Lee, M. H., & Kimble, J. (2008). C. elegans La-related protein, LARP-1, localizes to germline P bodies and attenuates Ras-MAPK signaling during oogenesis. *RNA*, *14*(7), 1378–1389. https://doi.org/10.1261/rna.1066008

Ogami, K., Oishi, Y., Sakamoto, K., Okumura, M., Yamagishi, R., Inoue, T., Hibino, M., Nogimori, T., Yamaguchi, N., Furutachi, K., Hosoda, N., Inagaki, H., & Hoshino, S. ichi. (2022). mTOR- and LARP1-dependent regulation of TOP mRNA poly(A) tail and ribosome loading. *Cell Reports*, *41*(4). https://doi.org/10.1016/j.celrep.2022.111548

Osman, C., Merkwirth, C., & Langer, T. (2009). Prohibitins and the functional compartmentalization of mitochondrial membranes. *Journal of Cell Science*, *122*(21), 3823–3830. https://doi.org/10.1242/jcs.037655

Pakos-Zebrucka, K., Koryga, I., Mnich, K., Ljujic, M., Samali, A., & Gorman, A. M. (2016). The integrated stress response. *EMBO Reports*, *17*(10), 1374–1395. https://doi.org/10.15252/embr.201642195

Panas, M. D., Ivanov, P., & Anderson, P. (2016). Mechanistic insights into mammalian stress granule dynamics. In *Journal of Cell Biology* (Vol. 215, Issue 3, pp. 313–323). Rockefeller University Press. https://doi.org/10.1083/jcb.201609081

Pan, Y., Cao, F., Guo, A., Chang, W., Chen, X., Ma, W., Gao, X., Guo, S., Fu, C., & Zhu, J. (2015). Endoplasmic reticulum ribosome-binding protein 1, RRBP1, promotes progression of colorectal cancer and predicts an unfavourable prognosis. *British Journal of Cancer*, *113*(5), 763–772. https://doi.org/10.1038/bjc.2015.260

Park, J., Kim, M., Yi, H., Baeg, K., Choi, Y., Lee, Y. suk, Lim, J., & Kim, V. N. (2023). Short poly(A) tails are protected from deadenylation by the LARP1–PABP complex. *Nature Structural and Molecular Biology*, *30*(3), 330–338. https://doi.org/10.1038/s41594-023-00930-y

Parrott, A. M., Walsh, M. R., Reichman, T. W., & Mathews, M. B. (2005). RNA binding and phosphorylation determine the intracellular distribution of nuclear factors 90 and 110. *Journal of Molecular Biology*, *348*(2), 281–293. https://doi.org/10.1016/j.jmb.2005.02.047

Patel, N., Chatterjee, S. K., Vrbanac, V., Chung, I., Mu, C. J., Olsen, R. R., Waghorne, C., & Zetter, B. R. (2010). Rescue of paclitaxel sensitivity by repression of Prohibitin1 in drug-resistant cancer cells. *Proceedings of the National Academy of Sciences of the United States of America*, *107*(6), 2503–2508. https://doi.org/10.1073/pnas.0910649107

Pearce, M. M. P., Wormer, D. B., Wilkens, S., & Wojcikiewicz, R. J. H. (2009). An endoplasmic reticulum (ER) membrane complex composed of SPFH1 and SPFH2 mediates the ER-associated degradation of inositol 1,4,5-trisphosphate receptors. *Journal of Biological Chemistry*, *284*(16), 10433–10445. https://doi.org/10.1074/jbc.M809801200

Pelletier, J., Thomas, G., & Volarevic, S. (2018). Ribosome Biogenesis and Cancer. *Nature Reviews Cancer*, *18*, 51–63.

Pérez-Perarnau, A., Preciado, S., Palmeri, C. M., Moncunill-Massaguer, C., Iglesias-Serret, D., González-Gironès, D. M., Miguel, M., Karasawa, S., Sakamoto, S., Cosialls, A. M., Rubio-Patiño, C., Saura-Esteller, J., Ramõn, R., Caja, L., Fabregat, I., Pons, G., Handa, H., Albericio, F., Gil, J., & Lavilla, R. (2014). A trifluorinated thiazoline scaffold leading to pro-apoptotic agents targeting prohibitins. *Angewandte Chemie - International Edition*, *53*(38), 10150–10154. https://doi.org/10.1002/anie.201405758

Pfeifer, I., Elsby, R., Fernandez, M., Faria, P. A., Nussenzveig, D. R., Lossos, I. S., Fontoura, B. M. A., Martin, W. D., & Barber, G. N. (2008). NFAR-1 and -2 modulate translation and are required for efficient host defense. *Proceedings of the National Academy of Sciences of the United States of America*, *105*(11), 4173–4178. https://doi.org/10.1073/pnas.0711222105

Philippe, L., Vasseur, J. J., Debart, F., & Thoreen, C. C. (2018). La-related protein 1 (LARP1) repression of TOP mRNA translation is mediated through its cap-binding domain and controlled by an adjacent regulatory region. *Nucleic Acids Research*, *46*(3), 1457–1469. https://doi.org/10.1093/nar/gkx1237

Pourdehnad, M., Truitt, M. L., Siddiqi, I. N., Ducker, G. S., Shokat, K. M., & Ruggero, D. (2013). Myc and mTOR converge on a common node in protein synthesis control that confers synthetic lethality in Myc-driven cancers. *Proceedings of the National Academy of Sciences of the United States of America*, *110*(29), 11988–11993. https://doi.org/10.1073/pnas.1310230110

Qiao, Z., Yokoyama, T., Yan, X. F., Beh, I. T., Shi, J., Basak, S., Akiyama, Y., & Gao, Y. G. (2022). Cryo-EM structure of the entire FtsH-HflKC AAA protease complex. *Cell Reports*, *39*(9). https://doi.org/10.1016/j.celrep.2022.110890

Rajalingam, K., Wunder, C., Brinkmann, V., Churin, Y., Hekman, M., Sievers, C., Rapp, U. R., & Rudel, T. (2005). Prohibitin is required for Ras-induced Raf-MEK-ERK activation and epithelial cell migration. *Nature Cell Biology*, *7*(8), 837–843. https://doi.org/10.1038/ncb1283

Ramakrishnan, V. (2002). Ribosome Structure and the Mechanism of Translation. *Cell*, *108*, 557–572.

Reichman, T. W., & Mathews, M. B. (2003). RNA binding and intramolecular interactions modulate the regulation of gene expression by nuclear factor 110. *RNA*, *9*(5), 543–554. https://doi.org/10.1261/rna.2181103

Reichman, T. W., Muñiz, L. C., & Mathews, M. B. (2002). The RNA Binding Protein Nuclear Factor 90 Functions as Both a Positive and Negative Regulator of Gene Expression in Mammalian Cells. *Molecular and Cellular Biology*, *22*(1), 343–356. https://doi.org/10.1128/mcb.22.1.343-356.2002

Ren, H. Z., Wang, J. S., Wang, P., Pan, G. Q., Wen, J. F., Fu, H., & Shan, X. Z. (2010). Increased expression of prohibitin and its relationship with poor prognosis in esophageal squamous cell carcinoma. *Pathology and Oncology Research*, *16*(4), 515–522. https://doi.org/10.1007/s12253-009-9242-1

Richter-Dennerlein, R., Korwitz, A., Haag, M., Tatsuta, T., Dargazanli, S., Baker, M., Decker, T., Lamkemeyer, T., Rugarli, E. I., & Langer, T. (2014). DNAJC19, a mitochondrial cochaperone associated with cardiomyopathy, forms a complex with prohibitins to regulate cardiolipin remodeling. *Cell Metabolism*, *20*(1), 158–171. https://doi.org/10.1016/j.cmet.2014.04.016

Saba, J. A., Huang, Z., Schole, K. L., Ye, X., Bhatt, S. D., Li, Y., Timp, W., Cheng, J., & Green, R. (2023). LARP1 senses free ribosomes to coordinate supply and demand of ribosomal proteins. *BioRxive*. https://doi.org/10.1101/2023.11.01.565189

Sakamoto, S., Aoki, K., Higuchi, T., Todaka, H., Morisawa, K., Tamaki, N., Hatano, E., Fukushima, A., Taniguchi, T., & Agata, Y. (2009). The NF90-NF45 Complex Functions as a Negative Regulator in the MicroRNA Processing Pathway. *Molecular and Cellular Biology*, *29*(13), 3754–3769. https://doi.org/10.1128/mcb.01836-08

Sancak, Y., Peterson, T. R., Shaul, Y. D., Lindquist, R. A., Thoreen, C. C., Bar-Peled, L., & Sabatini, D. M. (2008). The Rag GTPases Bind Raptor and Mediate Amino Acid Signaling to mTORC1. *Science*, *320*(5882), 1496–1501. https://doi.org/10.1126/science.1157535

Sánchez-Vera, I., Núñez-Vázquez, S., Saura-Esteller, J., Cosialls, A. M., Heib, J., Nadal Rodríguez, P., Ghashghaei, O., Lavilla, R., Pons, G., Gil, J., & Iglesias-Serret, D. (2023). The Prohibitin-Binding Compound Fluorizoline Activates the Integrated Stress Response through the eIF2α Kinase HRI. *International Journal of Molecular Sciences*, *24*(9). https://doi.org/10.3390/ijms24098064

Sarbassov, D. D., Ali, S. M., Kim, D.-H., Guertin, D. A., Latek, R. R., Erdjument-Bromage, H., Tempst, P., & Sabatini, D. M. (2004). Rictor, a Novel Binding Partner of mTOR, Defines a Rapamycin-Insensitive and Raptor-Independent Pathway that Regulates the Cytoskeleton. *Current Biology*, *14*, 1296–1302. https://doi.org/10.1016/j

Satoh, M., Shaheen, V. M., Kao, P. N., Okano, T., Shaw, M., Yoshida, H., Richards, H. B., & Reeves, W. H. (1999). Autoantibodies define a family of proteins with conserved double- stranded RNA-binding domains as well as DNA binding activity. *Journal of Biological Chemistry*, *274*(49), 34598–34604. https://doi.org/10.1074/jbc.274.49.34598

Saunders, L. R., Jurecic, V., & Barber, G. N. (2001). The 90- and 110-kDa human NFAR proteins are translated from two differentially spliced mRNAs encoded on chromosome 19p13. *Genomics*, *71*(2), 256–259. https://doi.org/10.1006/geno.2000.6423

Saunders, L. R., Perkins, D. J., Balachandran, S., Michaels, R., Ford, R., Mayeda, A., & Barber, G. N. (2001). Characterization of Two Evolutionarily Conserved, Alternatively Spliced Nuclear Phosphoproteins, NFAR-1 and -2, that Function in mRNA Processing and Interact with the Double-stranded RNA-dependent Protein Kinase, PKR. *Journal of Biological Chemistry*, *276*(34), 32300–32312. https://doi.org/10.1074/jbc.M104207200

Saxton, R. A., & Sabatini, D. M. (2017). mTOR Signaling in Growth, Metabolism, and Disease. *Cell*, *168*(6), 960–976. https://doi.org/10.1016/j.cell.2017.02.004

Schalm, S. S., Fingar, D. C., Sabatini, D. M., & Blenis, J. (2003). TOS Motif-Mediated Raptor Binding Regulates 4E-BP1 Multisite Phosphorylation and Function. *Current Biology*, *13*, 797–806. https://doi.org/10.1016/S0960-9822(03)00329-4

Schlosser, I., Hölzel, M., Mürnseer, M., Burtscher, H., Weidle, U. H., & Eick, D. (2003). A role for c-Myc in the regulation of ribosomal RNA processing. *Nucleic Acids Research*, *31*(21), 6148–6156. https://doi.org/10.1093/nar/gkg794

Schmidt, E. V. (2004). The role of c-myc in regulation of translation initiation. *Oncogene*, *23*(18), 3217–3221. https://doi.org/10.1038/sj.onc.1207548

Schwenzer, H., Abdel Mouti, M., Neubert, P., Morris, J., Stockton, J., Bonham, S., Fellermeyer, M., Chettle, J., Fischer, R., Beggs, A. D., & Blagden, S. P. (2021). LARP1 isoform expression in human cancer cell lines. *RNA Biology*, *18*(2), 237–247. https://doi.org/10.1080/15476286.2020.1744320

Shamanna, R. A., Hoque, M., Lewis-Antes, A., Azzam, E. I., Lagunoff, D., Pe'ery, T., & Mathews, M. B. (2011). The NF90/NF45 Complex Participates in DNA Break Repair via Nonhomologous End Joining. *Molecular and Cellular Biology*, *31*(23), 4832–4843. https://doi.org/10.1128/mcb.05849-11

Sharma, A., & Qadri, A. (2004). Vi polysaccharide of Salmonella typhi targets the prohibitin family of molecules in intestinal epithelial cells and suppresses early inflammatory responses. *Proc. Natl. Acad. Sci. USA*, *101*(50), 17492–17497. https://doi.org/doi/10.1073/pnas.0407536101

Shen, H. M., Zhang, D., Xiao, P., Qu, B., & Sun, Y. F. (2023). E2F1-mediated KDM4A-AS1 up-regulation promotes EMT of hepatocellular carcinoma cells by recruiting ILF3 to stabilize AURKA mRNA. *Cancer Gene Therapy*, *30*(7), 1007–1017. https://doi.org/10.1038/s41417-023-00607-0

Shigeoka, T., Koppers, M., Wong, H. H. W., Lin, J. Q., Cagnetta, R., Dwivedy, A., de Freitas Nascimento, J., van Tartwijk, F. W., Ströhl, F., Cioni, J. M., Schaeffer, J., Carrington, M., Kaminski, C. F., Jung, H., Harris, W. A., & Holt, C. E. (2019). On-Site Ribosome Remodeling by Locally Synthesized Ribosomal Proteins in Axons. *Cell Reports*, *29*(11), 3605-3619.e10. https://doi.org/10.1016/j.celrep.2019.11.025

Shi, L., Qiu, D., Zhao, G., Corthesy, B., Lees-Miller, S., Reeves, W. H., & Kao, P. N. (2007). Dynamic binding of Ku80, Ku70 and NF90 to the IL-2 promoter in vivo in activated T-cells. *Nucleic Acids Research*, *35*(7), 2302–2310. https://doi.org/10.1093/nar/gkm117

Shi, L., Zhao, G., Qiu, D., Godfrey, W. R., Vogel, H., Rando, T. A., Hu, H., & Kao, P. N. (2005). NF90 regulates cell cycle exit and terminal myogenic differentiation by direct binding to the 3'-untranslated region of MyoD and p21 WAF1/CIP1 mRNAs. *Journal of Biological Chemistry*, *280*(19), 18981–18989. https://doi.org/10.1074/jbc.M411034200

Shor, B., Wu, J., Shakey, Q., Toral-Barza, L., Shi, C., Follettie, M., & Yu, K. (2010). Requirement of the mTOR kinase for the regulation of Maf1 phosphorylation and control of RNA polymerase III-dependent transcription in cancer cells. *Journal of Biological Chemistry*, *285*(20), 15380–15392. https://doi.org/10.1074/jbc.M109.071639

Simsek, D., Tiu, G. C., Flynn, R. A., Byeon, G. W., Leppek, K., Xu, A. F., Chang, H. Y., & Barna, M. (2017). The Mammalian Ribo-interactome Reveals Ribosome Functional Diversity and Heterogeneity. *Cell*, *169*(6), 1051-1065.e18. https://doi.org/10.1016/j.cell.2017.05.022

Sonenberg, N., & Hinnebusch, A. G. (2009). Regulation of Translation Initiation in Eukaryotes: Mechanisms and Biological Targets. *Cell*, *136*(4), 731–745. https://doi.org/10.1016/j.cell.2009.01.042

Spahn, C. M. T., Beckmann, R., Eswar, N., Penczek, P. A., Sali, A., Nter Blobel, G., & Frank, J. (2001). Structure of the 80S Ribosome from Saccharomyces cerevisiae-tRNA-Ribosome and Subunit-Subunit Interactions. *Cell*, *107*, 373–386.

Stavraka, C., & Blagden, S. (2015). The La-related proteins, a family with connections to cancer. *Biomolecules*, *5*(4), 2701–2722. https://doi.org/10.3390/biom5042701

Steglich, G., Neupert, W., & Langer, T. (1999). Prohibitins Regulate Membrane Protein Degradation by the m -AAA Protease in Mitochondria . *Molecular and Cellular Biology*, *19*(5), 3435–3442. https://doi.org/10.1128/mcb.19.5.3435

Street, L., Rothamel, K., Brannan, K., Jin, W., Bokor, B., Dong, K., Rhine, K., Madrigal, A., Al-Azzam, N., Kim, J. K., Ma, Y., Abdou, A., Wolin, E., Doron-Mandel, E., Ahdout, J., Mujumdar, M., Jovanovic, M., & Yeo, G. W. (2023). Large-scale map of RNA binding protein interactomes across the mRNA life-cycle. *BioRxiv*. https://doi.org/10.1101/2023.06.08.544225

Subbarayalu, P., Yadav, P., Timilsina, S., Medina, D., Baxi, K., Hromas, R., Vadlamudi, R. K., Chen, Y., Sung, P., & Rao, M. K. (2023). The RNA Demethylase ALKBH5 Maintains Endoplasmic Reticulum Homeostasis by Regulating UPR, Autophagy, and Mitochondrial Function. *Cells*, *12*(9). https://doi.org/10.3390/cells12091283

Suzuki, C., Garces, R. G., Edmonds, K. A., Hiller, S., Hyberts, S. G., Marintchev, A., & Wagner, G. (2008). PDCD4 inhibits translation initiation by binding to eIF4A using both its MA3 domains. *PNAS*, *105*(9), 3274–3279.

Suzuki, T., Ito, S., Horikawa, S., Suzuki, T., Kawauchi, H., Tanaka, Y., & Suzuki, T. (2014). Human NAT10 is an ATP-dependent rna acetyltransferase responsible for N4-acetylcytidine formation in 18 S ribosomal RNA (rRNA). *Journal of Biological Chemistry*, *289*(52), 35724–35730. https://doi.org/10.1074/jbc.C114.602698

Tatsuta, T., & Langer, T. (2017). Prohibitins. *Current Biology*, *27*(13), 629–631. https://doi.org/10.1016/j.cub.2017.04.030

Tatsuta, T., Model, K., & Langer, T. (2005). Formation of Membrane-bound Ring Complexes by Prohibitins in Mitochondria. *Molecular Biology of the Cell*, *16*, 248–259. https://doi.org/10.1091/mbc.E04

Tcherkezian, J., Cargnello, M., Romeo, Y., Huttlin, E. L., Lavoie, G., Gygi, S. P., & Roux, P. P. (2014). Proteomic analysis of cap-dependent translation identifies LARP1 as a key regulator of 5'TOP mRNA translation. *Genes and Development*, *28*(4), 357–371. https://doi.org/10.1101/gad.231407.113

Tee, A. R., Manning, B. D., Roux, P. P., Cantley, L. C., & Blenis, J. (2003). Tuberous Sclerosis Complex Gene Products, Tuberin and Hamartin, Control mTOR Signaling by Acting as a GTPase-Activating Protein Complex toward Rheb. *Current Biology*, *13*, 1259–1268. https://doi.org/10.1016/S0960-9822(03)00506-2

Terashima, M., Kim, K. M., Adachi, T., Nielsen, P. J., Reth, M., Köhler, G., & Lamers, M. C. (1994). The IgM antigen receptor of B lymphocytes is associated with prohibitin and a prohibitin-related protein. *EMBO Journal*, *13*(16), 3782–3792. https://doi.org/10.1002/j.1460-2075.1994.tb06689.x

Thoreen, C. C., Chantranupong, L., Keys, H. R., Wang, T., Gray, N. S., & Sabatini, D. M. (2012). A unifying model for mTORC1-mediated regulation of mRNA translation. *Nature*, *485*(7396), 109–113. https://doi.org/10.1038/nature11083

Thuaud, F., Ribeiro, N., Nebigil, C. G., & Désaubry, L. (2013). Prohibitin ligands in cell death and survival: Mode of action and therapeutic potential. *Chemistry and Biology*, *20*(3), 316–331. https://doi.org/10.1016/j.chembiol.2013.02.006

Tominaga-Yamanaka, K., Abdelmohsen, K., Martindale, J. L., Yang, X., Taub, D. D., & Gorospe, M. (2012). NF90 and senescence associated secretory phenotype. *Aging* , *4*(10), 695–708.

Tsai, H. W., Chow, N. H., Lin, C. P., Chan, S. H., Chou, C. Y., & Ho, C. L. (2006). The significance of prohibitin and c-Met/hepatocyte growth factor receptor in the progression of cervical adenocarcinoma. *Human Pathology*, *37*(2), 198–204. https://doi.org/10.1016/j.humpath.2005.10.012

Tsai, H., Zeng, X., Liu, L., Xin, S., Wu, Y., Xu, Z., Zhang, H., Liu, G., Bi, Z., Su, D., Yang, M., Tao, Y., Wang, C., Zhao, J., Eriksson, J. E., Deng, W., Cheng, F., & Chen, H. (2021). NF45/NF90-mediated rDNA transcription provides a novel target for immunosuppressant development. *EMBO Molecular Medicine*, *13*(3). https://doi.org/10.15252/emmm.202012834

Tschochner, H., & Hurt, E. (2003). Pre-ribosomes on the road from the nucleolus to the cytoplasm. *Trends in Cell Biology*, *13*(5), 255–263. https://doi.org/10.1016/S0962-8924(03)00054-0

Ummanni, R., Junker, H., Zimmermann, U., Venz, S., Teller, S., Giebel, J., Scharf, C., Woenckhaus, C., Dombrowski, F., & Walther, R. (2008). Prohibitin identified by proteomic analysis of prostate biopsies distinguishes hyperplasia and cancer. *Cancer Letters*, *266*(2), 171–185. https://doi.org/10.1016/j.canlet.2008.02.047

Um, S. H., Frigerio, F., Watanabe, M., Picard, F., Joaquin, M., Sticker, M., Fumagalli, S., Allegrini, P. R., Kozma, S. C., Auwerx, J., & Thomas, G. (2004). Absence of S6K1 protects against age-and diet-induced obesity while enhancing insulin sensitivity. *Nature*, *431*, 200–206.

Van Dijk, E. L., Schilders, G., & Pruijn, G. J. M. (2007). Human cell growth requires a functional cytoplasmic exosome, which is involved in various mRNA decay pathways. *RNA*, *13*(7), 1027–1035. https://doi.org/10.1261/rna.575107

Van Riggelen, J., Yetil, A., & Felsher, D. W. (2010). MYC as a regulator of ribosome biogenesis and protein synthesis. *Nature Reviews Cancer*, *10*(4), 301–309. https://doi.org/10.1038/nrc2819

Vetter, I. R., Nowak, C., Nishimoto, T., È rgen Kuhlmann, J., & Wittinghofer, A. (1999). Structure of a Ran-binding domain complexed with Ran bound to a GTP analogue: implications for nuclear transport. *Nature*, *398*, 39–46.

Vrakas, C. N., Herman, A. B., Ray, M., Kelemen, S. E., Scalia, R., & Autieri, M. V. (2019). RNA stability protein ILF3 mediates cytokine-induced angiogenesis. *FASEB Journal*, *33*(3), 3304–3316. https://doi.org/10.1096/fj.201801315R

Vumbaca, F., Phoenix, K. N., Rodriguez-Pinto, D., Han, D. K., & Claffey, K. P. (2008). Double-Stranded RNA-Binding Protein Regulates Vascular Endothelial Growth Factor mRNA Stability, Translation, and Breast Cancer Angiogenesis. *Molecular and Cellular Biology*, *28*(2), 772–783. https://doi.org/10.1128/mcb.02078-06

Wandrey, F., Montellese, C., Koos, K., Badertscher, L., Bammert, L., Cook, A. G., Zemp, I., Horvath, P., & Kutay, U. (2015). The NF45/NF90 Heterodimer Contributes to the Biogenesis of 60S Ribosomal Subunits and Influences Nucleolar Morphology. *Molecular and Cellular Biology*, *35*(20), 3491–3503. https://doi.org/10.1128/mcb.00306-15

Wang, S., Fusaro, G., Padmanabhan, J., & Chellappan, S. P. (2002). Prohibitin co-localizes with Rb in the nucleus and recruits N-CoR and HDAC1 for transcriptional repression. *Oncogene*, *21*, 8388–8396. https://doi.org/10.1038/sj.onc

Wang, S., Nath, N., Adlam, M., & Chellappan, S. (1999). Prohibitin, a potential tumor suppressor, interacts with RB and regulates E2F function. *Oncogene*, *18*, 3501–3510. http://www.stockton-press.co.uk/onc

Wang, S., Nath, N., Fusaro, G., & Chellappan, S. (1999). Rb and Prohibitin Target Distinct Regions of E2F1 for Repression and Respond to Different Upstream Signals. *Molecular and Cellular Biology*, *19*(11), 7447–7460. https://doi.org/10.1128/mcb.19.11.7447

Wang, X., Li, W., Williams, M., Terada, N., Alessi, D. R., & Proud, C. G. (2001). Regulation of elongation factor 2 kinase by p90RSK1 and p70 S6 kinase. *EMBO Journal*, *20*(16), 4370–4379. https://doi.org/10.1093/emboj/20.16.4370

Wan, R., Bai, R., Zhan, X., & Shi, Y. (2020). Annual Review of Biochemistry How Is Precursor Messenger RNA Spliced by the Spliceosome? *Annual Review in Biochemistry*, *89*, 333–358. https://doi.org/10.1146/annurev-biochem-013118

Watson, S. F., Bellora, N., & MacIas, S. (2020). ILF3 contributes to the establishment of the antiviral type i interferon program. *Nucleic Acids Research*, *48*(1), 116–129. https://doi.org/10.1093/nar/gkz1060

Wei, Y., Chiang, W. C., Sumpter, R., Mishra, P., & Levine, B. (2017). Prohibitin 2 Is an Inner Mitochondrial Membrane Mitophagy Receptor. *Cell*, *168*(1–2), 224-238.e10. https://doi.org/10.1016/j.cell.2016.11.042

Werner, A., Iwasaki, S., McGourty, C. A., Medina-Ruiz, S., Teerikorpi, N., Fedrigo, I., Ingolia, N. T., & Rape, M. (2015). Cell-fate determination by ubiquitin-dependent regulation of translation. *Nature*, *525*(7570), 523–527. https://doi.org/10.1038/nature14978

Wilbertz, J. H., Voigt, F., Horvathova, I., Roth, G., Zhan, Y., & Chao, J. A. (2019). Single-Molecule Imaging of mRNA Localization and Regulation during the Integrated Stress Response. *Molecular Cell*, *73*(5), 946-958.e7. https://doi.org/10.1016/j.molcel.2018.12.006

Wilson, D. N., & Cate, J. H. D. (2012). The structure and function of the eukaryotic ribosome. *Cold Spring Harbor Perspectives in Biology*, *4*(5), 5. https://doi.org/10.1101/cshperspect.a011536

Winter, A., Kämäräinen, O., & Hofmann, A. (2007). Molecular modeling of prohibitin domains. *Proteins: Structure, Function and Genetics*, *68*(1), 353–362. https://doi.org/10.1002/prot.21355

Wolkowicz, U. M., & Cook, A. G. (2012). NF45 dimerizes with NF90, Zfr and SPNR via a conserved domain that has a nucleotidyltransferase fold. *Nucleic Acids Research*, *40*(18), 9356–9368. https://doi.org/10.1093/nar/gks696

Wu, T. H., Shi, L., Adrian, J., Shi, M., Nair, R. V., Snyder, M. P., & Kao, P. N. (2018). NF90/ILF3 is a transcription factor that promotes proliferation over differentiation by hierarchical regulation in K562 erythroleukemia cells. *PLoS ONE*, *13*(3). https://doi.org/10.1371/journal.pone.0193126

Wyant, G. A., Abu-Remaileh, M., Frenkel, E. M., Laqtom, N. N., Dharamdasani, V., Lewis, C. A., Chan, S. H., Heinze, I., Ori, A., & Sabatini, D. M. (2018). NUFIP1 is a ribosome receptor for starvation-induced ribophagy. *Science*, *360*, 751–758.

Xie, C., Huang, L., Xie, S., Xie, D., Zhang, G., Wang, P., Peng, L., & Gao, Z. (2013). LARP1 predict the prognosis for early-stage and AFP-normal hepatocellular carcinoma. *Journal of Translational Medicine*, *11*(1). https://doi.org/10.1186/1479-5876-11-272

Xu, Z., Xu, J., Lu, H., Lin, B., Cai, S., Guo, J., Zang, F., & Chen, R. (2017). LARP1 is regulated by the XIST/miR-374a axis and functions as an oncogene in non-small cell lung carcinoma. *Oncology Reports*, *38*(6), 3659–3667. https://doi.org/10.3892/or.2017.6040

Yan, C., Gong, L., Chen, L., Xu, M., Abou-Hamdan, H., Tang, M., Désaubry, L., & Song, Z. (2020). PHB2 (prohibitin 2) promotes PINK1-PRKN/Parkin-dependent mitophagy

by the PARL-PGAM5-PINK1 axis. *Autophagy*, *16*(3), 419–434. https://doi.org/10.1080/15548627.2019.1628520

Yang, G., Murashige, D. S., Humphrey, S. J., & James, D. E. (2015). A Positive Feedback Loop between Akt and mTORC2 via SIN1 Phosphorylation. *Cell Reports*, *12*(6), 937–943. https://doi.org/10.1016/j.celrep.2015.07.016

Yang, H., Rudge, D. G., Koos, J. D., Vaidialingam, B., Yang, H. J., & Pavletich, N. P. (2013). MTOR kinase structure, mechanism and regulation. *Nature*, *497*(7448), 217–223. https://doi.org/10.1038/nature12122

Yang, J., Li, B., & He, Q. Y. (2018). Significance of prohibitin domain family in tumorigenesis and its implication in cancer diagnosis and treatment review-article. In *Cell Death and Disease* (Vol. 9, Issue 6). Nature Publishing Group. https://doi.org/10.1038/s41419-018-0661-3

Yan, G., Yang, J., Li, W., Guo, A., Guan, J., & Liu, Y. (2023). Genome-wide CRISPR screens identify ILF3 as a mediator of mTORC1-dependent amino acid sensing. *Nature Cell Biology*, *25*(5), 754–764. https://doi.org/10.1038/s41556-023-01123-x

Ye, L., Lin, S. tao, Mi, Y. shuai, Liu, Y., Ma, Y., Sun, H. min, Peng, Z. hai, & Fan, J. wei. (2016). Overexpression of LARP1 predicts poor prognosis of colorectal cancer and is expected to be a potential therapeutic target. *Tumor Biology*, *37*(11), 14585–14594. https://doi.org/10.1007/s13277-016-5332-3

Yurugi, H., Marini, F., Weber, C., David, K., Zhao, Q., Binder, H., Désaubry, L., & Rajalingam, K. (2017). Targeting prohibitins with chemical ligands inhibits KRAS-mediated lung tumours. *Oncogene*, *36*(33), 4778–4789. https://doi.org/10.1038/onc.2017.93

Yurugi, H., Tanida, S., Ishida, A., Akita, K., Toda, M., Inoue, M., & Nakada, H. (2012). Expression of prohibitins on the surface of activated T cells. *Biochemical and Biophysical Research Communications*, *420*(2), 275–280. https://doi.org/10.1016/j.bbrc.2012.02.149

Yu, Y., Yoon, S.-O., Poulogiannis, G., Yang, Q., Ma, X. M., Villén, J., Kubica, N., Hoffman, G. R., Cantley, L. C., Gygi, S. P., & Blenis, J. (2011). Phosphoproteomic Analysis Identifies Grb10 as an mTORC1 Substrate That Negatively Regulates Insulin Signaling. *Science*, *332*(6035), 1322–1326. https://doi.org/10.1126/science.1199484

Zhang, J., Yin, Y., Wang, J., Zhang, J., Liu, H., Feng, W., Yang, W., Zetter, B., & Xu, Y. (2021). Prohibitin regulates mTOR pathway via interaction with FKBP8. *Frontiers of Medicine*, *15*(3), 448–459. https://doi.org/10.1007/s11684-020-0805-6

Zhao, J., Hyman, L., & Moore, C. (1999). Formation of mRNA 3 Ends in Eukaryotes: Mechanism, Regulation, and Interrelationships with Other Steps in mRNA Synthesis. *Microbiology and Molecular Biology Reviews*, *63*(2), 405–445.

Zhong, N., Cui, Y., Zhou, X., Li, T., & Han, J. (2015). Identification of prohibitin 1 as a potential prognostic biomarker in human pancreatic carcinoma using modified aqueous two-phase partition system combined with 2D-MALDI-TOF-TOF-MS/MS. *Tumor Biology*, *36*(2), 1221–1231. https://doi.org/10.1007/s13277-014-2742-y

Zhou, Z., Licklider, L. J., Gygi, S. P., & Reed, R. (2002). Comprehensive proteomic analysis of the human spliceosome. *Nature*, *419*, 182–185. www.nature.com/nature